Baryon spectroscopy via measurement of polarization observables

Institutsseminar Kern- und Hadronenphysik

Farah Noreen Afzal

25.11.2019

Universität Bonn

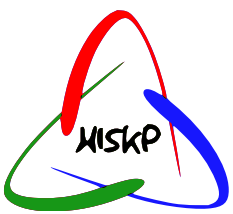

Table of contents

Baryon spectroscopy

Motivation

UNIVERSITÄT BONN

Different scales of matter

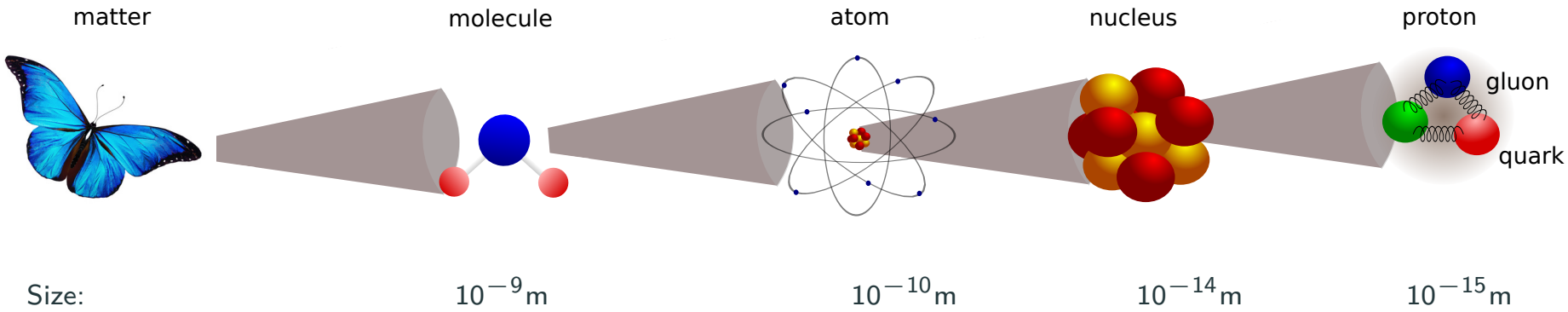

Size:	10^{-9}m	10^{-10}m	10^{-14}m	10^{-15}m

- How can we study different scales of matter?
  $\rightarrow$ **Spectroscopy**, e.g. atomic spectroscopy or baryon spectroscopy

Atomic spectroscopy

- Study dynamics inside the atom
- Atomic spectroscopy $\leftrightarrow$ QED

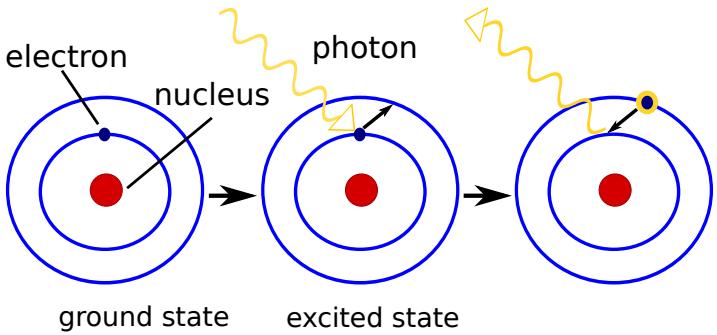

Atomic spectroscopy

- Study dynamics inside the atom
- Atomic spectroscopy $\leftrightarrow$ QED

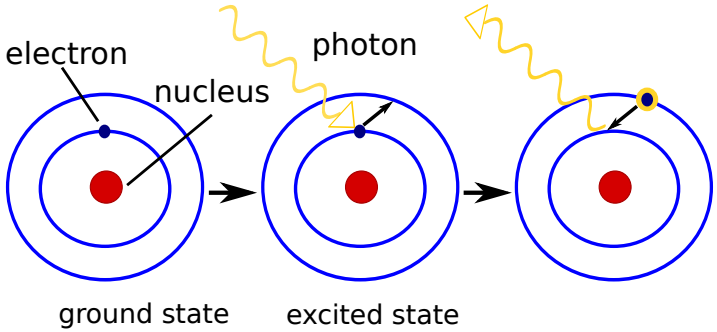

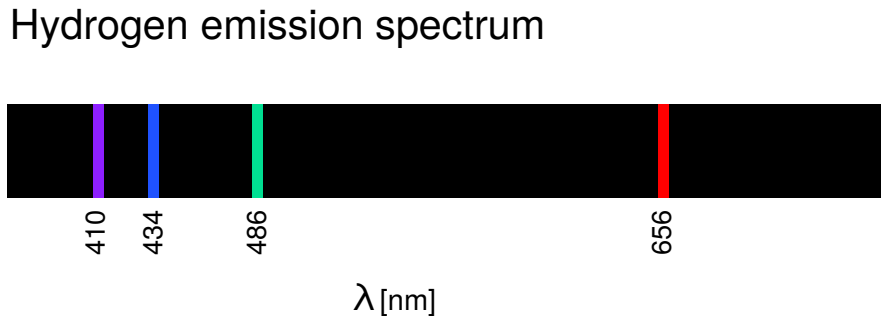

http:ch301.cm.utexas.edu/atomic/#H-atom/H-atom-all.php

- Study dynamics inside the atom
- Atomic spectroscopy $\leftrightarrow$ QED

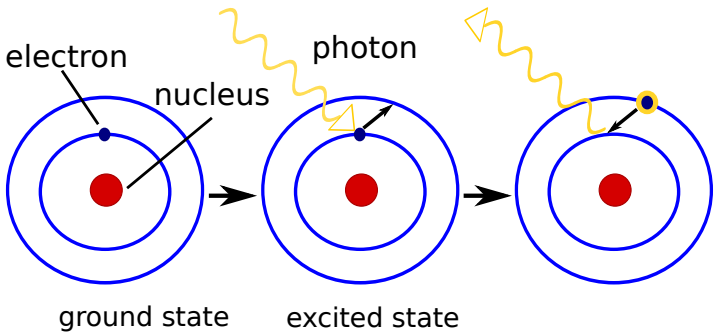

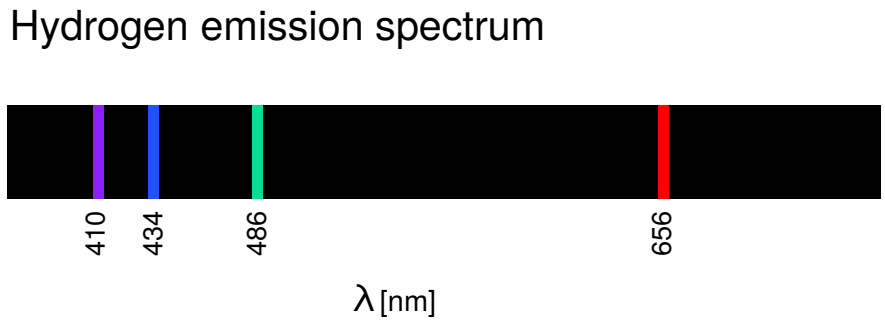

http:ch301.cm.utexas.edu/atomic/#H-atom/H-atom-all.php

- Well separated emission lines!

Baryon spectroscopy

- Study dynamics of constituents inside the nucleon
- Baryon spectroscopy $\leftrightarrow$ QCD

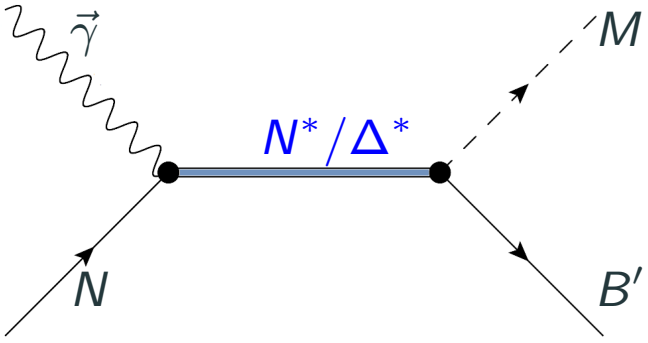

Baryon spectroscopy

- Study dynamics of constituents inside the nucleon
- Baryon spectroscopy $\leftrightarrow$ QCD

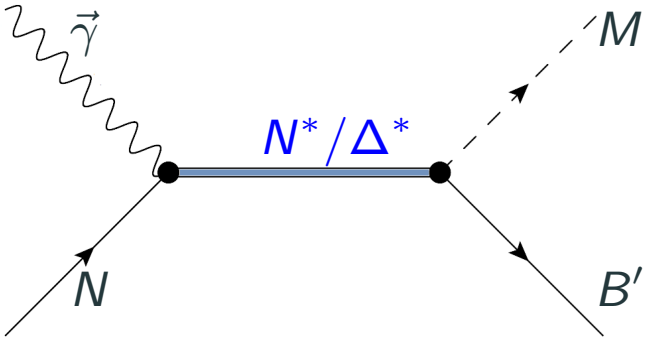

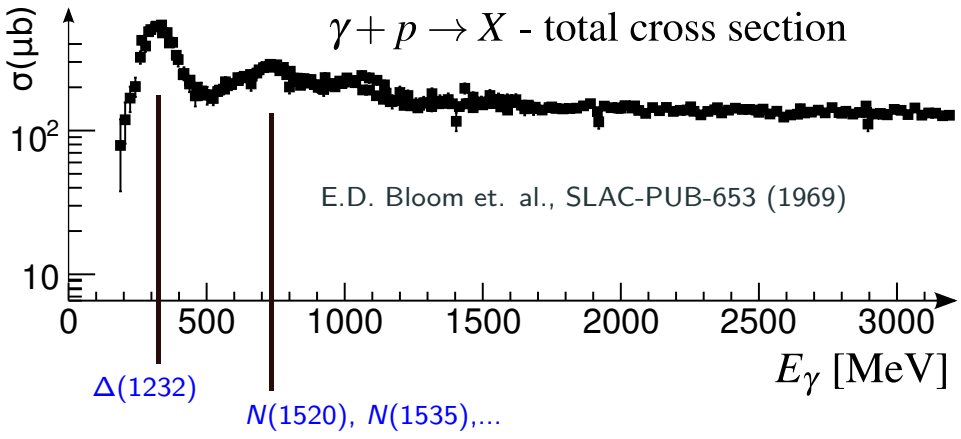

Baryon spectroscopy

- Study dynamics of constituents inside the nucleon
- Baryon spectroscopy $\leftrightarrow$ QCD

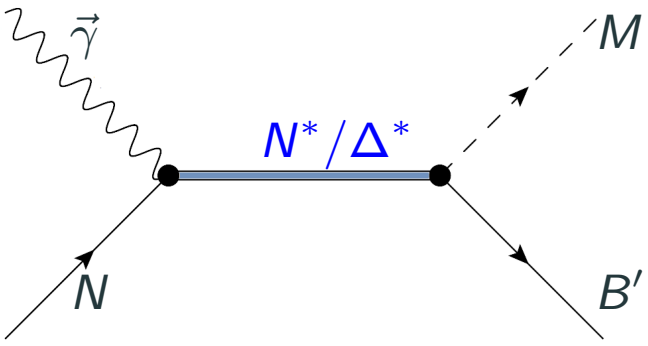

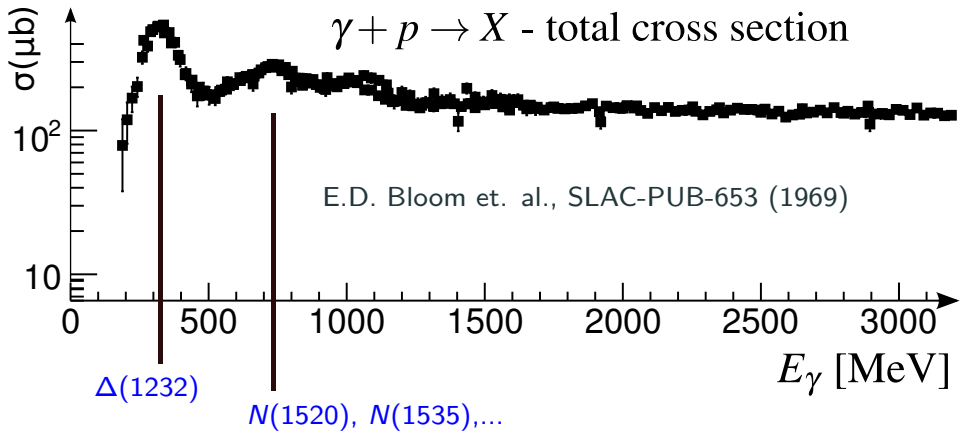

- Disentanglement of the contributing resonances is a challenging task!

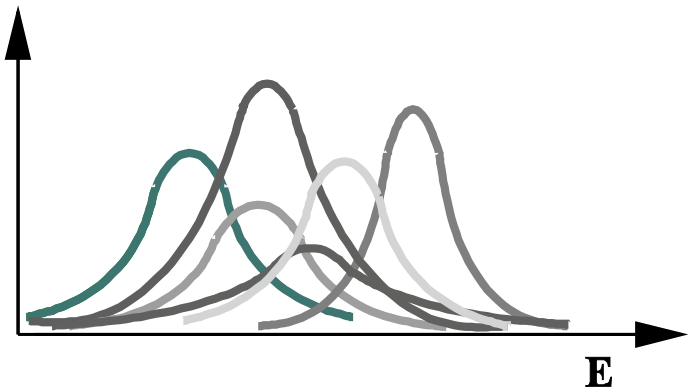

Theoretical description of nucleon excitation spectra

- How can we predict the nucleon excitation spectrum?

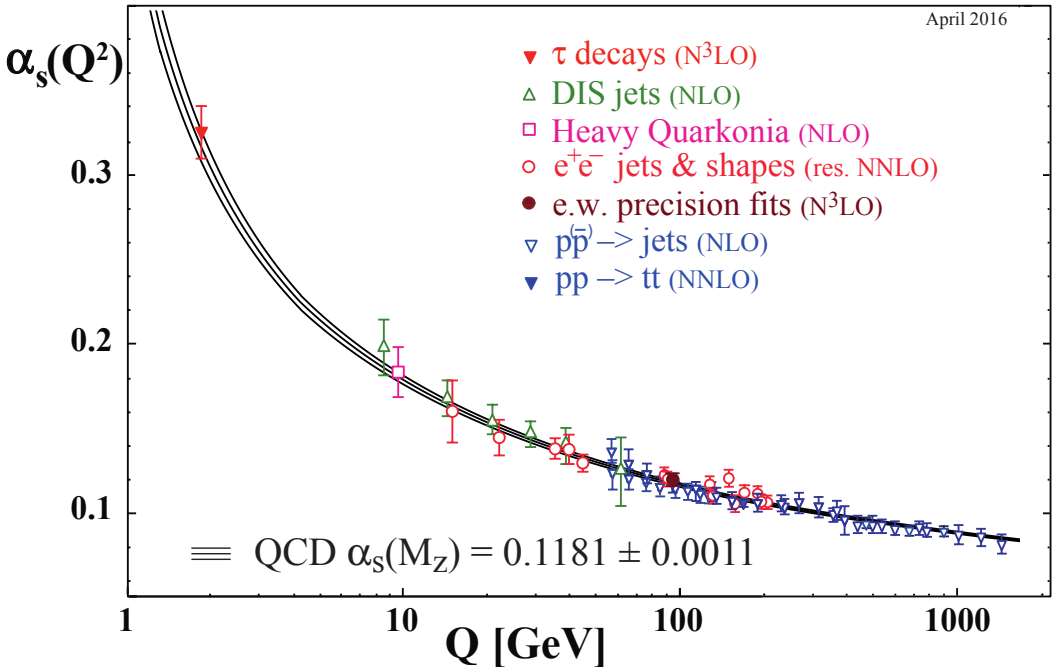

M. Tanabashi et al., Review of Particle Physics

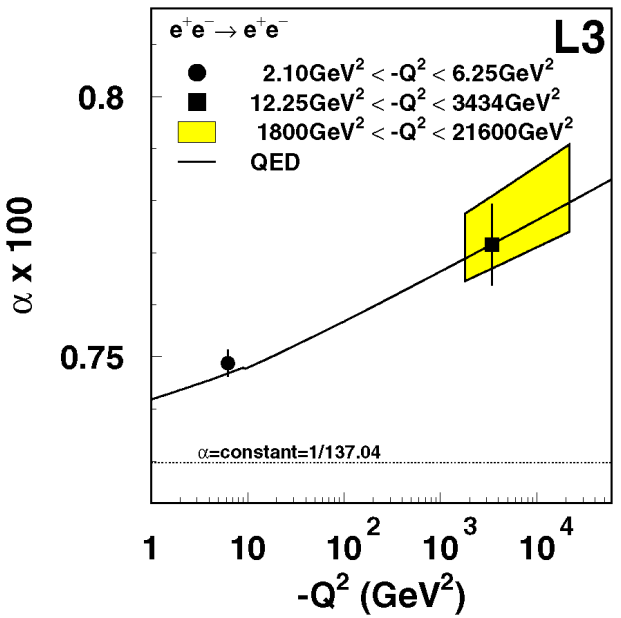

P. Achard et al., Physics Letter B 623 (2005) 26

- α_s is large at energy scale of proton mass
  $\rightarrow$ perturbation theory is not possible!

Theoretical description of nucleon excitation spectra

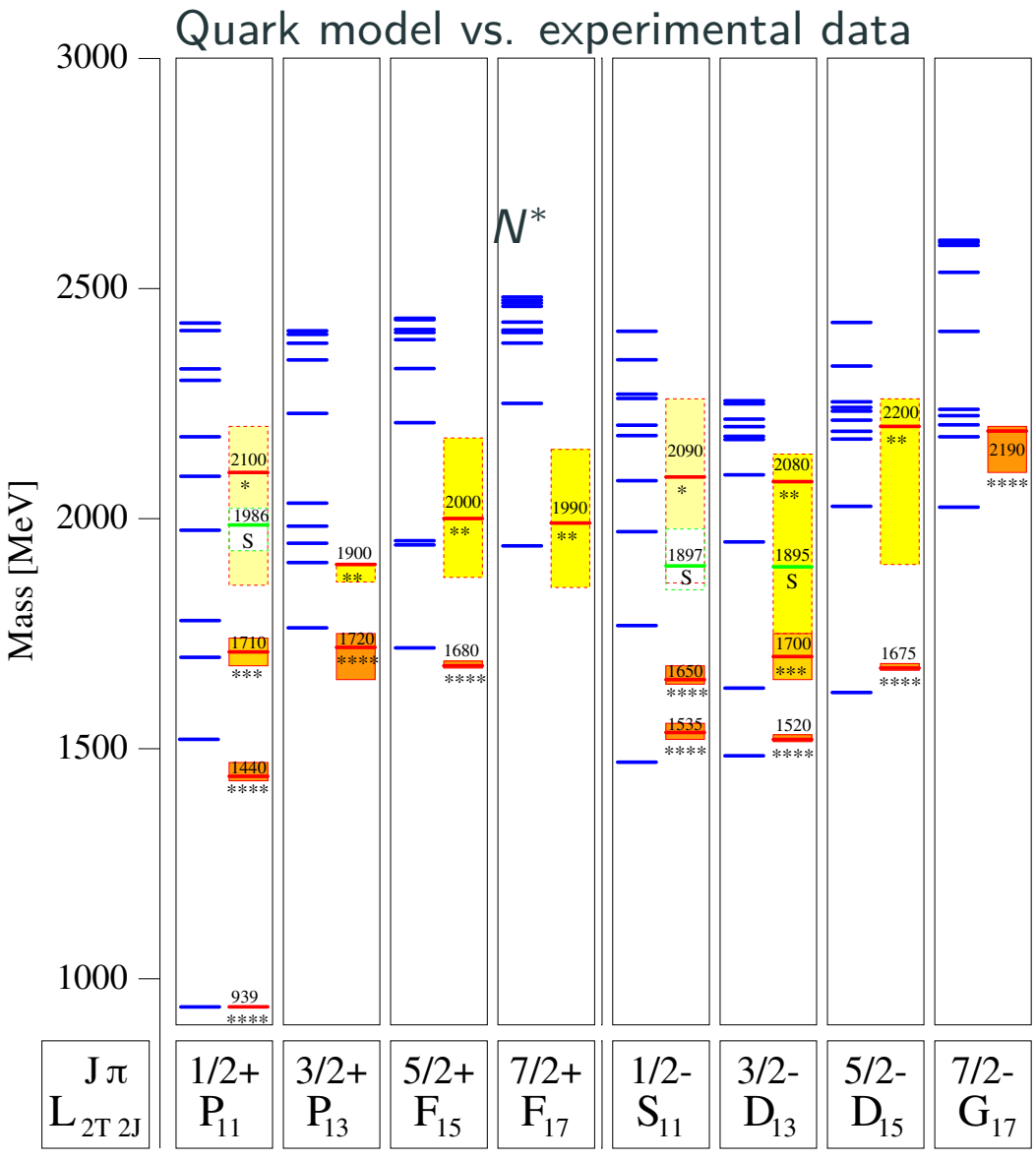

U. Loering, B.C. Metsch, H.R. Petry, EPJA 10 (2001) 395-446

Quark models:

- constituent quarks with defined rest masses
- confinement potential
- some residual interaction

Theoretical description of nucleon excitation spectra

Lattice QCD predictions

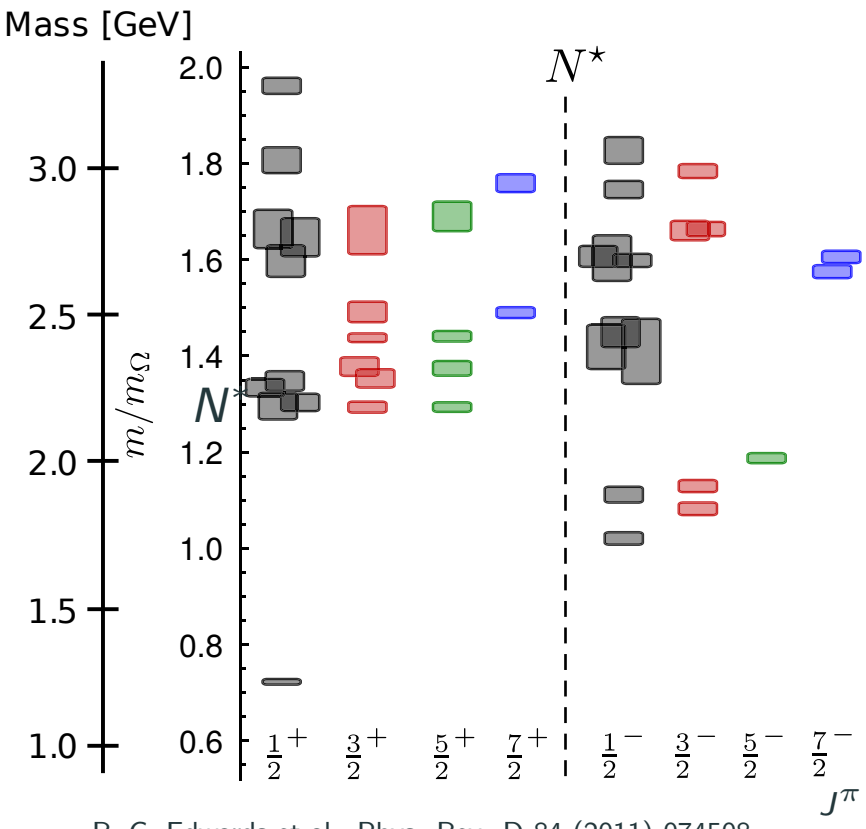

R. G. Edwards et al., Phys. Rev. D 84 (2011) 074508

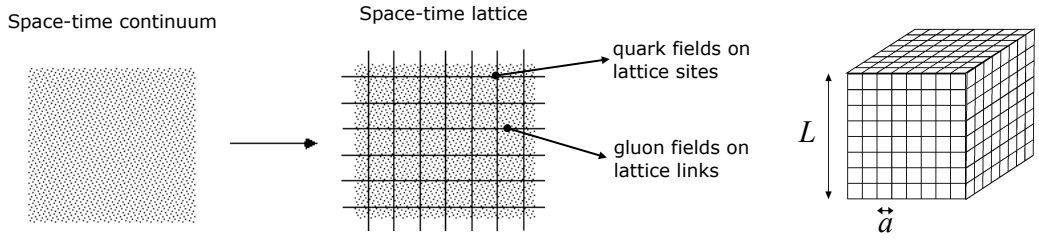

A. Ukawa

Lattice QCD:

- QCD Lagrangian is discretized
- numerical evaluation requires an enormous computational effort
- unphysical π^0 mass ($m_\pi \approx 396$ MeV)

Theoretical description of nucleon excitation spectra

UNIVERSITÄT BONN

Quark model vs. experimental data

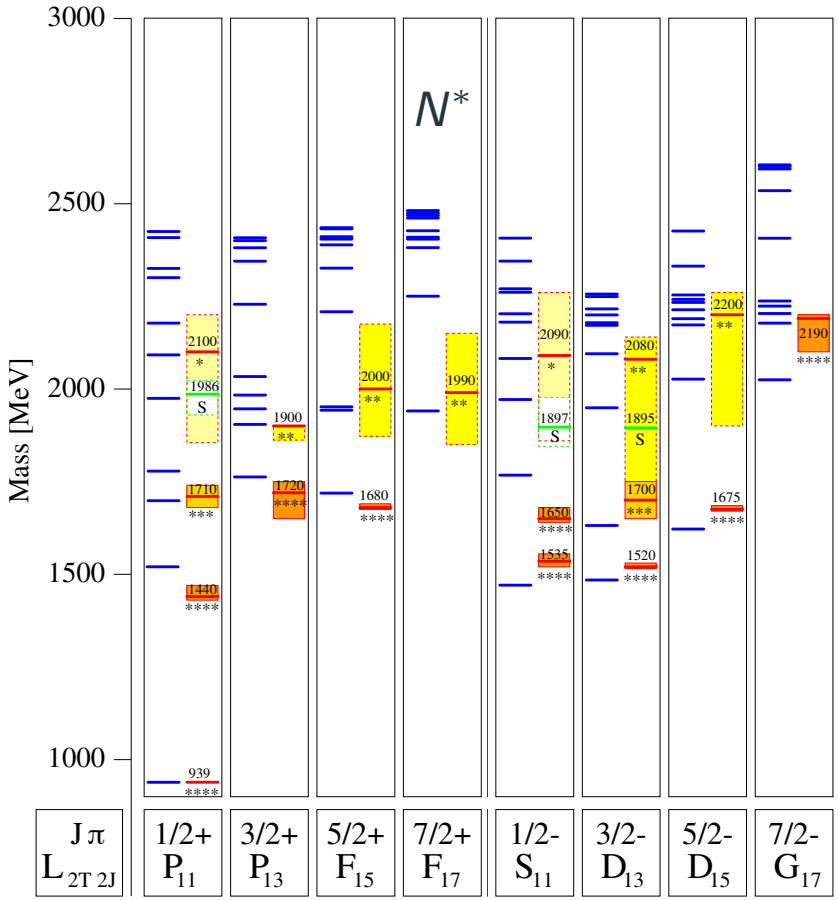

U. Loering, B.C. Metsch, H.R. Petry, EPJA 10 (2001) 395-446

Lattice QCD predictions

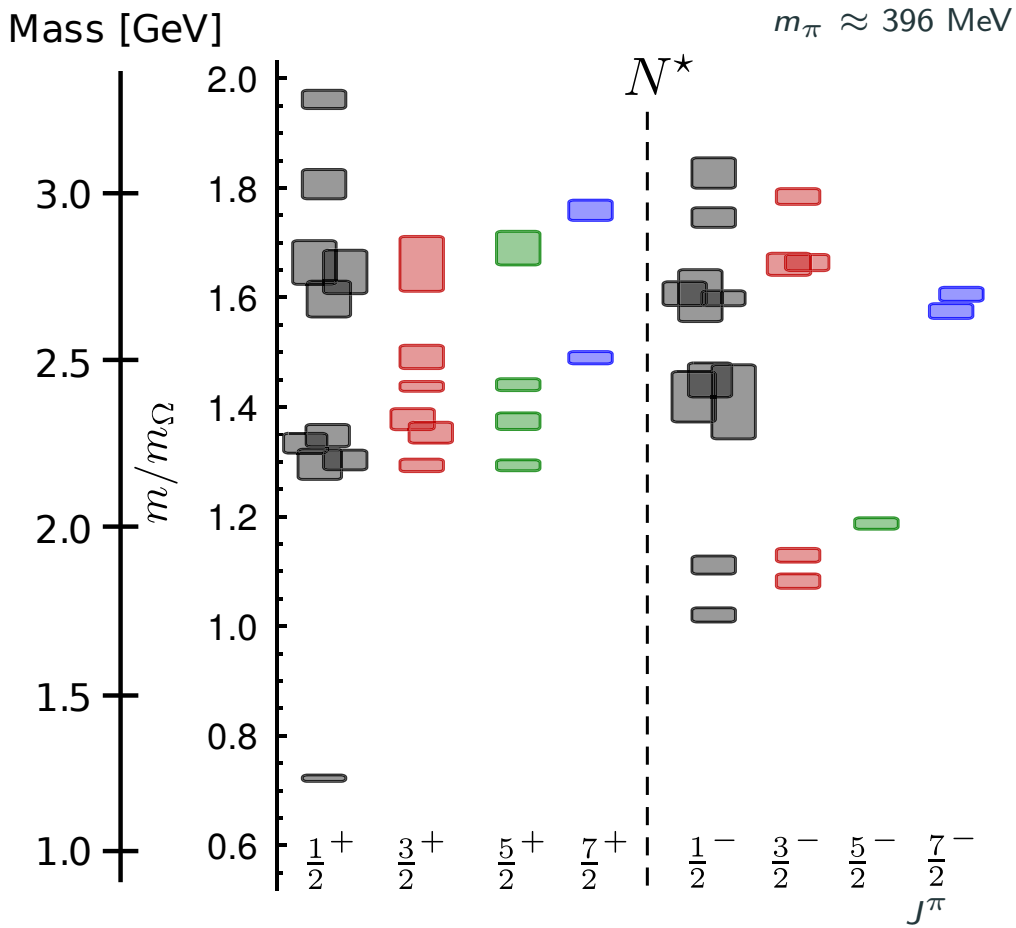

R. G. Edwards et al., Phys. Rev. D 84 (2011) 074508

- Discrepancy between theory and experiment: missing resonances, ordering of states

Theoretical description of nucleon excitation spectra

UNIVERSITÄT BONN

Quark model vs. experimental data

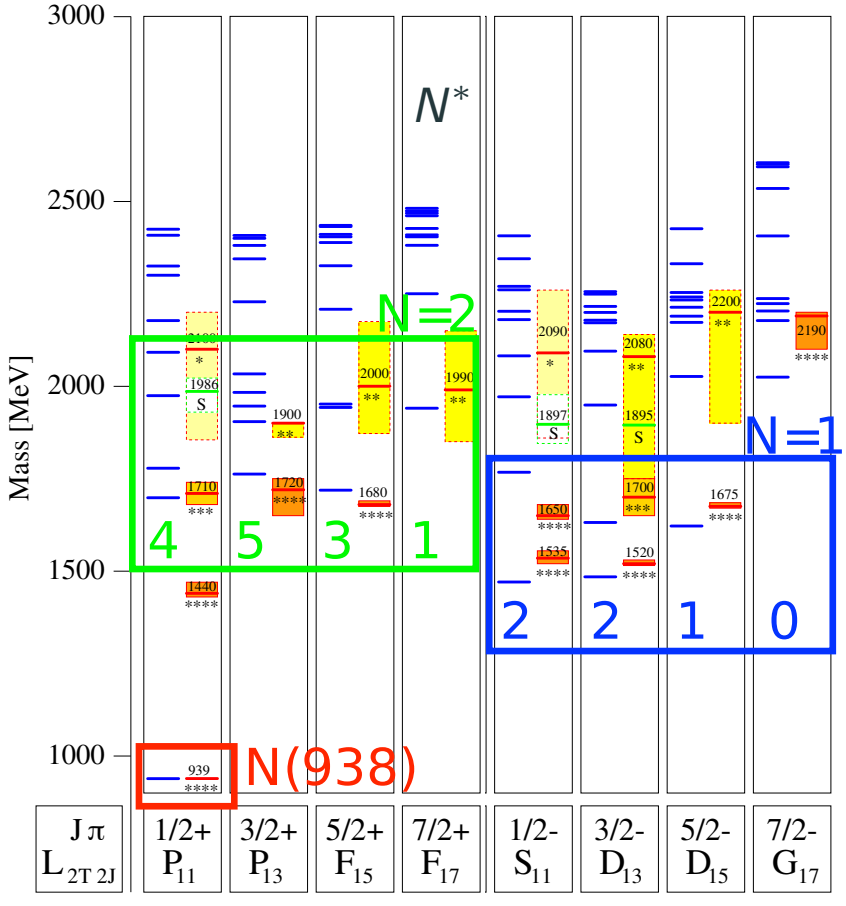

U. Loering, B.C. Metsch, H.R. Petry, Eur.Phys.J.A10:395-446,2001

Lattice QCD predictions

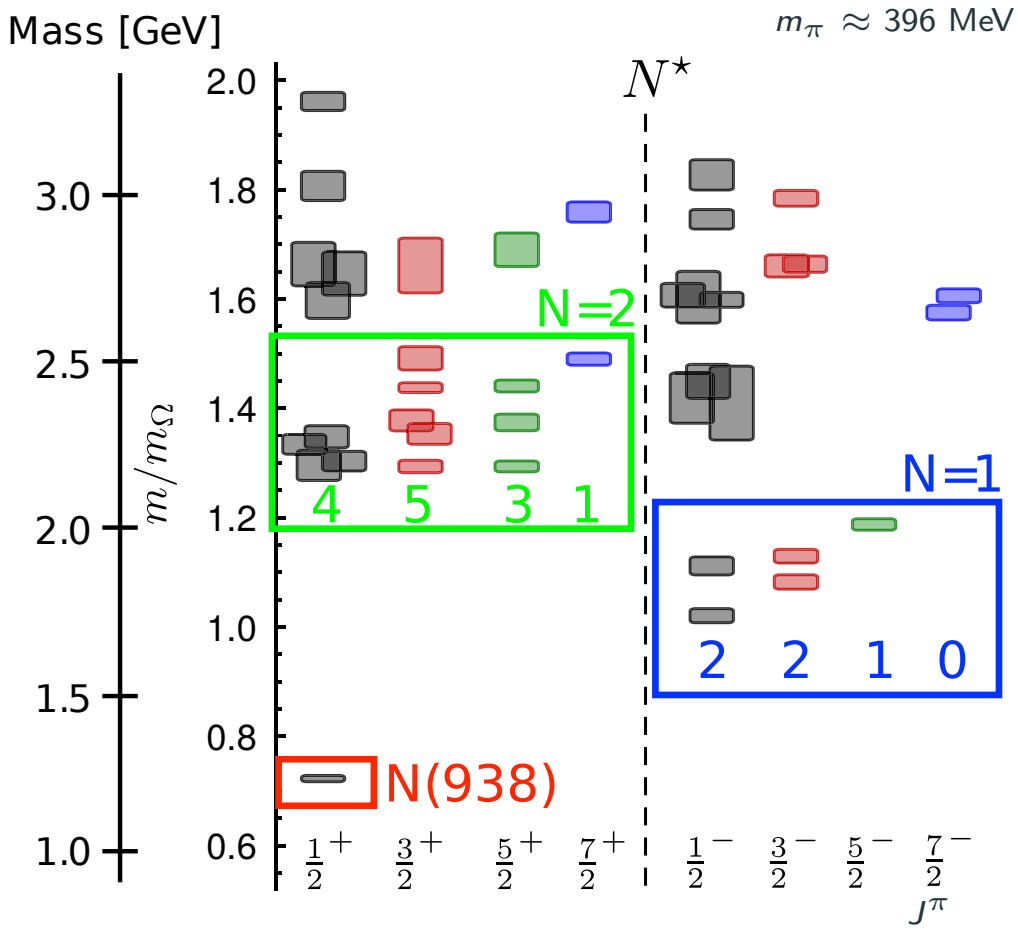

R. G. Edwards et al., Phys. Rev. D 84 (2011) 074508

- Discrepancy between theory and experiment: missing resonances, ordering of states
- most resonances observed in πN $\rightarrow$ experimental bias?

Photoproduction reactions

Study of different reaction channels gives access to different resonant structures

$\Rightarrow$ Worldwide effort to get high precision data (ELSA,MAMI, JLab, ...)

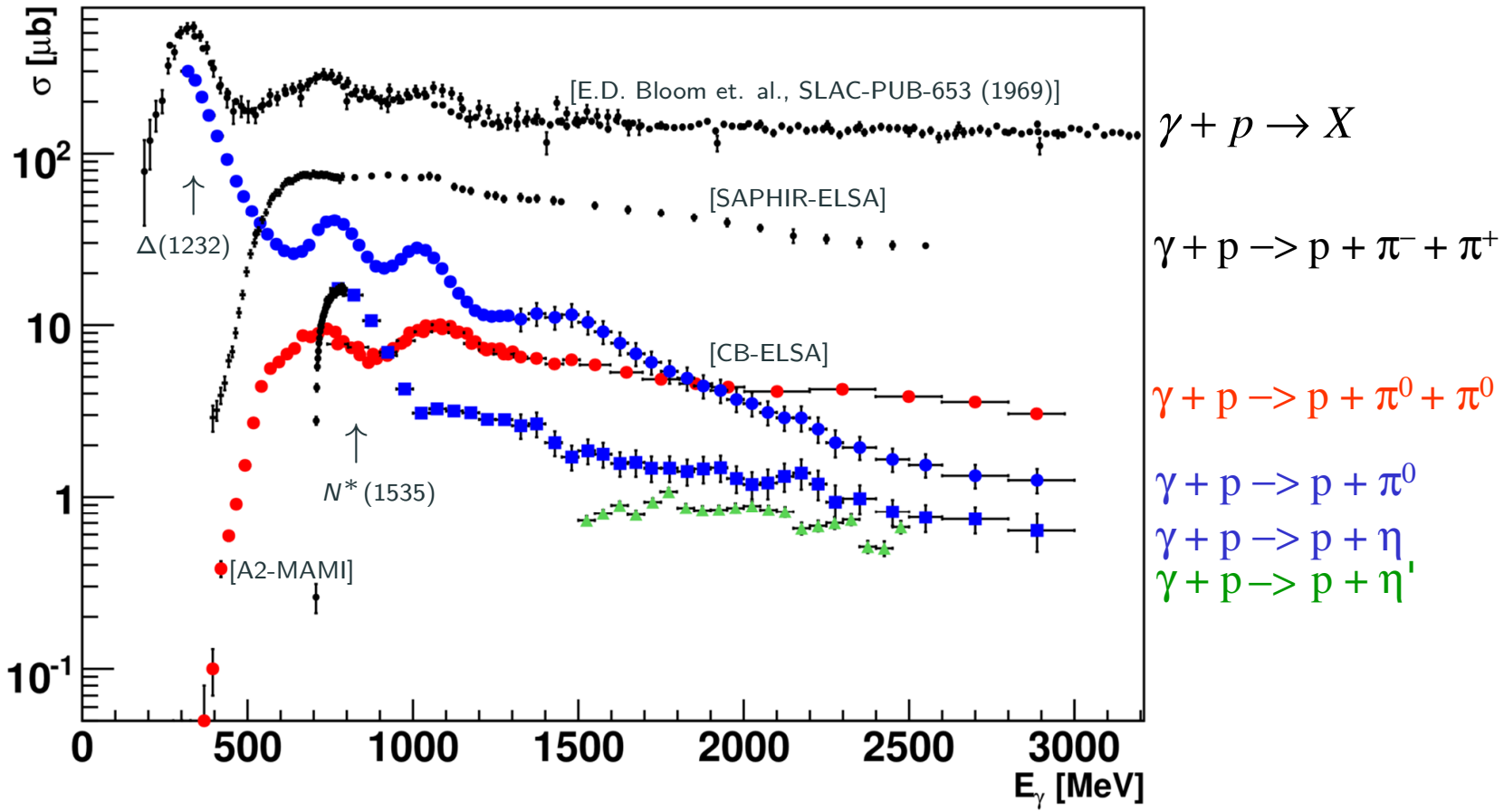

Photoproduction reactions are an excellent tool to probe nucleon excitation spectra!

Unpolarized cross section

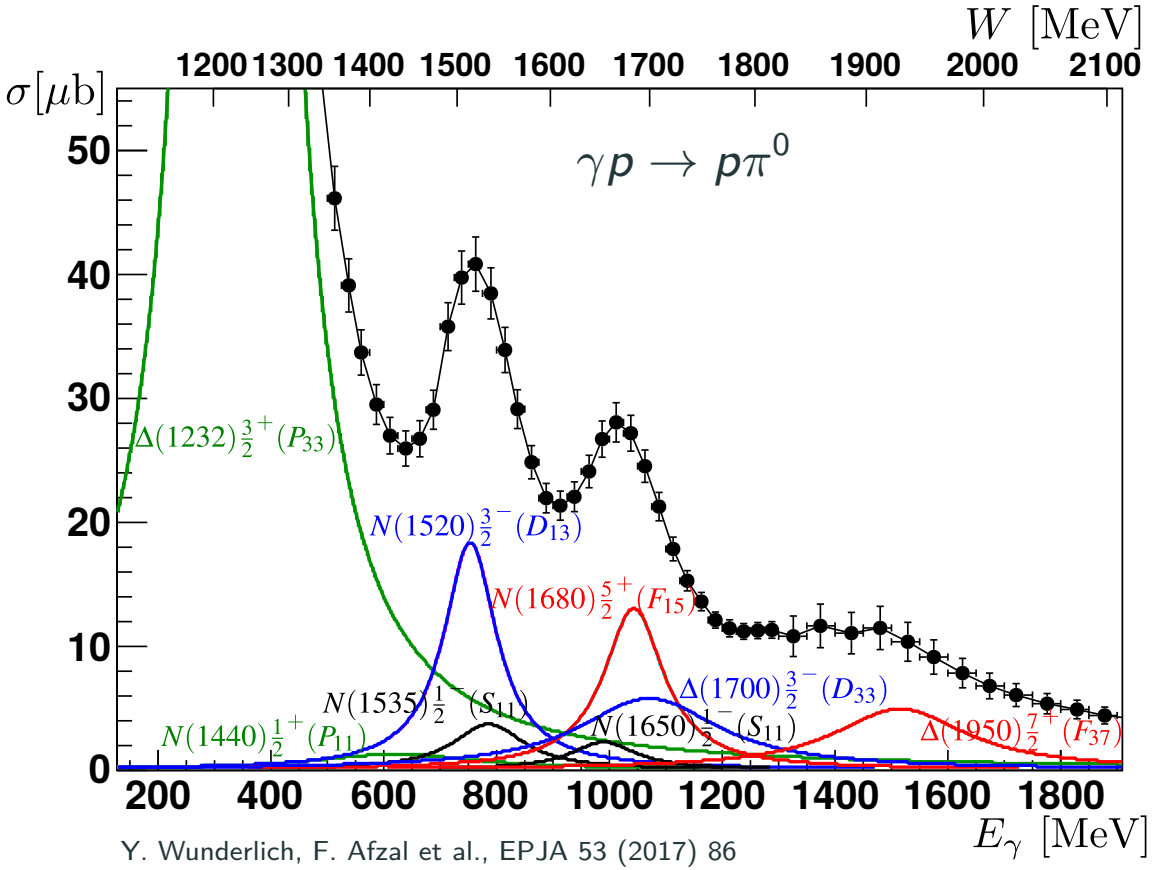

Y. Wunderlich, F. Afzal et al., EPJA 53 (2017) 86

Unpolarized cross section

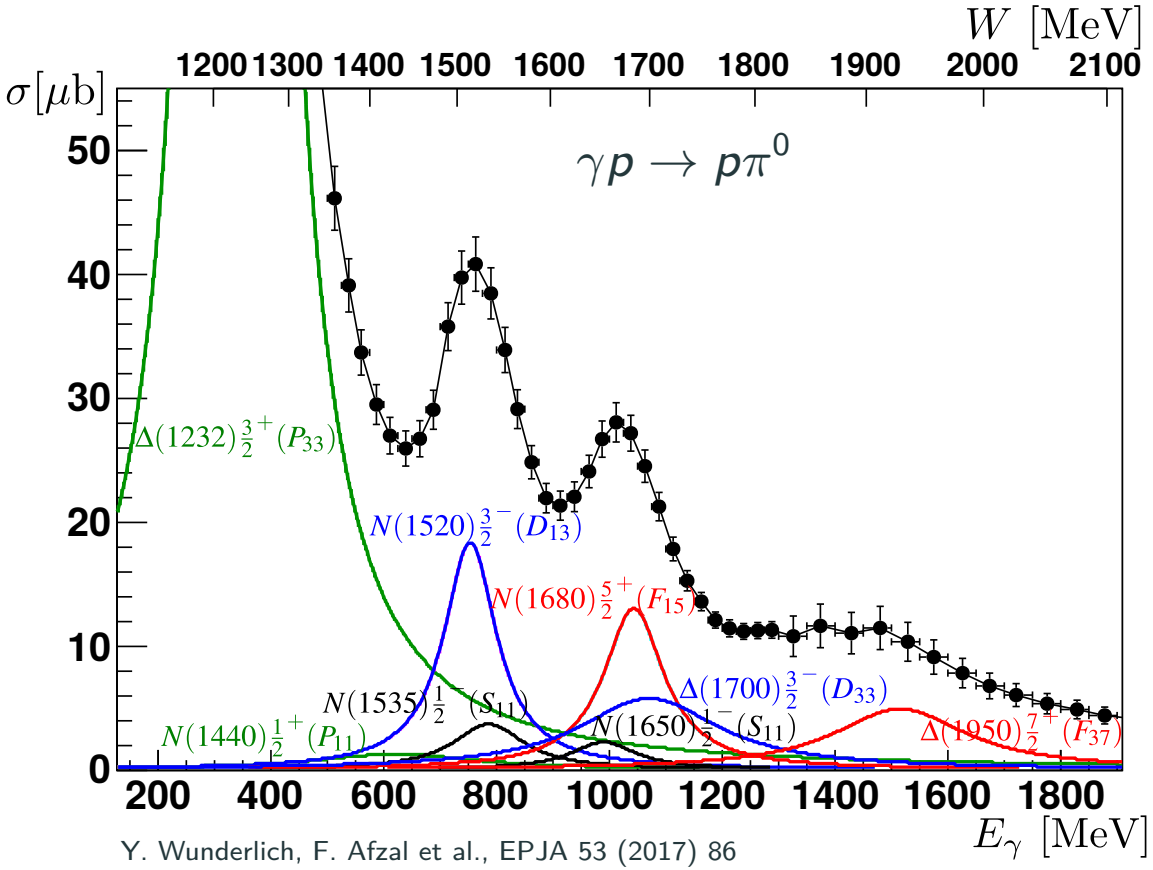

Y. Wunderlich, F. Afzal et al., EPJA 53 (2017) 86

$$\frac{d\sigma}{d\Omega}_0(W,\theta) \propto \sum_{\text{spins}} | < f|\mathcal{F}|i > |^2$$

Unpolarized cross section

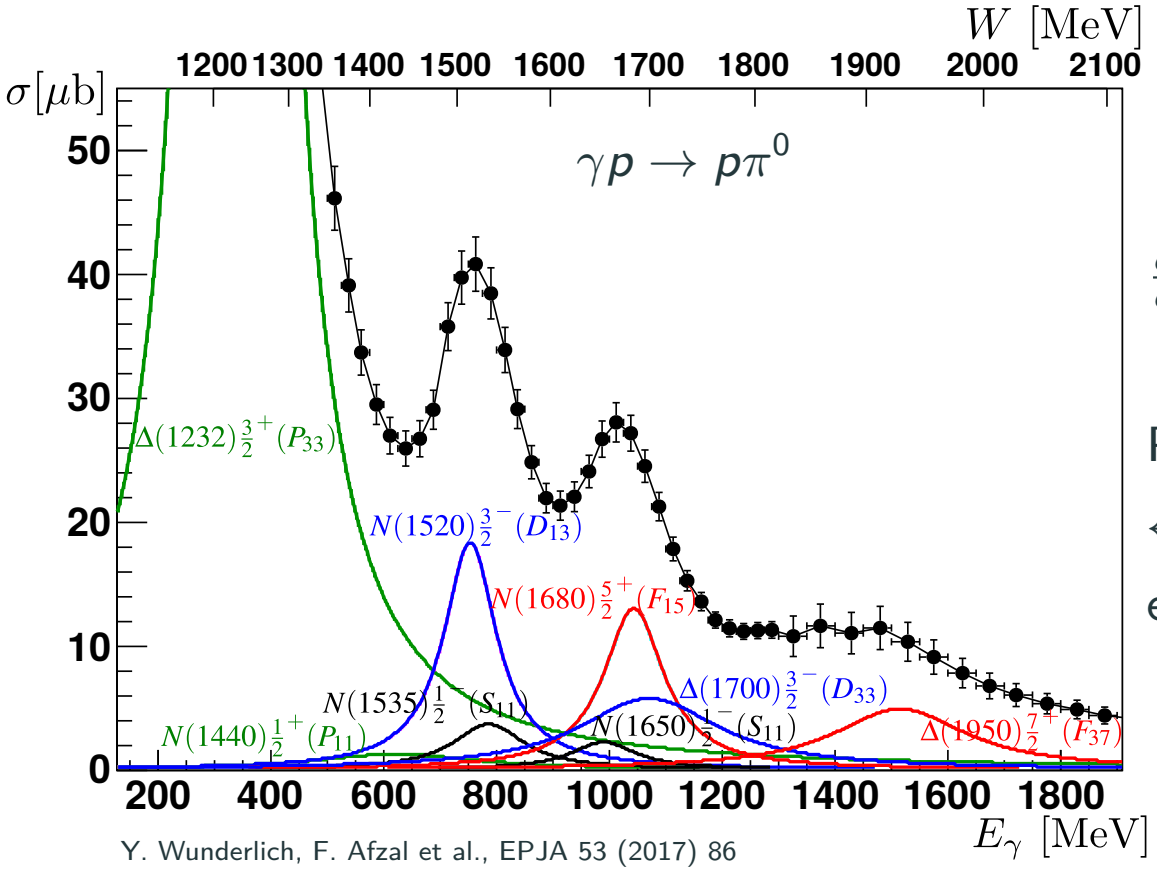

Y. Wunderlich, F. Afzal et al., EPJA 53 (2017) 86

$$\frac{d\sigma}{d\Omega}_0(W,\theta) \propto \sum_{\text{spins}} | < f|\mathcal{F}|i > |^2$$

Photoproduction amplitude $\mathcal{F}$

$\leftrightarrow$ 4 complex amplitudes

e.g. CGLN amplitudes: F_1, F_2, F_3, F_4

Unpolarized cross section

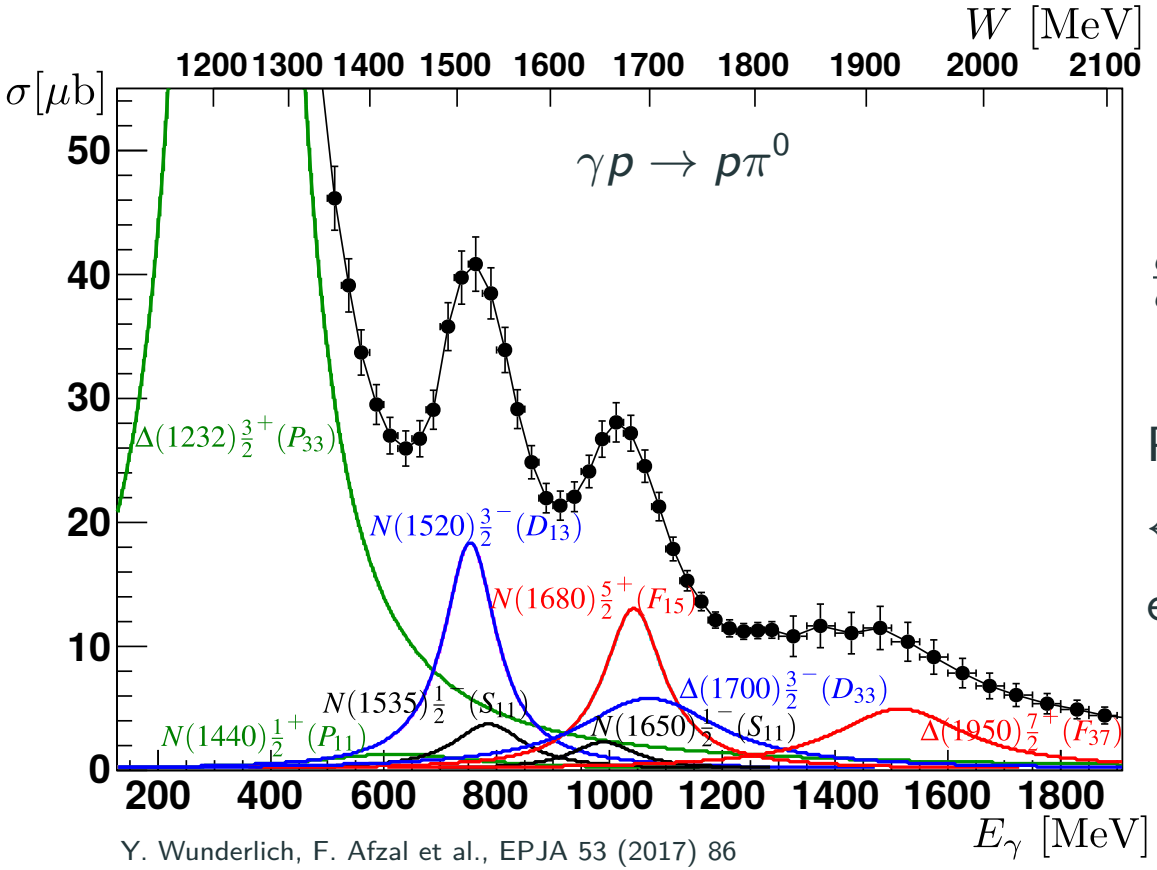

Y. Wunderlich, F. Afzal et al., EPJA 53 (2017) 86

$$\frac{d\sigma}{d\Omega}_0(W,\theta) \propto \sum_{\text{spins}} | < f|\mathcal{F}|i > |^2$$

Photoproduction amplitude $\mathcal{F}$

$\leftrightarrow$ 4 complex amplitudes

e.g. CGLN amplitudes: F_1, F_2, F_3, F_4

- PWA: $F_1 = \sum_{l=0}^{\infty}(lM_{l+} + E_{l+})P'_{l+1} + [(l+1)M_{l-} + E_{l-}]P'_{l-1}$
  - $E_{l\pm}(W), M_{l\pm}(W)$: Multipoles
  - $P'_{l\pm1}(\cos\theta_{cm})$: Legendre polynomials

Unpolarized cross section

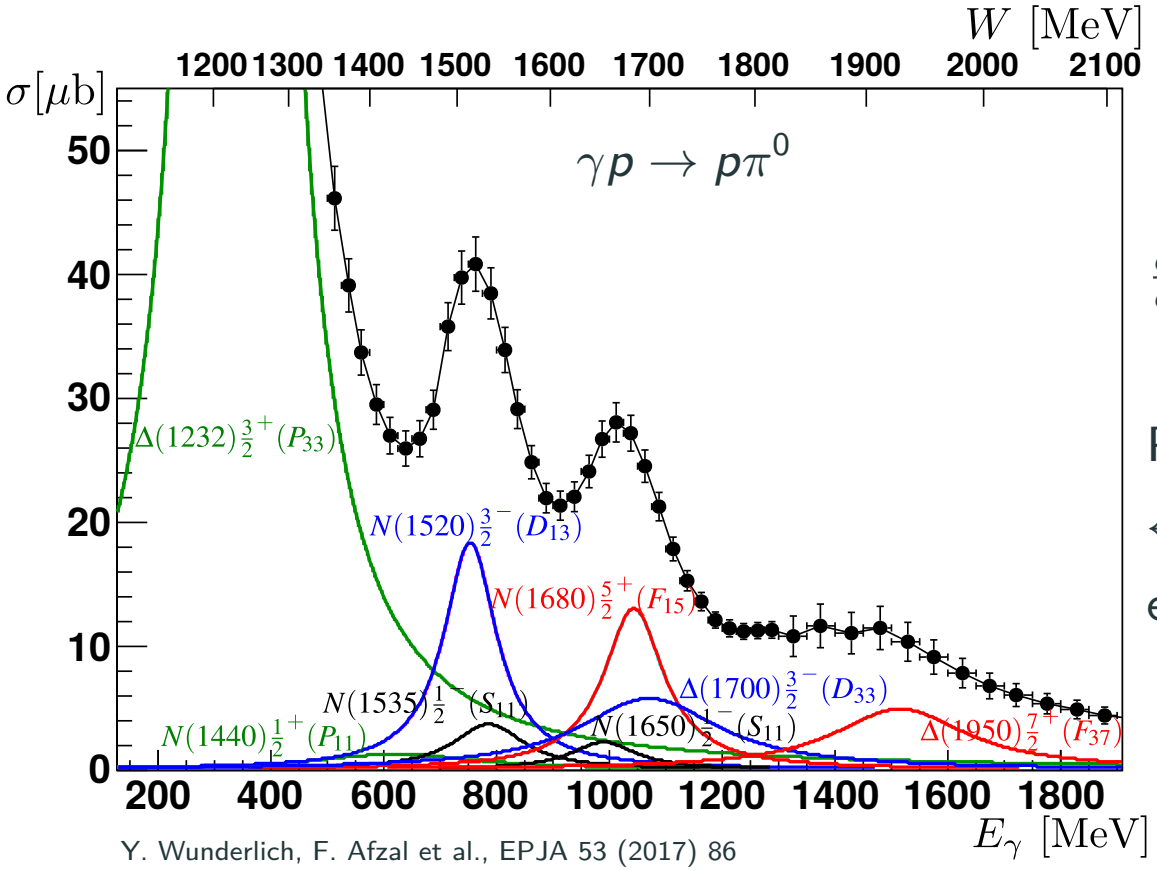

Y. Wunderlich, F. Afzal et al., EPJA 53 (2017) 86

$$\frac{d\sigma}{d\Omega}_0(W,\theta) \propto \sum_{\text{spins}} | < f|\mathcal{F}|i > |^2$$

Photoproduction amplitude $\mathcal{F}$

$\leftrightarrow$ 4 complex amplitudes

e.g. CGLN amplitudes: F_1, F_2, F_3, F_4

- PWA: $F_1 = \sum_{l=0}^{\infty}(lM_{l+} + E_{l+})P'_{l+1} + [(l+1)M_{l-} + E_{l-}]P'_{l-1}$
  - $E_{l\pm}(W), M_{l\pm}(W)$: Multipoles
  - $P'_{l\pm1}(\cos\theta_{cm})$: Legendre polynomials

- $\sigma \sim |E_{0+}|^2 + |E_{1+}|^2 + |M_{1+}|^2 + |M_{1-}|^2 + ...$
  $\to$ unpolarized total cross section is sensitive to dominant contributing resonances

Polarization observables

For a unique determination of the complex amplitudes:

Photon polarization		Target polarization	Recoil nucleon polarization	Target and recoil polarizations
		X Y $Z_{(beam)}$	X' Y' Z'	X' X' Z' Z' X Z X Z
unpolarized	σ	- T -	- P -	$T_{x'}$ $L_{x'}$ $T_{z'}$ $L_{z'}$
linear	-Σ	H (-P) -G	$O_{x'}$ (-T) $O_{z'}$	$(-L_{z'})$ $(T_{z'})$ $(L_{x'})$ $(-T_{x'})$
circular	-	F - -E	$C_{x'}$ - $C_{z'}$	- - - -

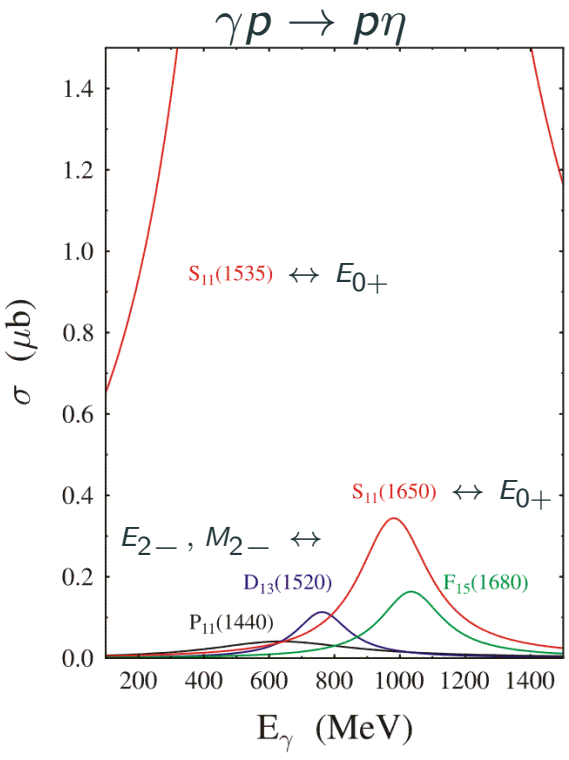

courtesy of L. Tiator

Polarization observables

For a unique determination of the complex amplitudes:

Photon polarization		Target polarization	Recoil nucleon polarization	Target and recoil polarizations
		X Y $Z_{(beam)}$	X' Y' Z'	X' X' Z' Z' X Z X Z
unpolarized	σ	- T -	- P -	$T_{x'}$ $L_{x'}$ $T_{z'}$ $L_{z'}$
linear	-Σ	H (-P) -G	$O_{x'}$ (-T) $O_{z'}$	$(-L_{z'})$ $(T_{z'})$ $(L_{x'})$ $(-T_{x'})$
circular	-	F - -E	$C_{x'}$ - $C_{z'}$	- - - -

$$\Sigma \sim \underbrace{-2E_{0+}^{*}E_{2+} + 2E_{0+}^{*}E_{2-} - 2E_{0+}^{*}M_{2+} + 2E_{0+}^{*}M_{2-}}_{< S, D >} + \ldots$$

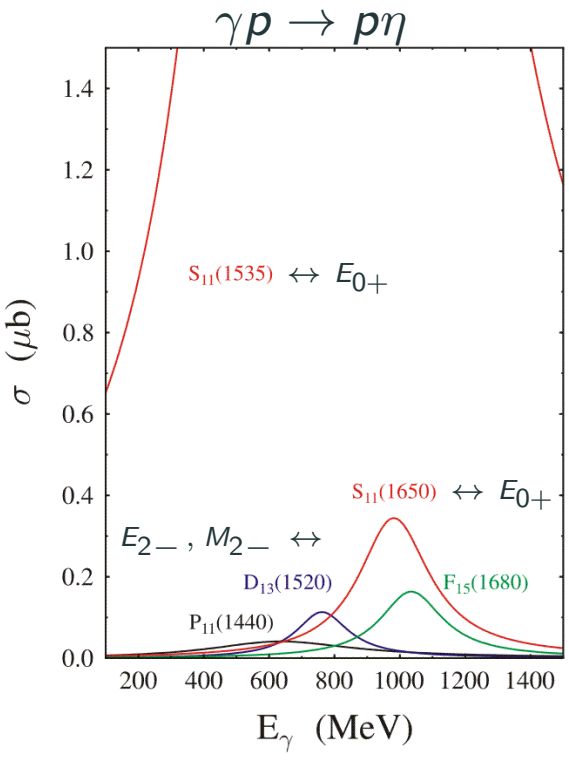

courtesy of L. Tiator

→Polarization observables are sensitive to interferences between dominant partial wave (*S*-wave, E_{0+} multipole) and smaller partial waves (*D*-waves, $E_{2\pm}, M_{2\pm}$ multipoles)!

Goal

Goal: Study nucleon resonances that couple to π^0/η

↓

Need to measure polarization observables

Photon polarization		Target polarization			Recoil nucleon polarization			Target and recoil polarizations			
		X	Y	$Z_{(beam)}$	X'	Y'	Z'	X' X	X' Z	Z' X	Z' Z
unpolarized	σ	-	T	-	-	P	-	$T_{x'}$	$L_{x'}$	$T_{z'}$	$L_{z'}$
linear	-Σ	H	(-P)	-G	$O_{x'}$	(-T)	$O_{z'}$	$(-L_{z'})$	$(T_{z'})$	$(L_{x'})$	$(-T_{x'})$
circular	-	F	-	-E	$C_{x'}$	-	$C_{z'}$	-	-	-	-

experiment in Mainz

Measurement of E (and G) at the A2 experiment

MAinz MIcrotron (MAMI)

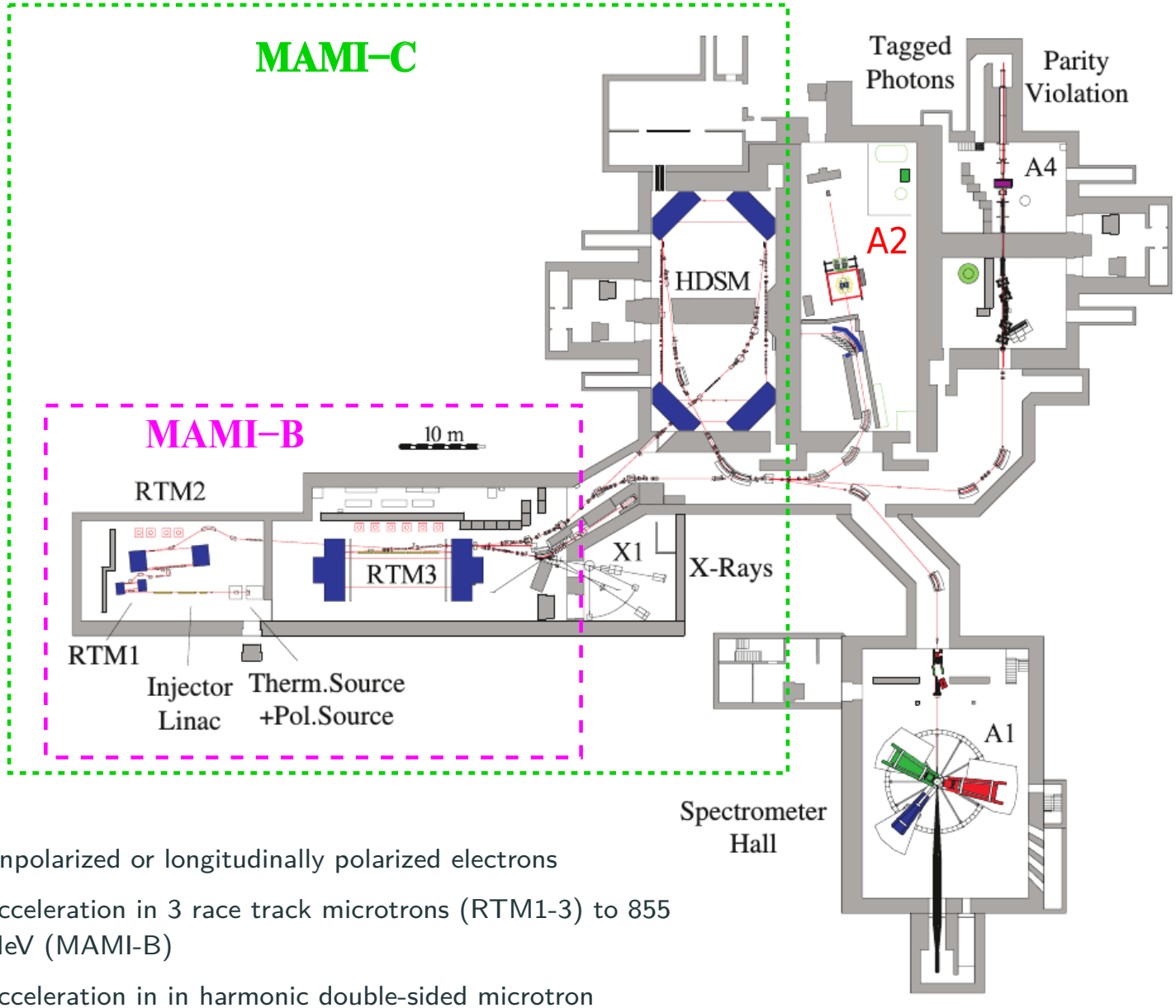

- Unpolarized or longitudinally polarized electrons
- Acceleration in 3 race track microtrons (RTM1-3) to 855 MeV (MAMI-B)
- Acceleration in in harmonic double-sided microtron (HDSM) to 1600 MeV (MAMI-C)

The A2 experiment at MAMI (Mainz)

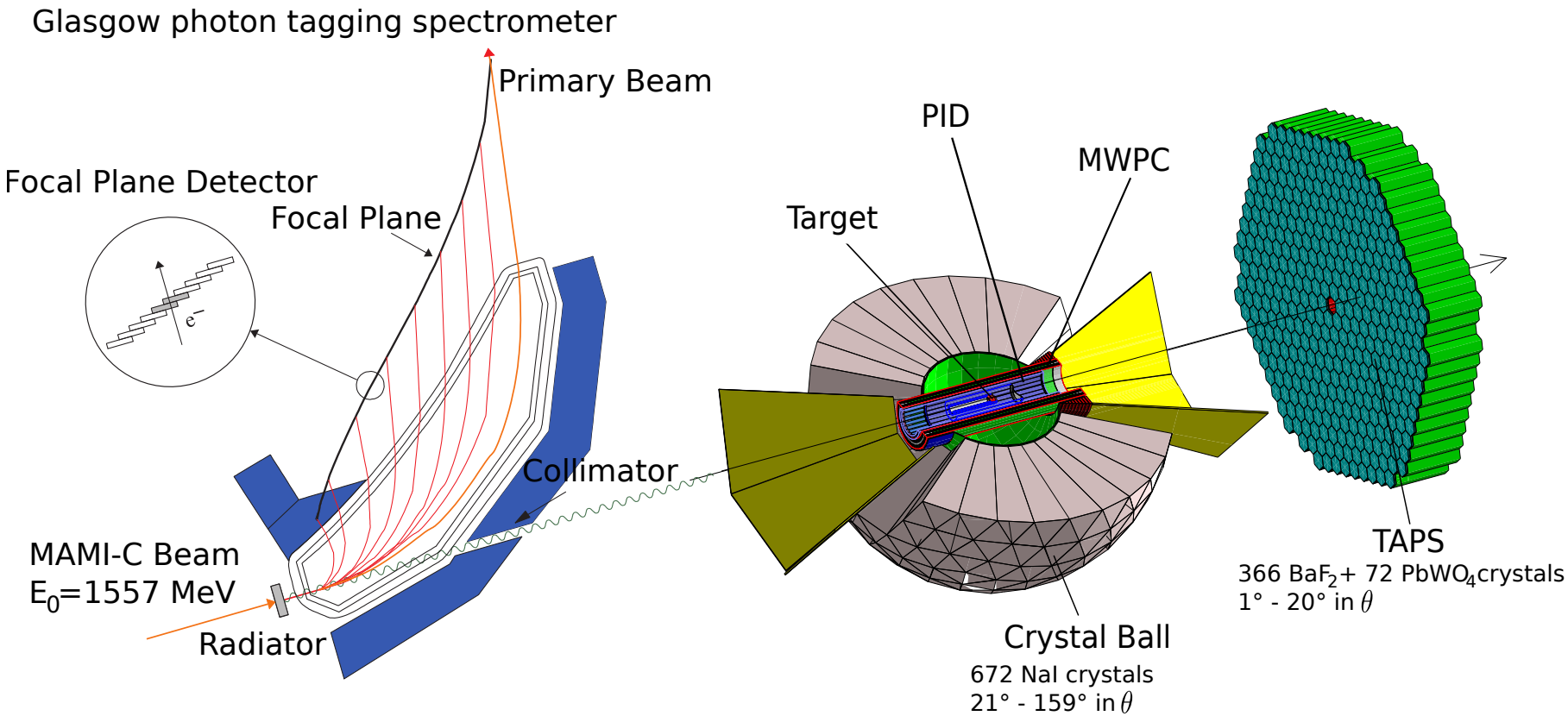

The A2 experiment at MAMI (Mainz)

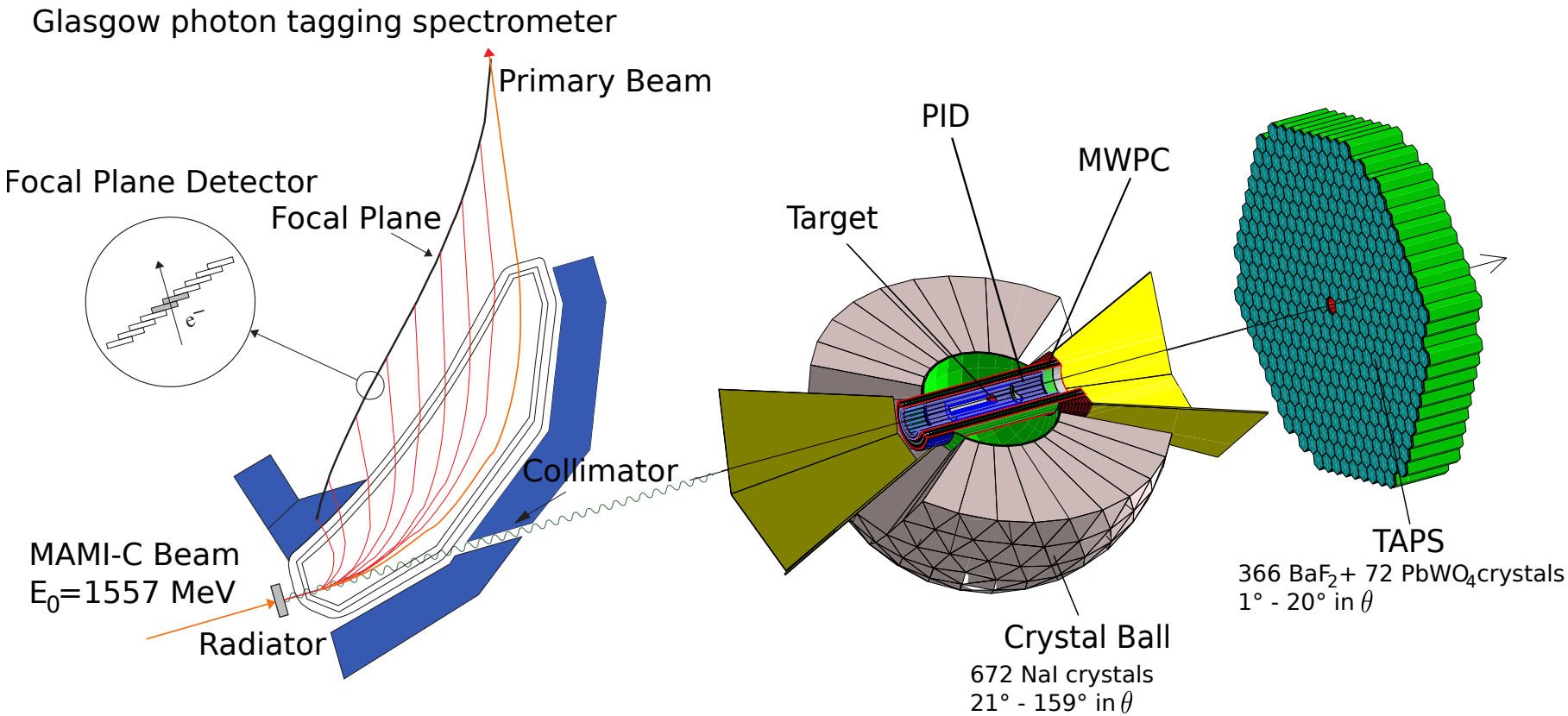

Ideally suited to identify charged and neutral final states!

Coherent and incoherent bremsstrahlung

incoherent bremsstrahlung

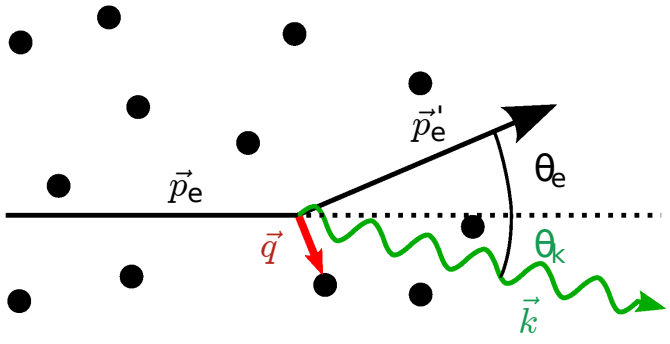

coherent bremsstrahlung

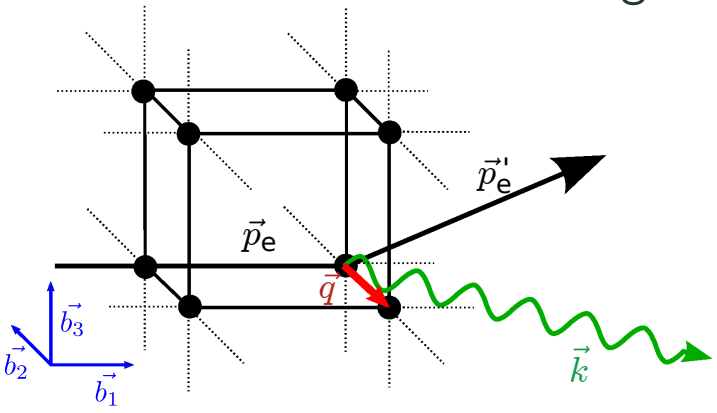

Coherent and incoherent bremsstrahlung

incoherent bremsstrahlung

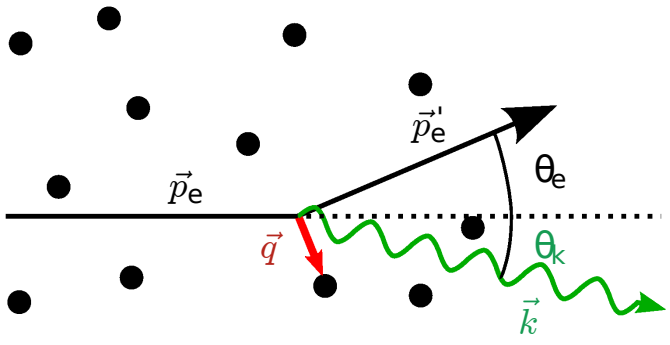

coherent bremsstrahlung

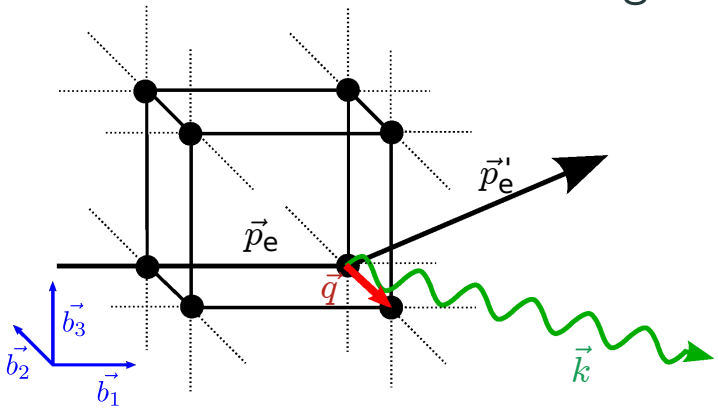

- coherent bremsstrahlung produced on diamond crystal
- Bragg: if $\vec{q} = n \cdot \vec{g} \rightarrow$ constructive interference

Coherent and incoherent bremsstrahlung

incoherent bremsstrahlung

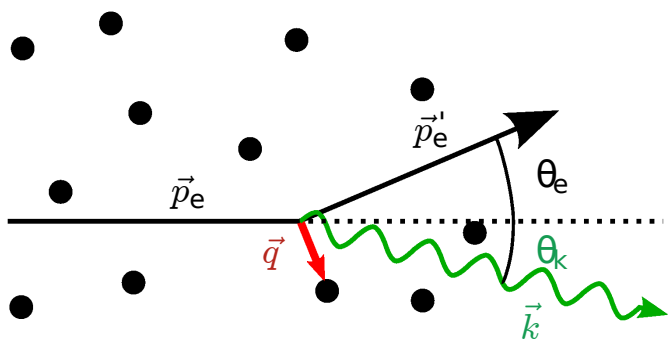

coherent bremsstrahlung

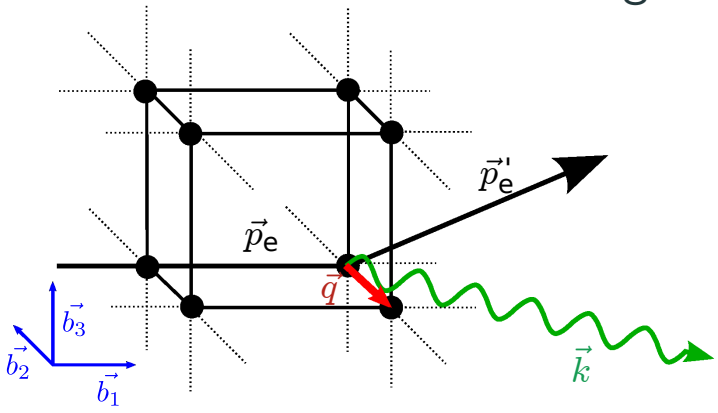

- coherent bremsstrahlung produced on diamond crystal
- Bragg: if $\vec{q} = n \cdot \vec{g} \rightarrow$ constructive interference

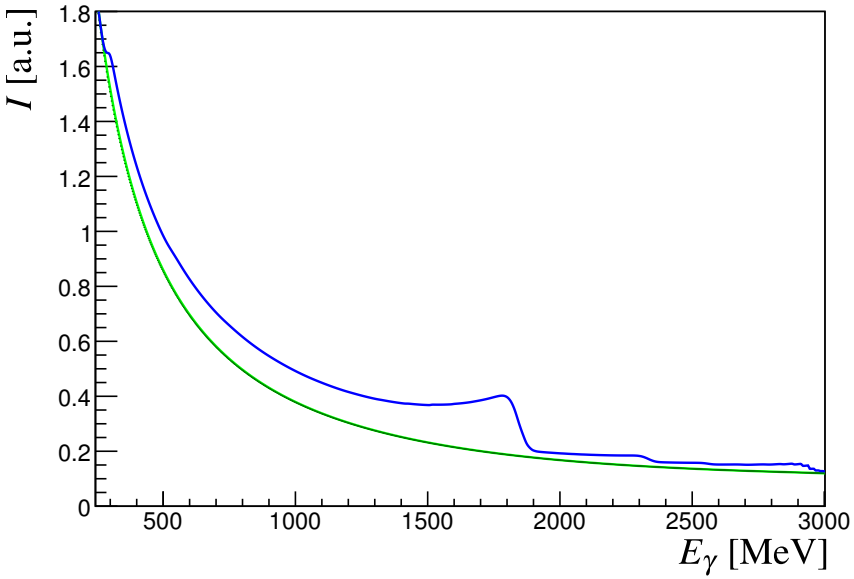

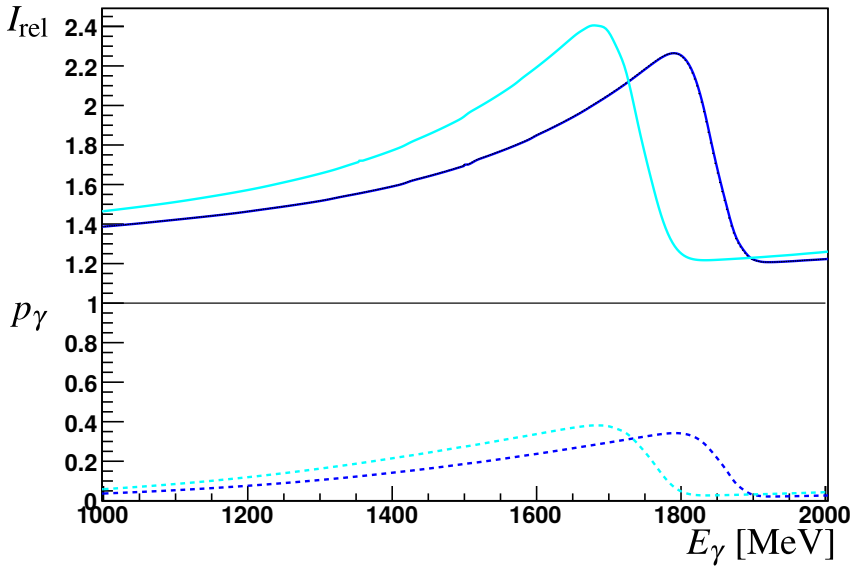

Elliptically polarized photons

- longitudinally pol. electrons + diamond radiator
  $\rightarrow$ elliptically polarized photons

- **First simultaneous measurement of *E* (circ. pol.) and *G* (lin. pol.)!**

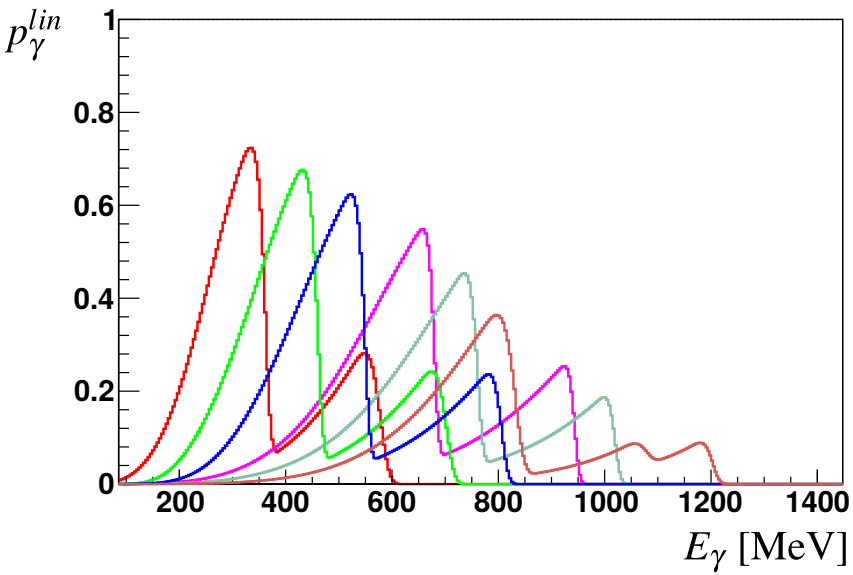

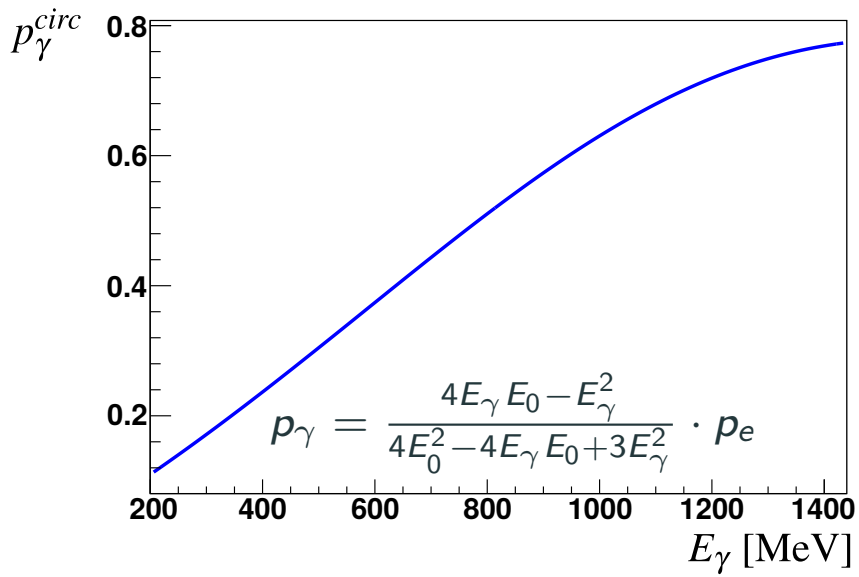

Dubna-Mainz frozen spin polarized target

- polarization via Dynamic Nuclear Polarization DNP
- 70 GHz microwave irradiation at 2.5 T is used to transfer the electrons polarization to protons
- ^{3}He/^{4}He dilution cryostat with 27 mK and holding coil field of 0.63 T

Butanol Target

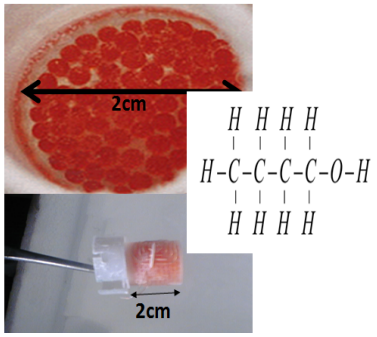

Carbon Target

Dubna-Mainz frozen spin polarized target

- polarization via Dynamic Nuclear Polarization DNP
- 70 GHz microwave irradiation at 2.5 T is used to transfer the electrons polarization to protons
- $^3He/^4He$ dilution cryostat with 27 mK and holding coil field of 0.63 T

Butanol Target

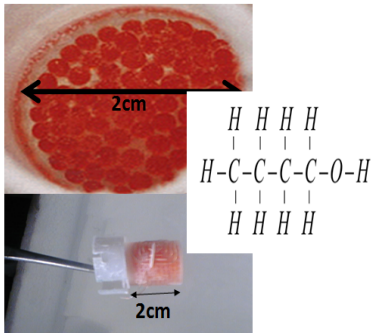

Carbon Target

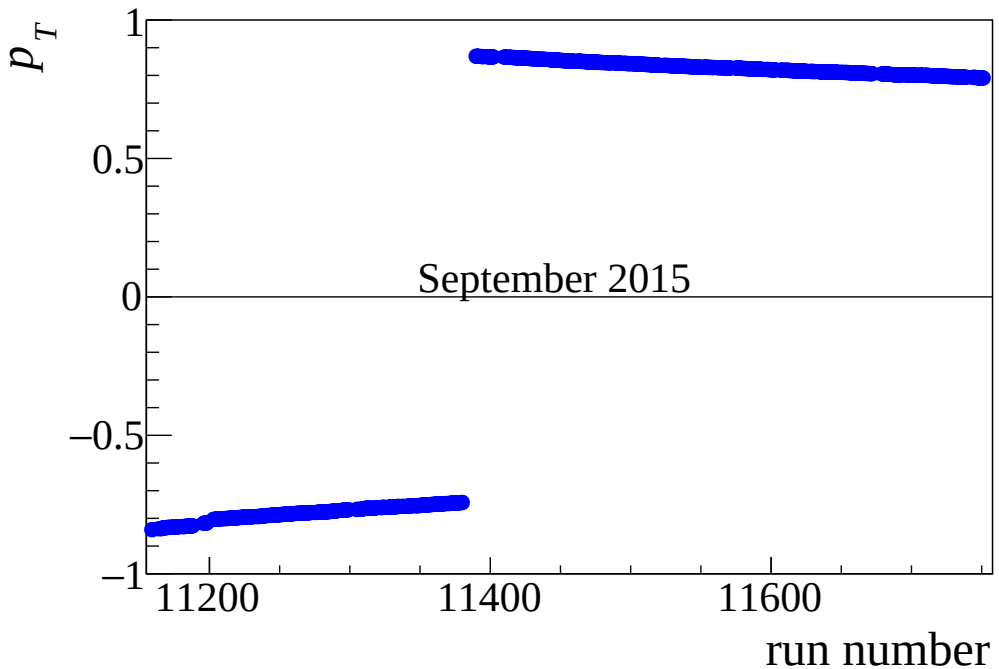

Event selection process

Time cut

Selected events had to fulfill the following constraints:

- at least 2 hits in calorimeters: $2\gamma + (p)$ (2 or 3 PED events)
- Beam photon: time coincidence with reaction products

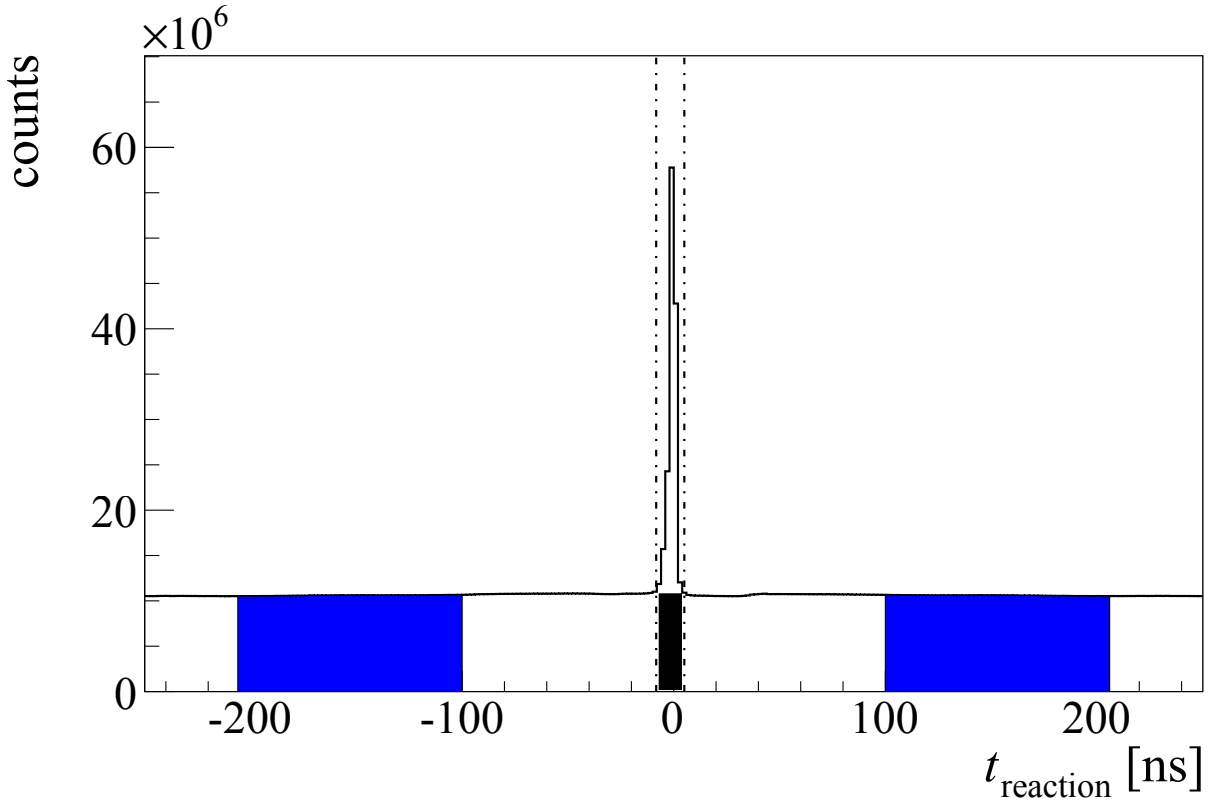

Kinematic cuts

Selected events had to fulfill the following constraints:

- at least 2 hits in calorimeters: $2\gamma + (p)$ (2 or 3 PED events)
- no charge information
- Proton: calculated as missing particle of $\gamma p \rightarrow \gamma\gamma X$
- Angular-cuts (if p is detected):
  - Coplanarity-cut: $\Delta\phi = |\phi_{meson} - \phi_p| = 180°$ within 2σ
  - Agreement of missing particle and measured charged particle in polar angle θ

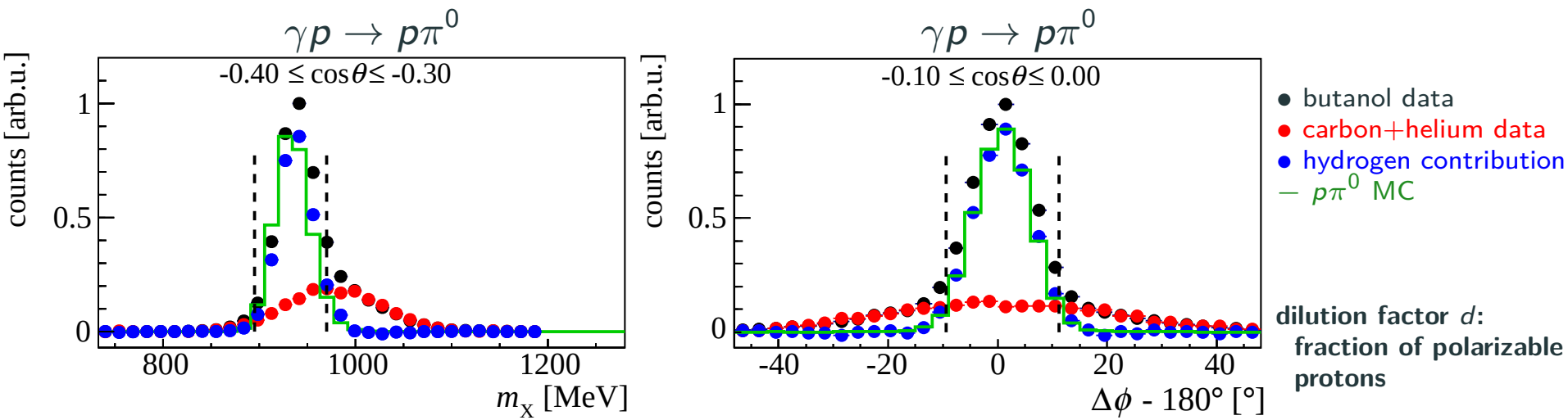

PSA cut

$\gamma p \to p\pi^0$

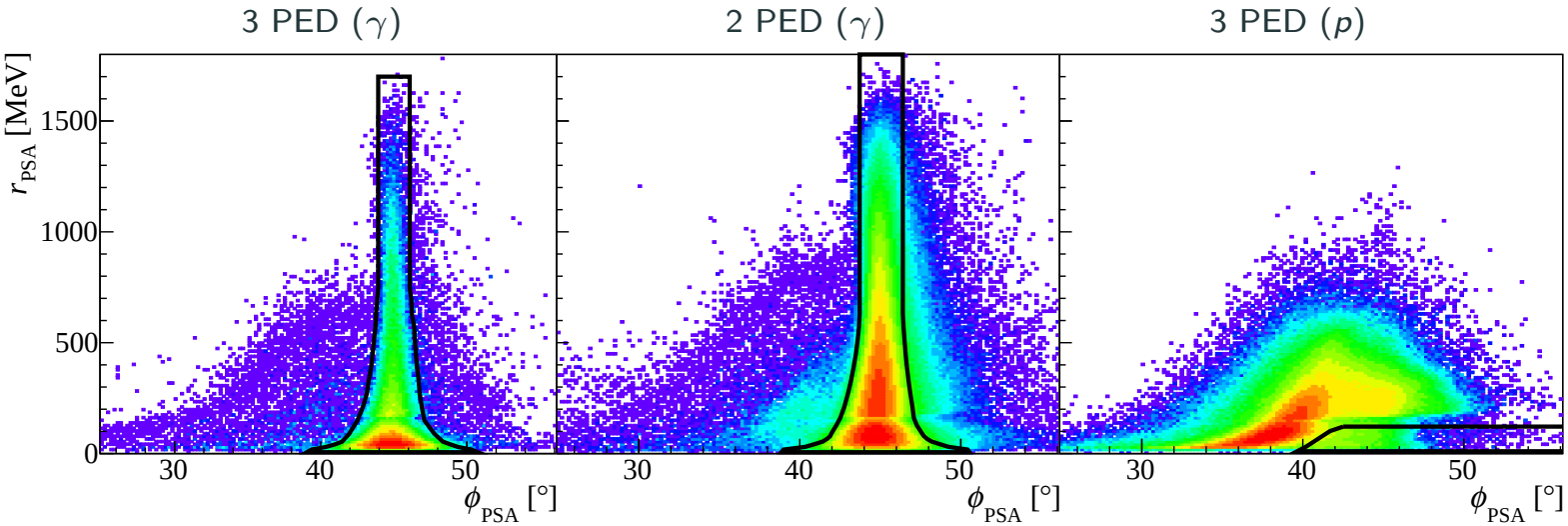

$\gamma p \to p\eta$

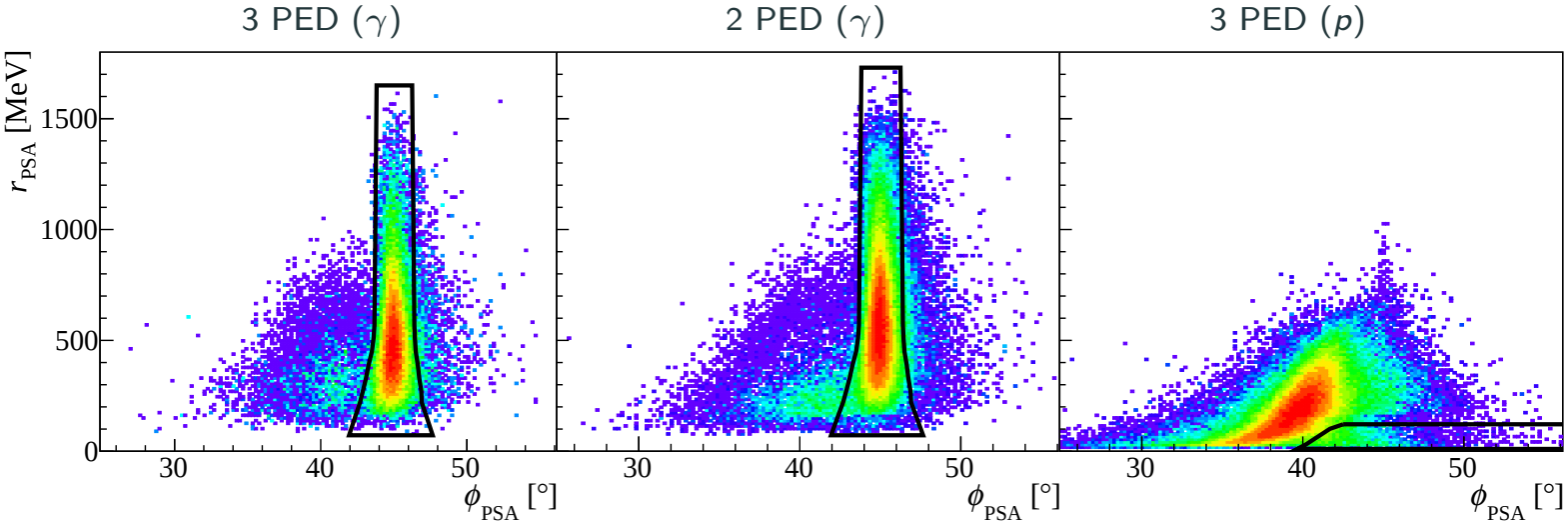

$$\phi_{\mathrm{PSA}} = \arctan \frac{E_S}{E_L}$$

$$r_{\mathrm{PSA}} = \sqrt{E_S^2 + E_L^2}$$

$\Delta E - E$ spectra (check for charged particles)

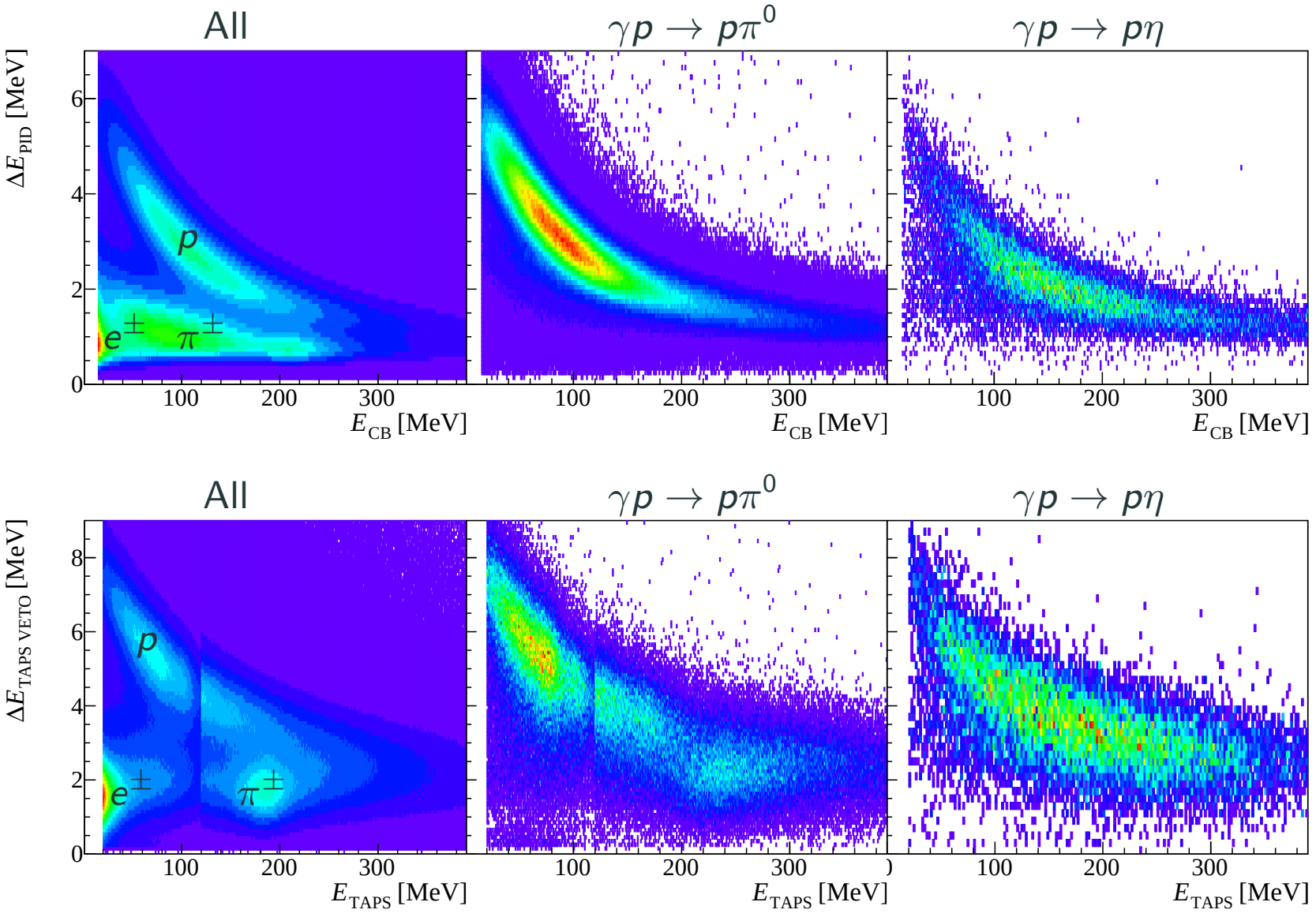

Impact of selection cuts

Selected events had to fulfill kinematic constraints:

- at least 2 hits in calorimeters ($2\gamma + (p)$)
- Invariant mass $m_{\gamma\gamma}$: 2σ cut around π^0/η mass

3 PED

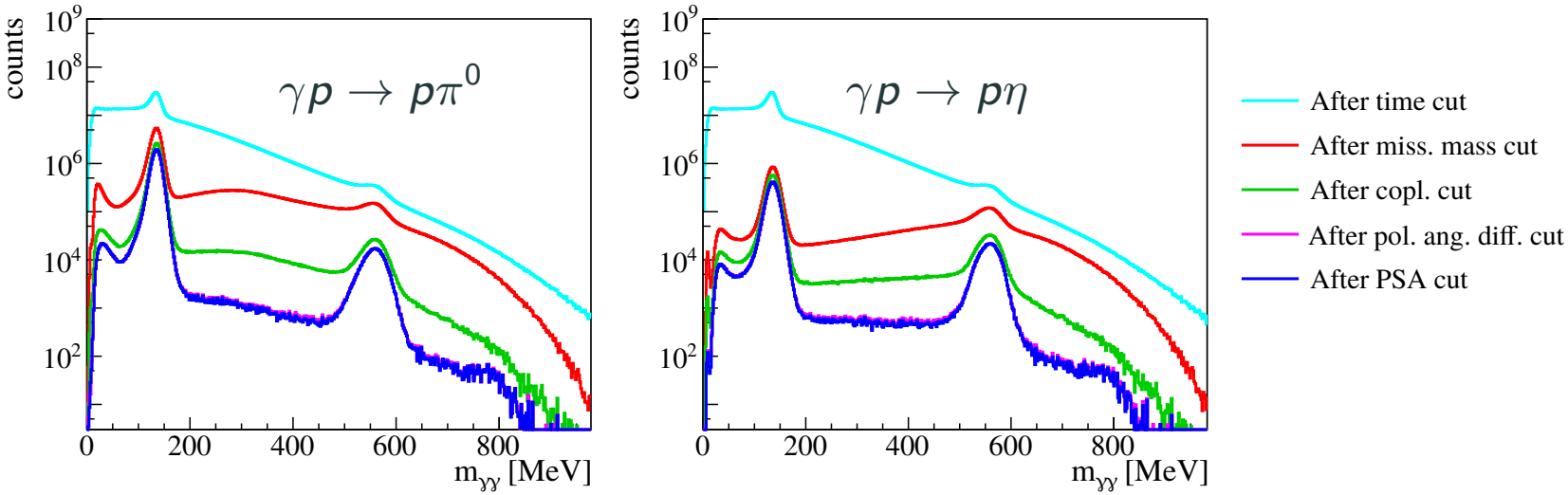

- low background: $\leq 2\%$ ($p\pi^0$) and $\leq 6\%$ ($p\eta$)

Determination of E

Determination of E

Differential cross section for pseudo-scalar meson photoproduction using elliptically polarized photons and longitudinally polarized target:

$$\frac{d\sigma}{d\Omega}(\theta,\phi) = \frac{d\sigma}{d\Omega}_0(\theta)\Big[1 - P_{lin}\mathbf{\Sigma}\cos(2(\alpha-\phi)) - P_z\Big(-P_{lin}\mathbf{G}\sin(2(\alpha-\phi)) + P_{circ}\mathbf{E}\Big)\Big]$$

Integrating over ϕ:

$$N_B\Big|_{\pm 1}^{\pm P_z}(\theta) = N_B(\theta)\cdot\Big[1 - dP_{circ}P_z\mathbf{E}\Big]$$

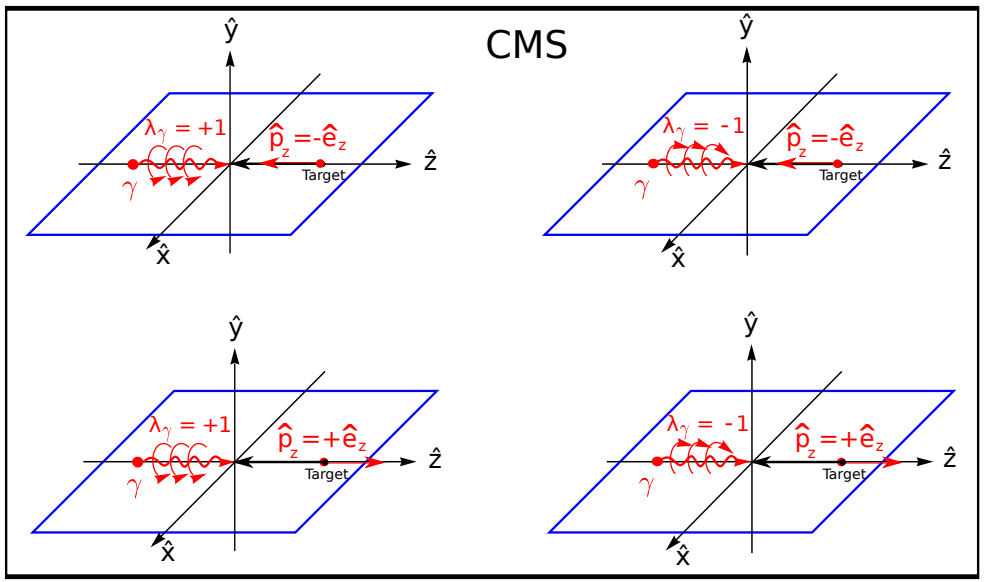

$$\mathrm{E} = \frac{\sigma^{1/2} - \sigma^{3/2}}{\sigma^{1/2} + \sigma^{3/2}} = \frac{N_B^{1/2} - N_B^{3/2}}{N_B^{1/2} + N_B^{3/2}} \cdot \frac{1}{d} \cdot \frac{1}{P_{circ}P_z}$$

Dilution factor

- Need to study the unpolarized background in butanol target (carbon, helium)
- Scale carbon+helium data to butanol data

$$s^C \cdot N^C_{\text{non-hydrogen region}} = N^{\text{but}}_{\text{non-hydrogen region}}$$

$$s^C = \frac{N^{\text{but}}_{\text{non-hydrogen region}}}{N^C_{\text{non-hydrogen region}}}$$

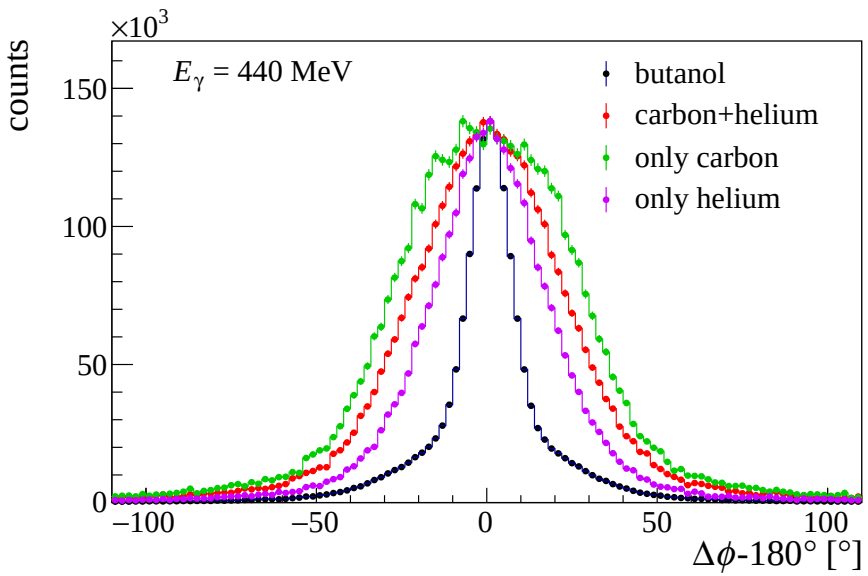

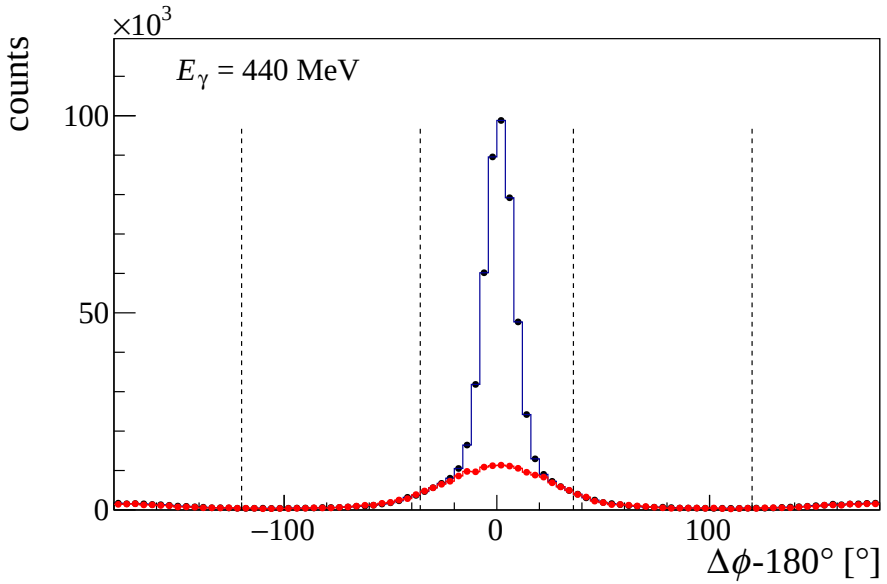

Comparison of diamond and amorphous data

- diamond runs with coherent edge at 450 MeV (elliptically polarized photons)
- Møller runs (amorphous radiator with circularly polarized photons)

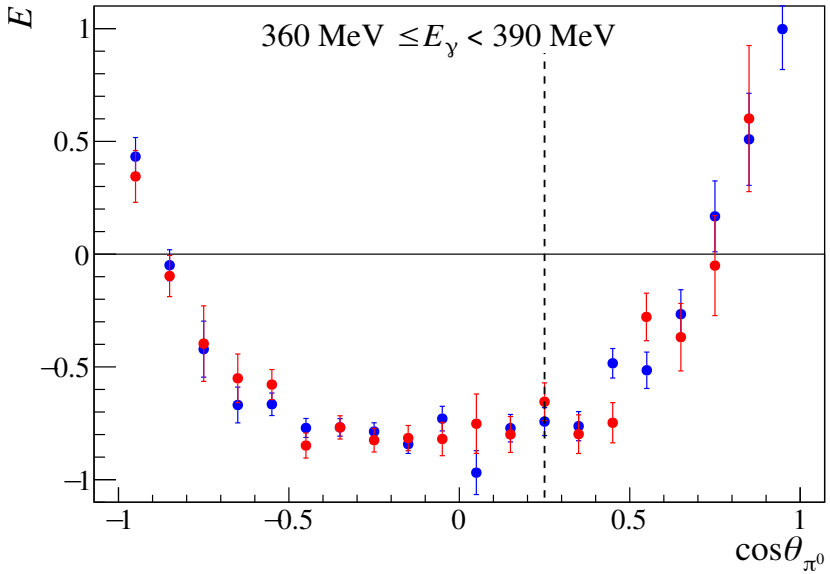

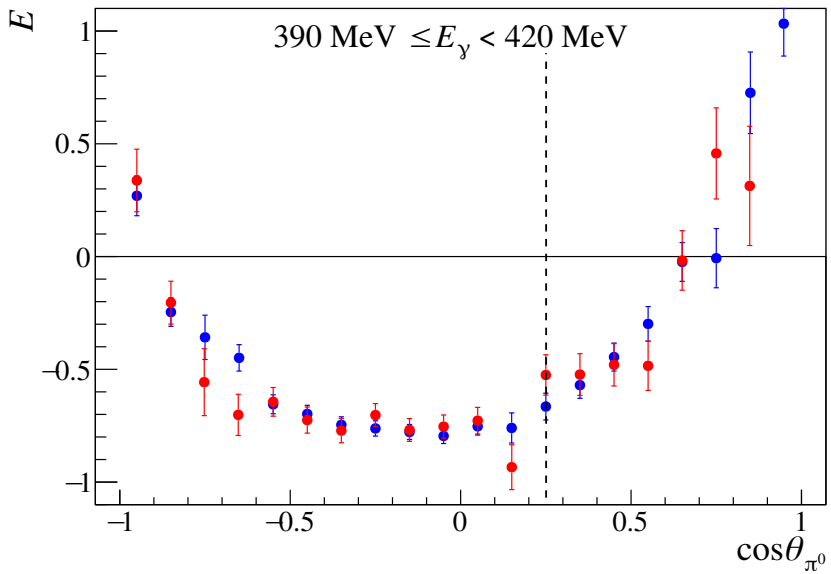

- first experimental evidence that the degree of circular polarization can be calculated in the same way for a diamond radiator as it is done for an amorphous radiator in a first approximation within 3%
- E and G can be determined using longitudinally polarized electrons and a diamond radiator

The helicity asymmetry E in π^0 photoproduction

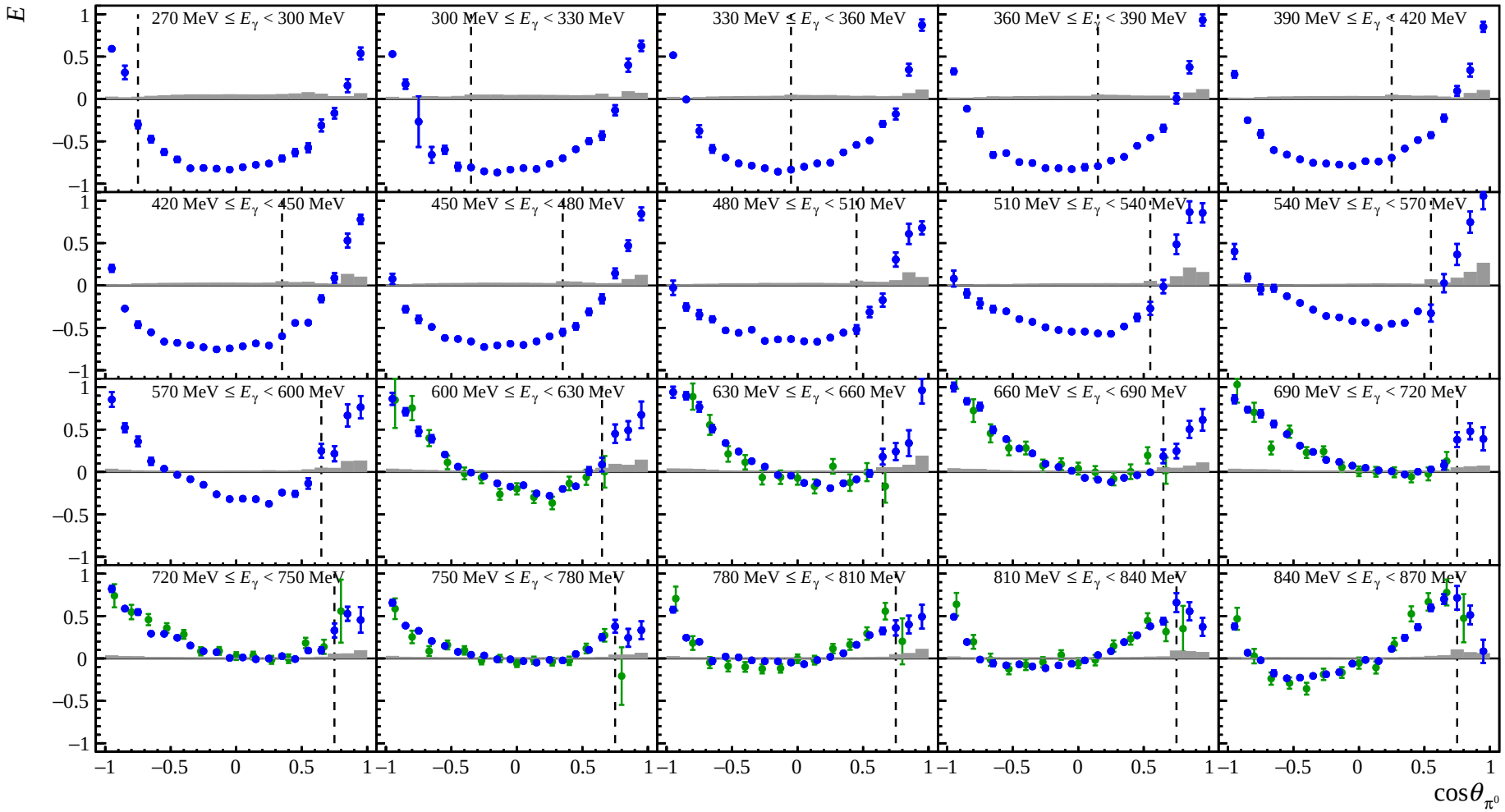

- A2 data (this work)
- CBELSA/TAPS data (M. Gottschall et al., , 2013)

The helicity asymmetry E in π^0 photoproduction

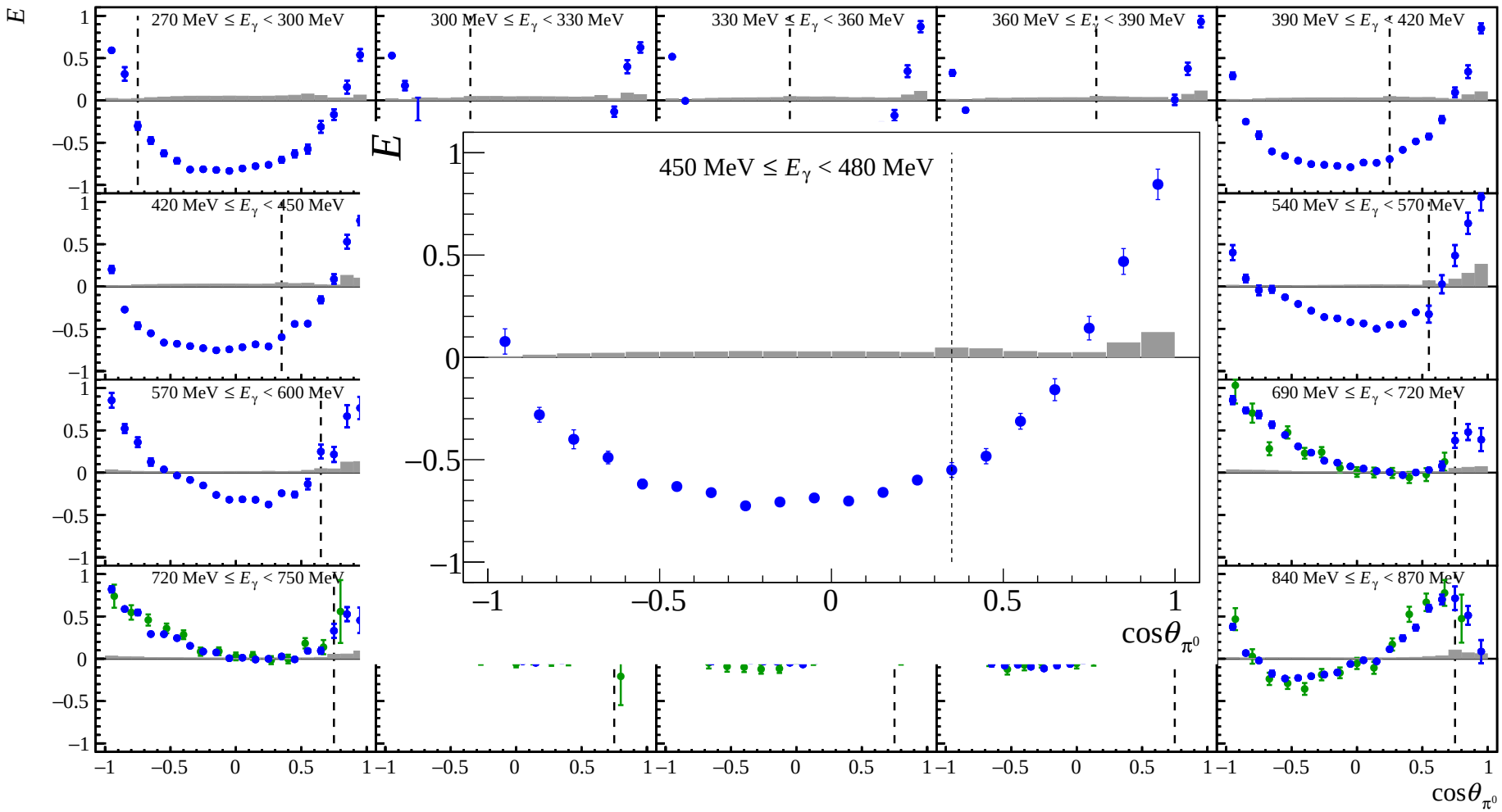

- A2 data (this work)
- CBELSA/TAPS data (M. Gottschall et al., , 2013)

The helicity asymmetry E in π^0 photoproduction

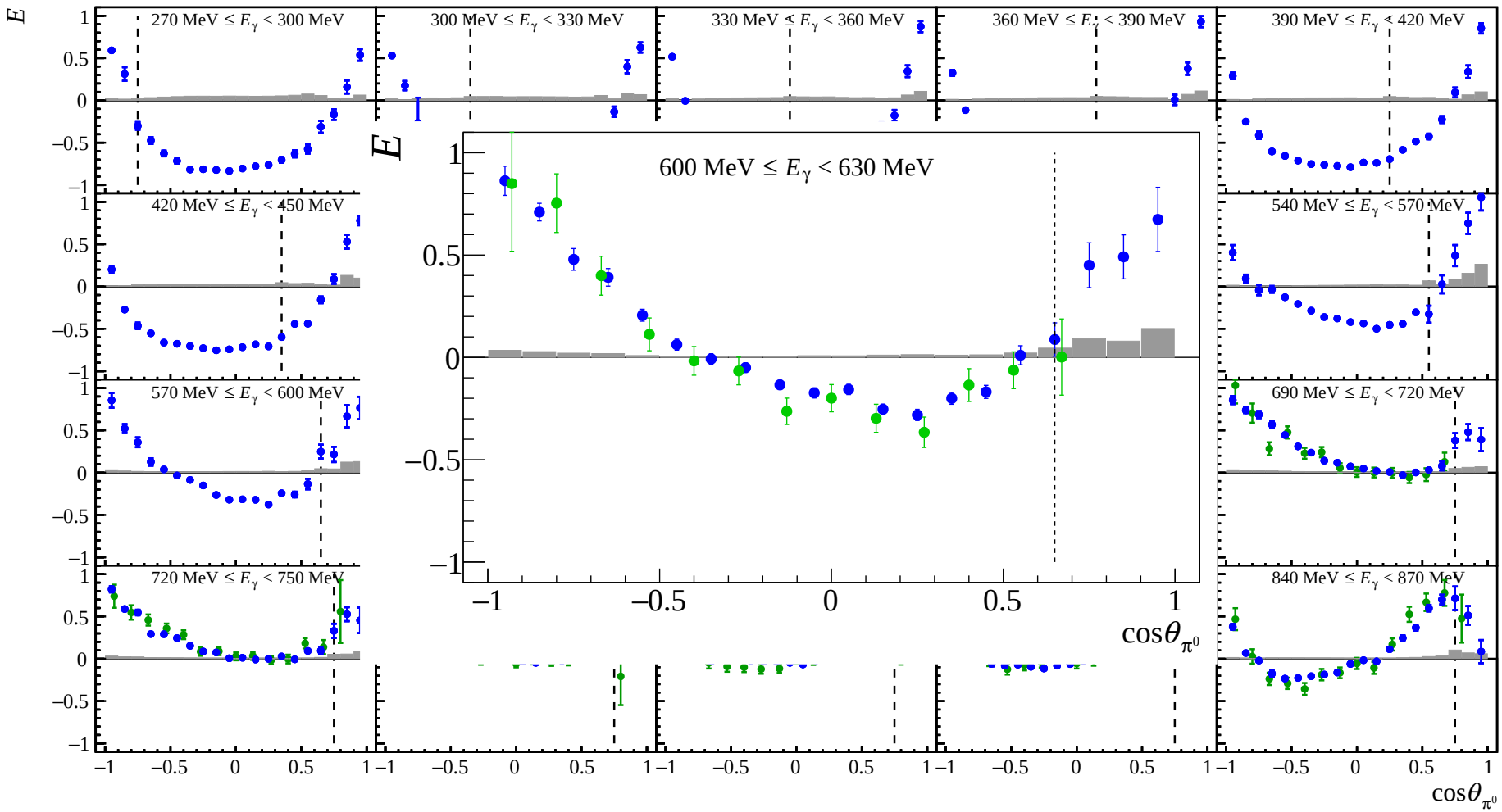

- A2 data (this work)
- CBELSA/TAPS data (M. Gottschall et al., , 2013)

The helicity asymmetry E in π^0 photoproduction

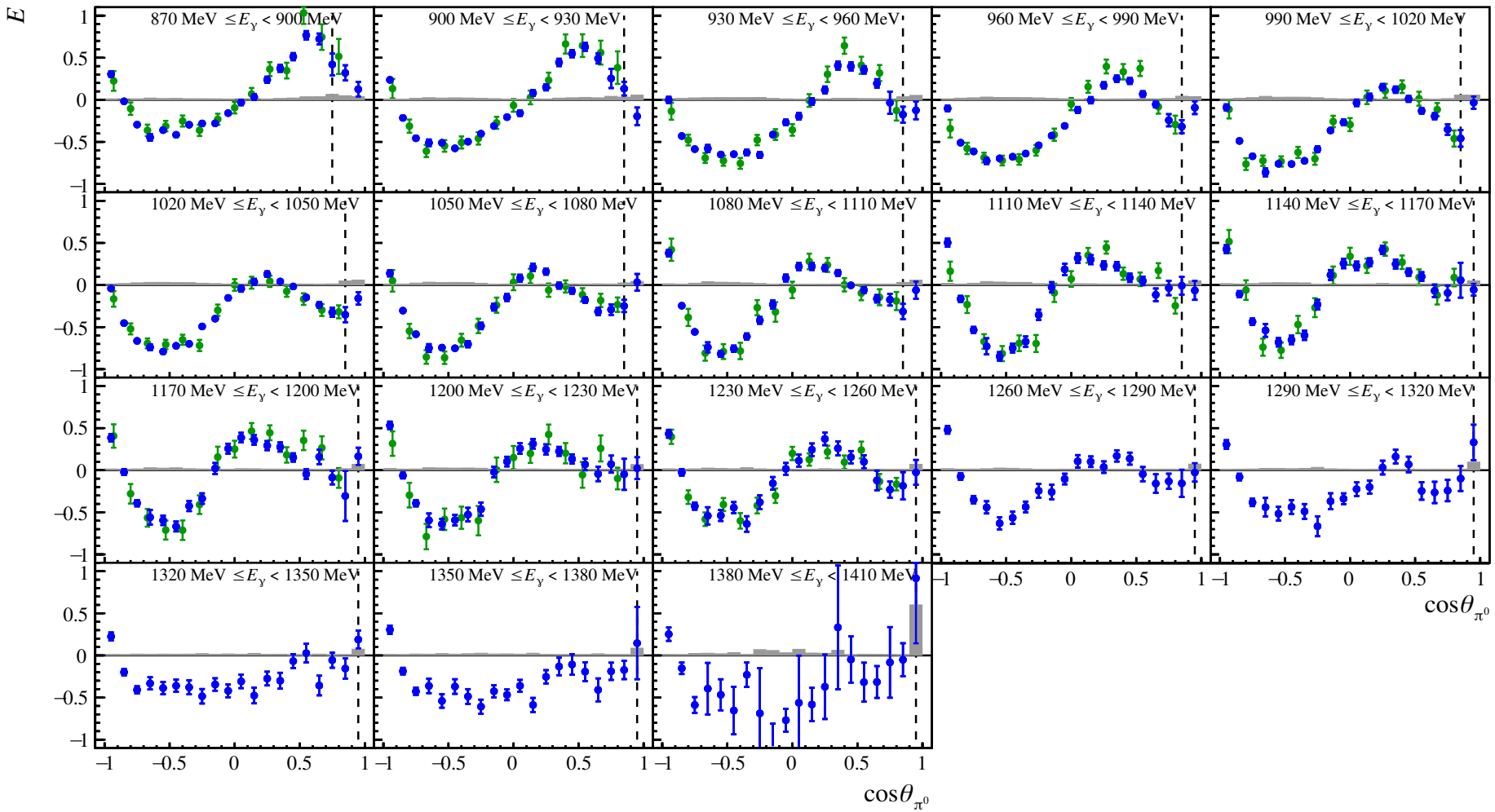

- A2 data (this work)
- CBELSA/TAPS data (M. Gottschall et al., , 2013)

The helicity asymmetry E in π^0 photoproduction

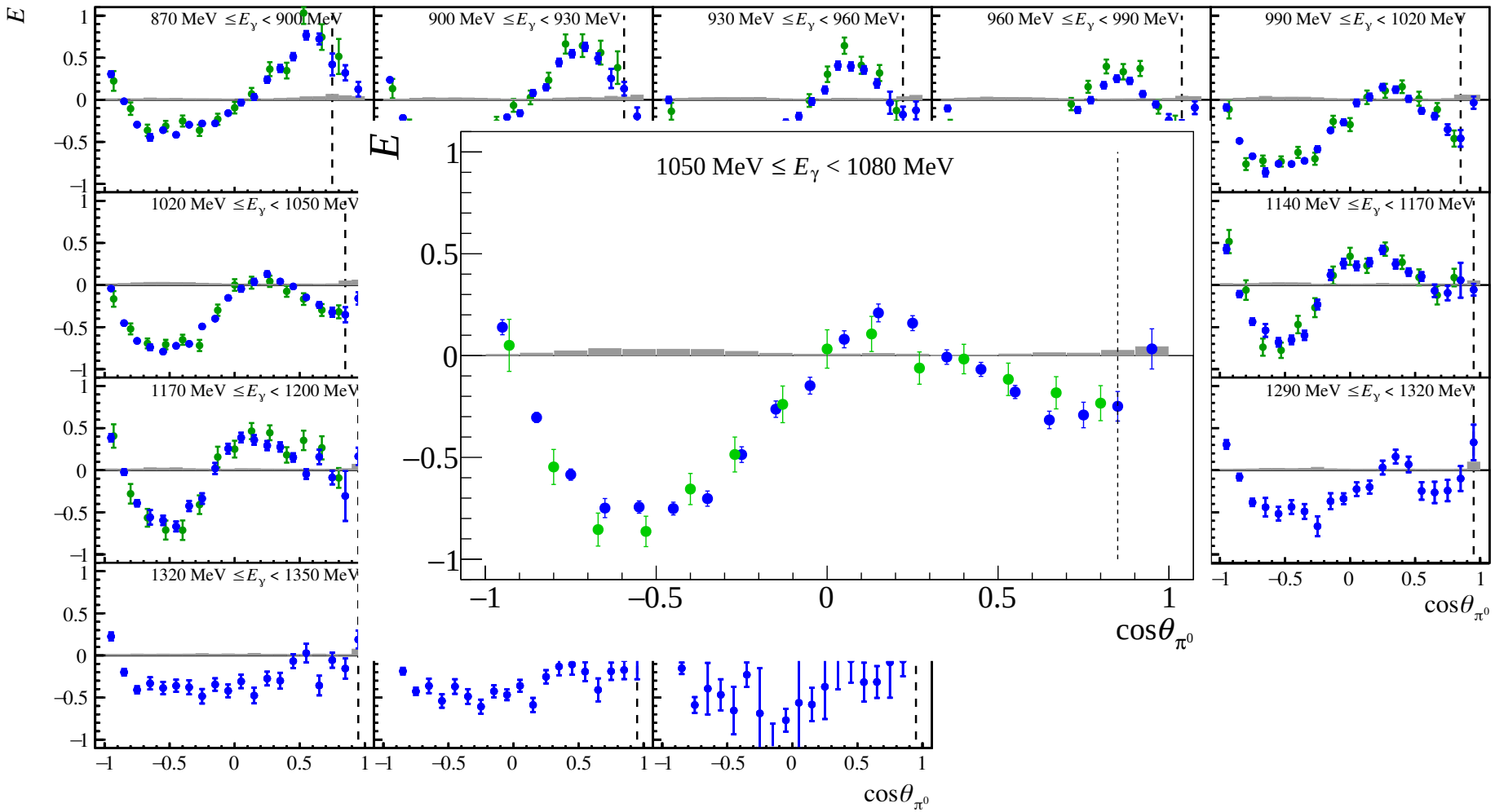

- A2 data (this work)
- CBELSA/TAPS data (M. Gottschall et al., , 2013)

The helicity asymmetry E in η photoproduction

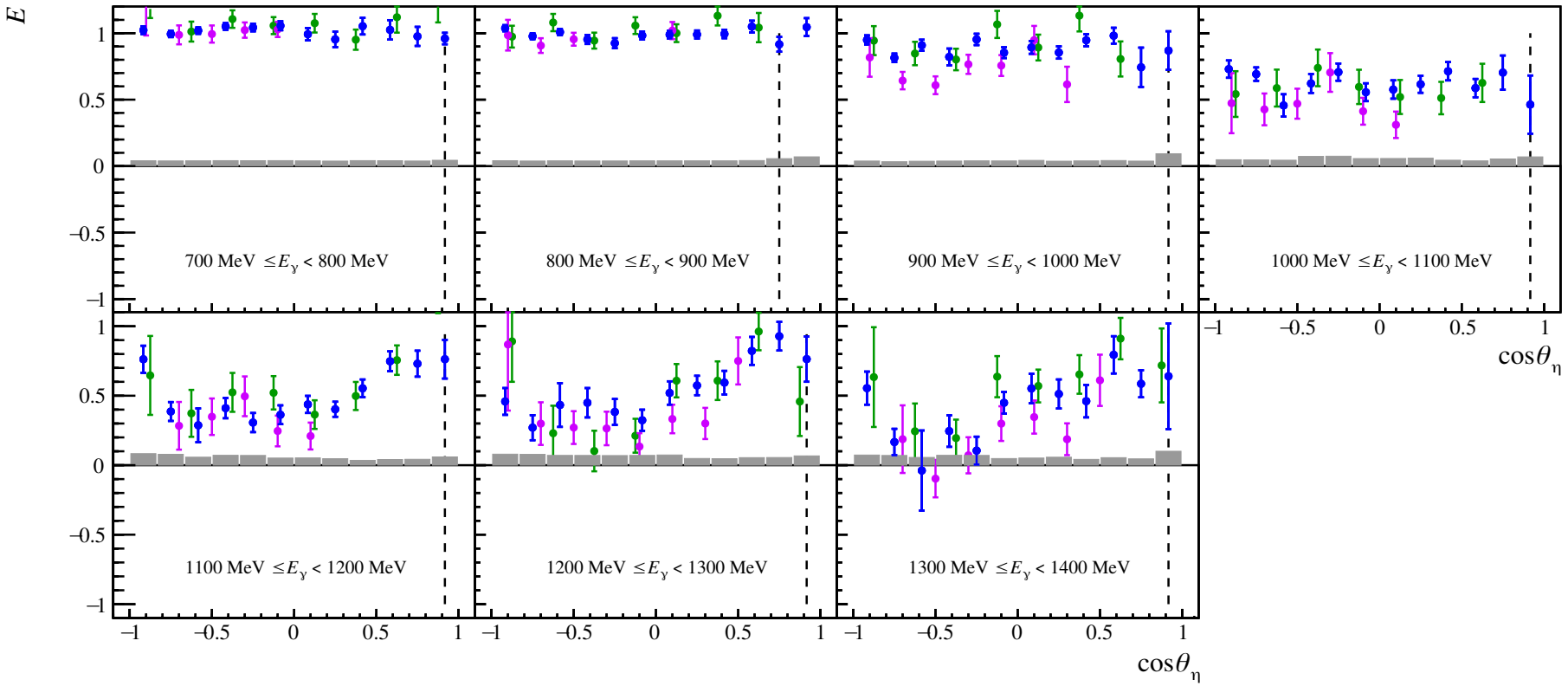

- A2 data (this work)
- CBELSA/TAPS data (J. Müller et al.)
- CLAS data (I. Senderovich et al., Phys. Lett. B 755 (2016))

The helicity asymmetry E in η photoproduction

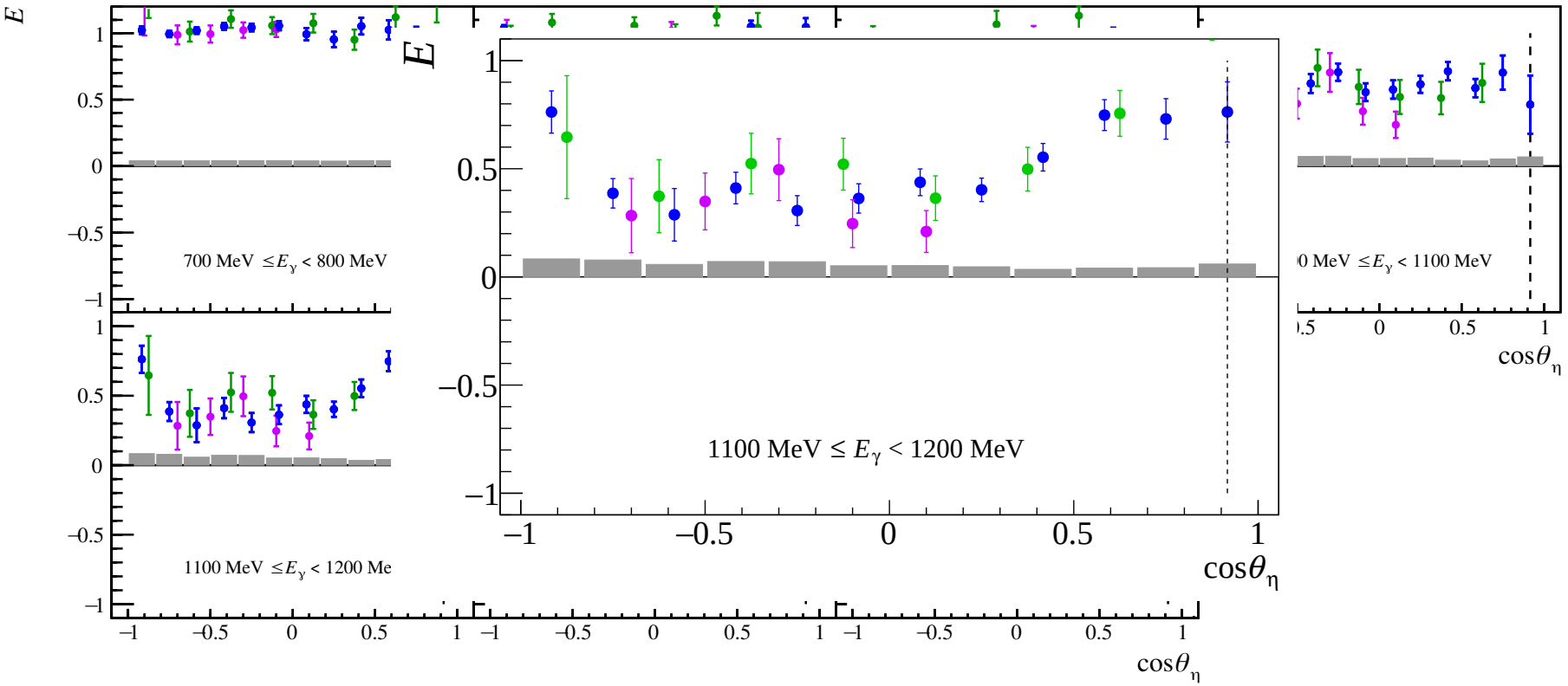

- A2 data (this work)
- CBELSA/TAPS data (J. Müller et al.)
- CLAS data (I. Senderovich et al., Phys. Lett. B 755 (2016))

The helicity asymmetry E in π^0 photoproduction

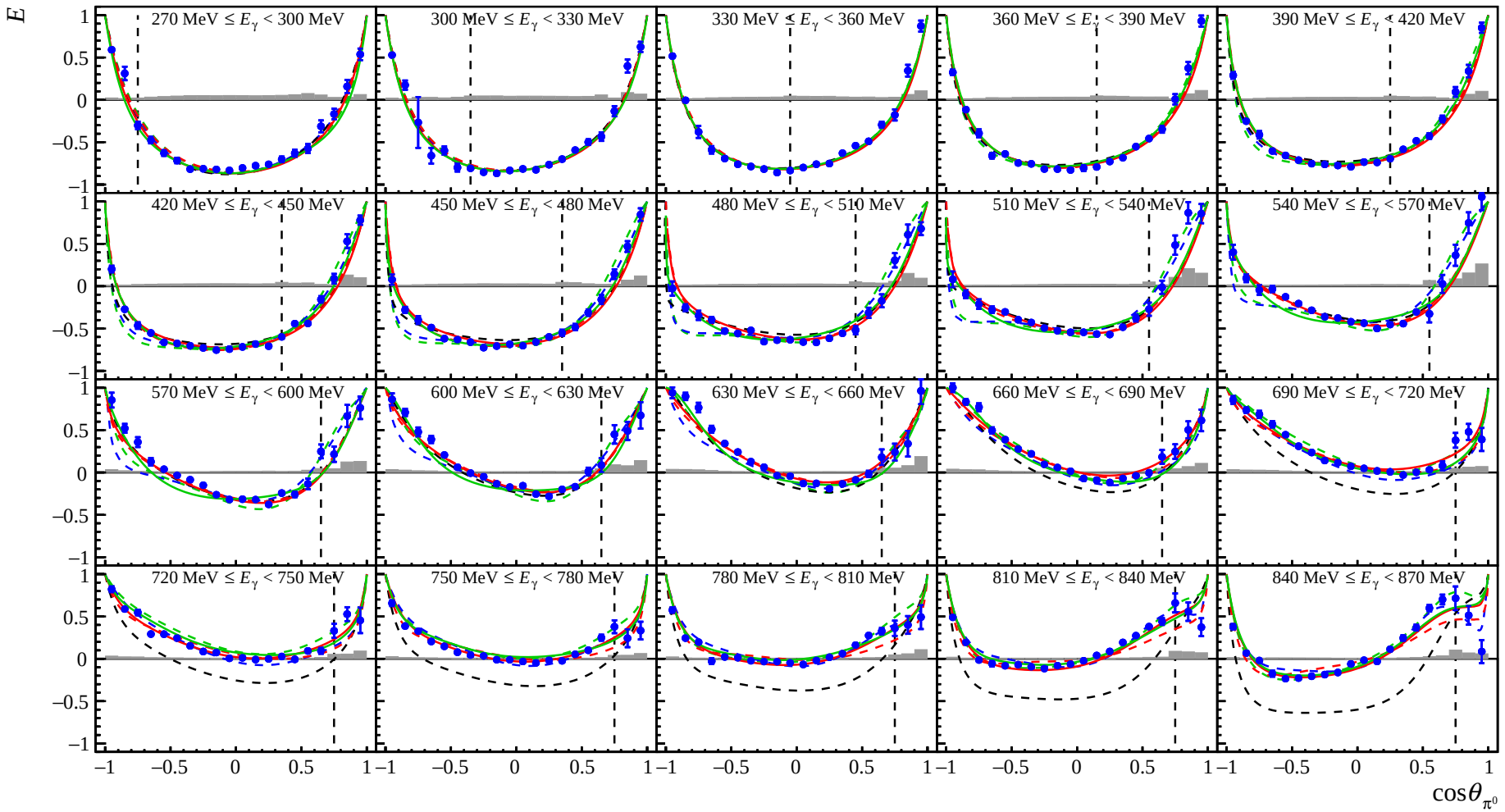

- A2 data (this work)
- BnGa-2011-02
- JüBo-2015-FitB
- SAID-CM12
- BnGa-2017
- JüBo-2017
- MAID2007

The helicity asymmetry E in π^0 photoproduction

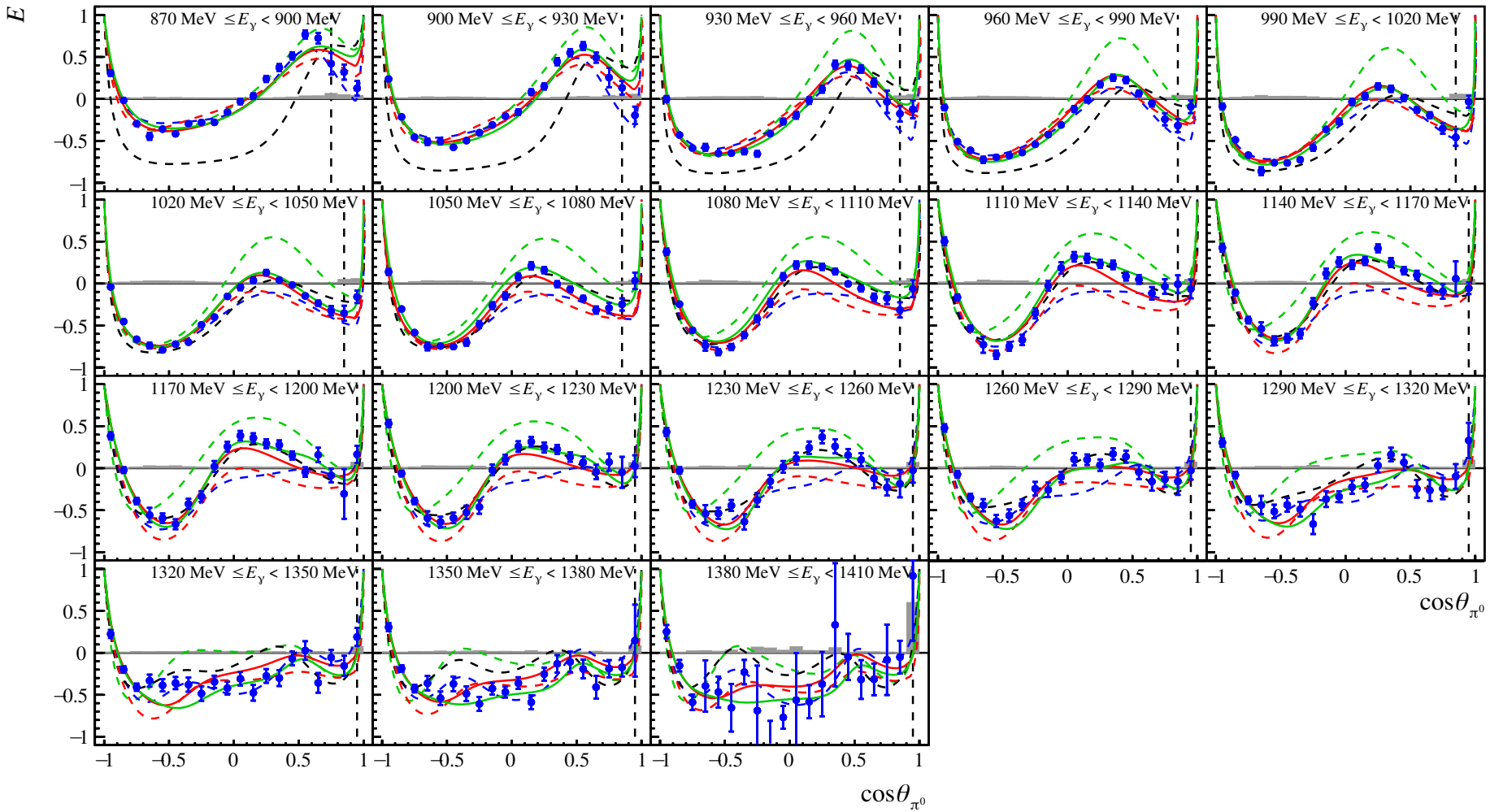

- A2 data (this work)
- BnGa-2011-02
- JüBo-2015-FitB
- SAID-CM12
- BnGa-2017
- JüBo-2017
- MAID2007

The helicity asymmetry E in η photoproduction

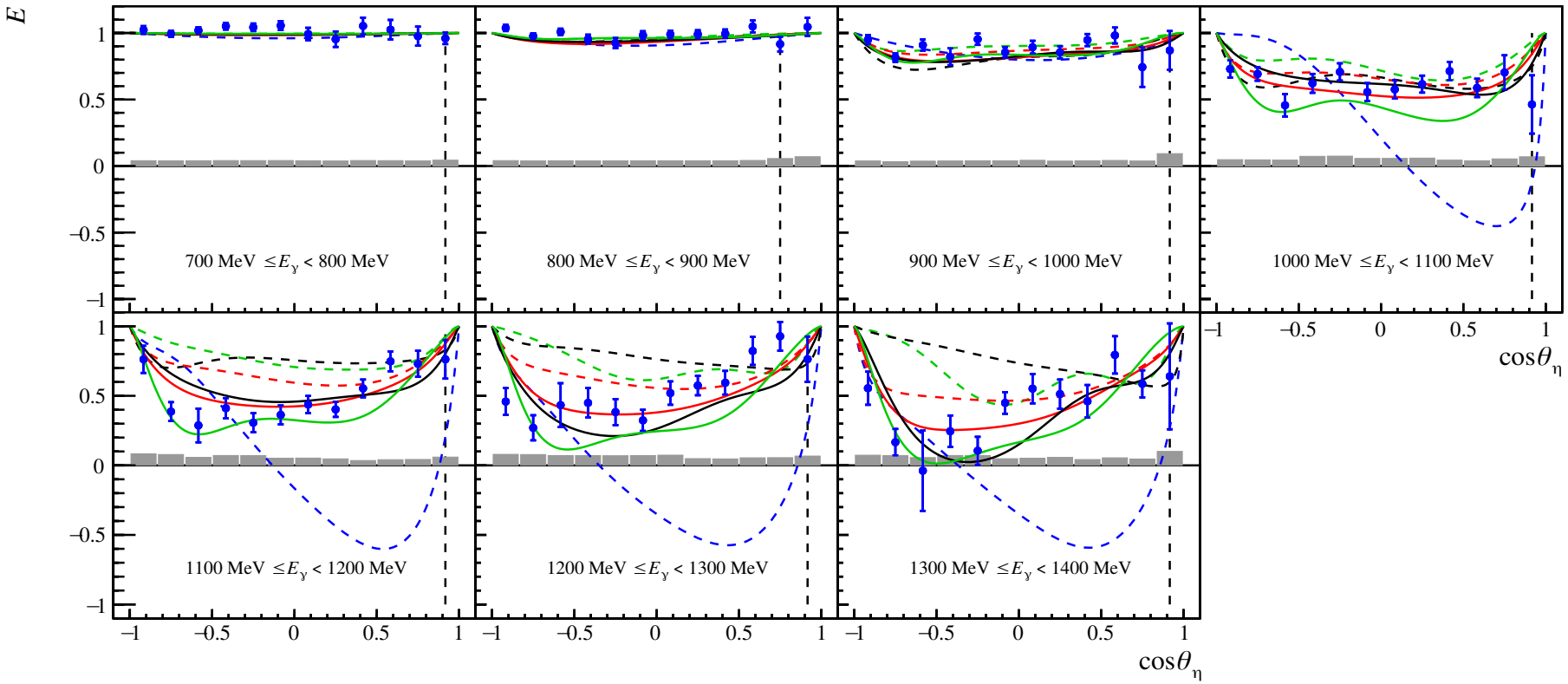

- A2 data (this work)
- BnGa-2014-02
- JüBo-2015-FitB
- ηMAID
- SAID-GE09
- BnGa-2017
- JüBo-2017
- ηMAID-2018

Discussion of results

Dominant partial wave contributions in polarization observables

$$\check{\mathrm{E}}(W, \cos\theta) = \mathrm{E}(W, \cos\theta) \cdot \frac{d\sigma}{d\Omega}(W, \cos\theta) = \sum_{k=0}^{2L_{max}} (a_L(W))_k \cdot P_k^0(\cos\theta)$$

Dominant partial wave contributions in polarization observables

$$\check{\mathrm{E}}(W,\cos\theta) = \mathrm{E}(W,\cos\theta)\cdot\frac{d\sigma}{d\Omega}(W,\cos\theta) = \sum_{k=0}^{2L_{max}} (a_L(W))_k \cdot P_k^0(\cos\theta)$$

$$(a_2)_2^{\check{E}}(W) = \left(E_{0+}^*, E_{1+}^*, \ldots, M_{2-}^*\right)$$

$$\left(\begin{array}{c|ccc|cccc}
0 & 0 & 0 & 0 & 6 & 1 & 3 & -3 \\ \hline
0 & 6 & 0 & -3 & 0 & 0 & 0 & 0 \\
0 & 0 & 2 & -1 & 0 & 0 & 0 & 0 \\
0 & -3 & -1 & 0 & 0 & 0 & 0 & 0 \\ \hline
6 & 0 & 0 & 0 & 12 & \frac{24}{7} & \frac{60}{7} & 0 \\
1 & 0 & 0 & 0 & \frac{24}{7} & 2 & -\frac{15}{7} & 0 \\
3 & 0 & 0 & 0 & \frac{60}{7} & -\frac{15}{7} & \frac{12}{7} & -\frac{27}{7} \\
-3 & 0 & 0 & 0 & 0 & 0 & -\frac{27}{7} & 6
\end{array}\right)
\begin{pmatrix} E_{0+} \\ E_{1+} \\ M_{1+} \\ M_{1-} \\ E_{2+} \\ E_{2-} \\ M_{2+} \\ M_{2-} \end{pmatrix}$$

$$\check{\mathrm{E}}(W,\cos\theta) = \mathrm{E}(W,\cos\theta)\cdot\frac{d\sigma}{d\Omega}(W,\cos\theta) = \sum_{k=0}^{2L_{max}} (a_L(W))_k \cdot P_k^0(\cos\theta)$$

$$(a_2)_2^{\check{E}}(W) = \left(E_{0+}^*, E_{1+}^*, \ldots, M_{2-}^*\right)$$

$$\left(\begin{array}{c|ccc|cccc} 0 & 0 & 0 & 0 & 6 & 1 & 3 & -3 \\ \hline 0 & 6 & 0 & -3 & 0 & 0 & 0 & 0 \\ 0 & 0 & 2 & -1 & 0 & 0 & 0 & 0 \\ 0 & -3 & -1 & 0 & 0 & 0 & 0 & 0 \\ \hline 6 & 0 & 0 & 0 & 12 & \frac{24}{7} & \frac{60}{7} & 0 \\ 1 & 0 & 0 & 0 & \frac{24}{7} & 2 & -\frac{15}{7} & 0 \\ 3 & 0 & 0 & 0 & \frac{60}{7} & -\frac{15}{7} & \frac{12}{7} & -\frac{27}{7} \\ -3 & 0 & 0 & 0 & 0 & 0 & -\frac{27}{7} & 6 \end{array}\right) \left(\begin{array}{c} E_{0+} \\ E_{1+} \\ M_{1+} \\ M_{1-} \\ E_{2+} \\ E_{2-} \\ M_{2+} \\ M_{2-} \end{array}\right)$$

$$\begin{aligned} &= 6E_{2+}^*E_{0+} + E_{2-}^*E_{0+} + 3M_{2+}^*E_{0+} + 3M_{2-}^*E_{0+} + 6|E_{1+}|^2 - 3M_{1-}^*E_{1+} + |M_{1+}|^2 \\ &- M_{1-}^*M_{1+} - 3E_{1+}^*M_{1-} - M_{1+}^*M_{1-} + 6E_{0+}^*E_{2+} + 12|E_{2+}|^2 + \frac{24}{7}E_{2-}^*E_{2+} \\ &+ \frac{60}{7}M_{2+}^*E_{2+} + E_{0+}^*E_{2-} + \frac{24}{7}E_{2+}^*E_{2-} + 2|E_{2-}|^2 - \frac{15}{7}M_{2+}^*E_{2-} + 3E_{0+}^*M_{2+} \\ &+ \frac{60}{7}E_{2+}^*M_{2+} - \frac{15}{7}E_{2-}^*M_{2+} + \frac{12}{7}|M_{2+}|^2\frac{27}{7}M_{2-}^*M_{2+} - 3E_{0+}^*M_{2-} - \frac{27}{7}M_{2+}^*M_{2-} \\ &+ 6|M_{2-}|^2 \end{aligned}$$

$$\check{\mathrm{E}}(W,\cos\theta) = \mathrm{E}(W,\cos\theta)\cdot\frac{d\sigma}{d\Omega}(W,\cos\theta) = \sum_{k=0}^{2L_{max}} (a_L(W))_k \cdot P_k^0(\cos\theta)$$

$$(a_2)_2^{\check{E}}(W) = \left(E_{0+}^*, E_{1+}^*, \ldots, M_{2-}^*\right)$$

$$\left(\begin{array}{c|ccc|cccc} 0 & 0 & 0 & 0 & 6 & 1 & 3 & -3 \\ \hline 0 & 6 & 0 & -3 & 0 & 0 & 0 & 0 \\ 0 & 0 & 2 & -1 & 0 & 0 & 0 & 0 \\ 0 & -3 & -1 & 0 & 0 & 0 & 0 & 0 \\ \hline 6 & 0 & 0 & 0 & 12 & \frac{24}{7} & \frac{60}{7} & 0 \\ 1 & 0 & 0 & 0 & \frac{24}{7} & 2 & -\frac{15}{7} & 0 \\ 3 & 0 & 0 & 0 & \frac{60}{7} & -\frac{15}{7} & \frac{12}{7} & -\frac{27}{7} \\ -3 & 0 & 0 & 0 & 0 & 0 & -\frac{27}{7} & 6 \end{array}\right) \left(\begin{array}{c} E_{0+} \\ E_{1+} \\ M_{1+} \\ M_{1-} \\ E_{2+} \\ E_{2-} \\ M_{2+} \\ M_{2-} \end{array}\right)$$

$$\begin{aligned} &= 6E_{2+}^*E_{0+} + E_{2-}^*E_{0+} + 3M_{2+}^*E_{0+} + 3M_{2-}^*E_{0+} + 6|E_{1+}|^2 - 3M_{1-}^*E_{1+} + |M_{1+}|^2 \\ &- M_{1-}^*M_{1+} - 3E_{1+}^*M_{1-} - M_{1+}^*M_{1-} + 6E_{0+}^*E_{2+} + 12|E_{2+}|^2 + \frac{24}{7}E_{2-}^*E_{2+} \\ &+ \frac{60}{7}M_{2+}^*E_{2+} + E_{0+}^*E_{2-} + \frac{24}{7}E_{2+}^*E_{2-} + 2|E_{2-}|^2 - \frac{15}{7}M_{2+}^*E_{2-} + 3E_{0+}^*M_{2+} \\ &+ \frac{60}{7}E_{2+}^*M_{2+} - \frac{15}{7}E_{2-}^*M_{2+} + \frac{12}{7}|M_{2+}|^2\frac{27}{7}M_{2-}^*M_{2+} - 3E_{0+}^*M_{2-} - \frac{27}{7}M_{2+}^*M_{2-} \\ &+ 6|M_{2-}|^2 \\ &= < P,P > + < S,D > + < D,D > \end{aligned}$$

Dominant partial wave contributions (E (A2), $\gamma p \rightarrow p\pi^0$)

$$\check{\mathrm{E}}(W, \cos\theta) = \mathrm{E}(W, \cos\theta) \cdot \frac{d\sigma}{d\Omega}(W, \cos\theta) = \sum_{k=0}^{2L_{max}+1} (a_L(W))_k \cdot P_k^0(\cos\theta)$$

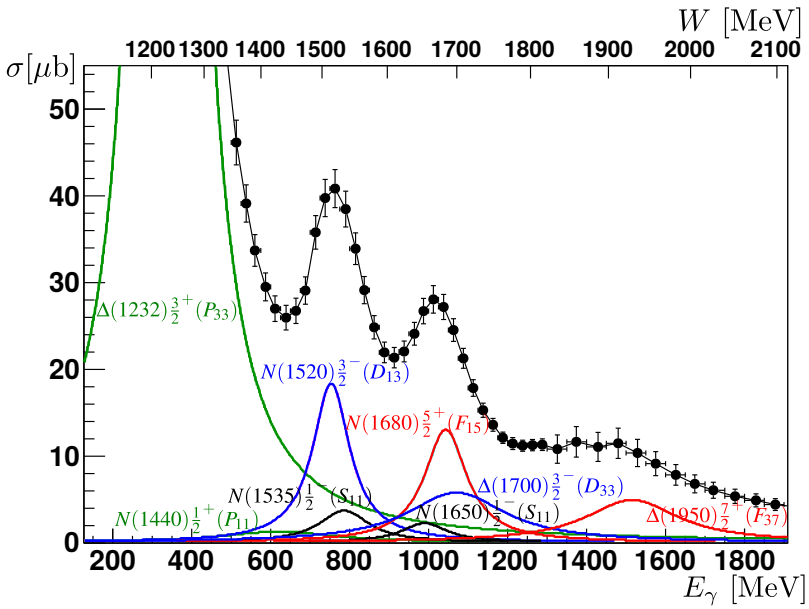

Y. Wunderlich, F. Afzal et al., EPJA 53 (2017) 86

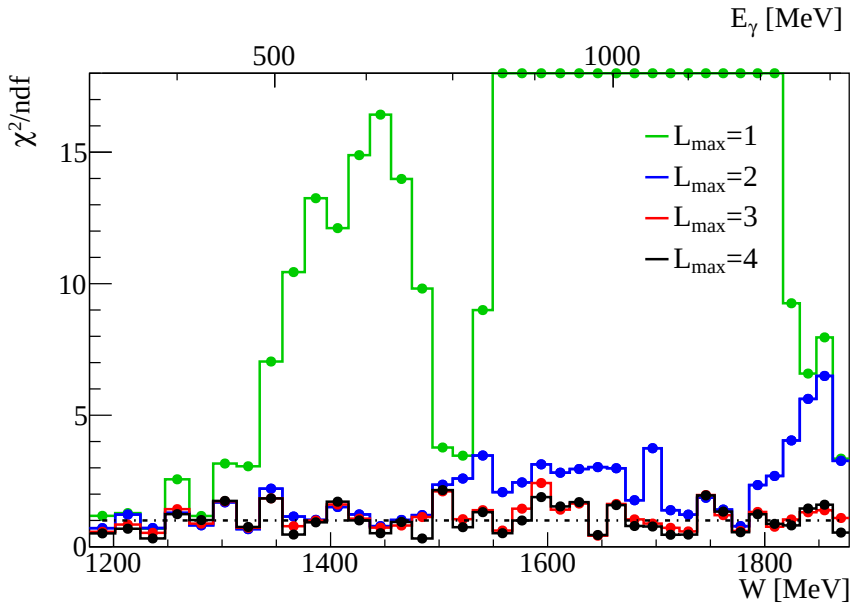

Dominant partial wave contributions (E (A2), $\gamma p \to p\pi^0$)

$$\check{\mathrm{E}}(W,\cos\theta) = \mathrm{E}(W,\cos\theta)\cdot\frac{d\sigma}{d\Omega}(W,\cos\theta) = \sum_{k=0}^{2L_{max}+1}(a_L(W))_k \cdot P_k^0(\cos\theta)$$

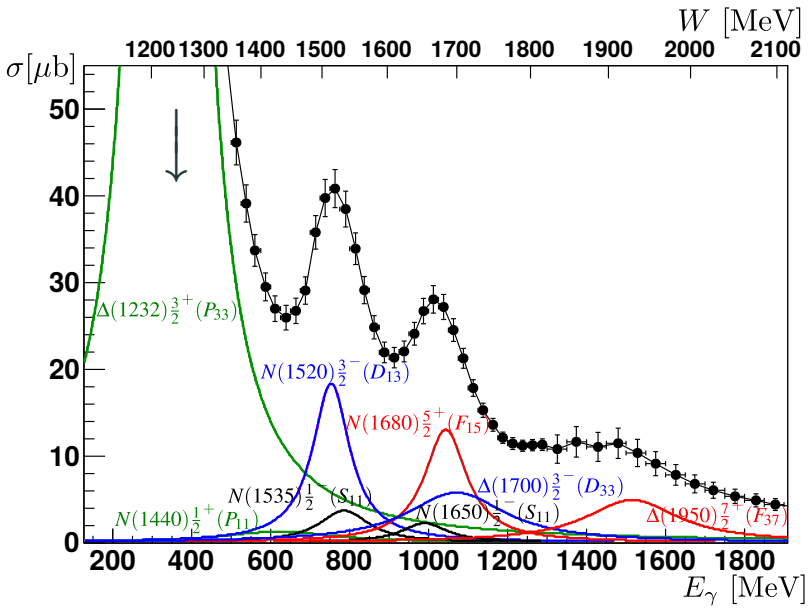

Y. Wunderlich, F. Afzal et al., EPJA 53 (2017) 86

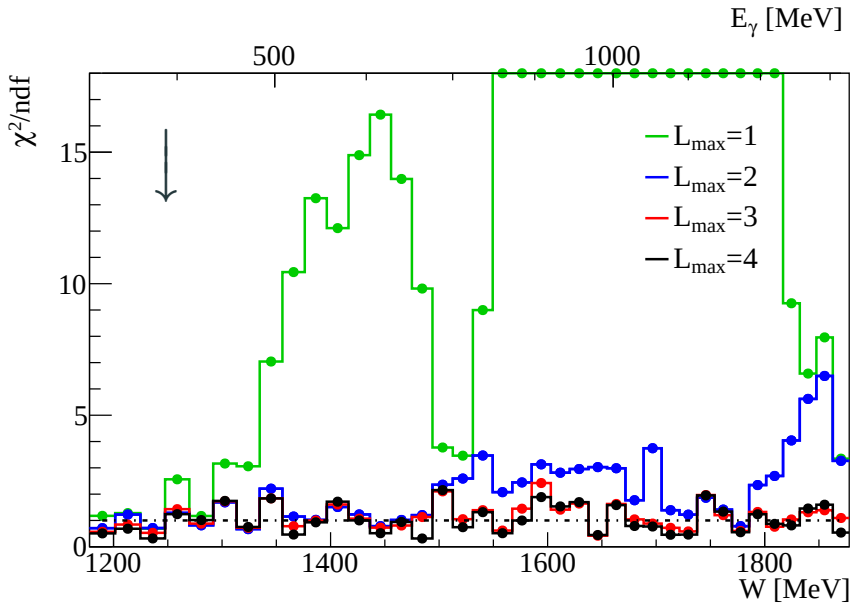

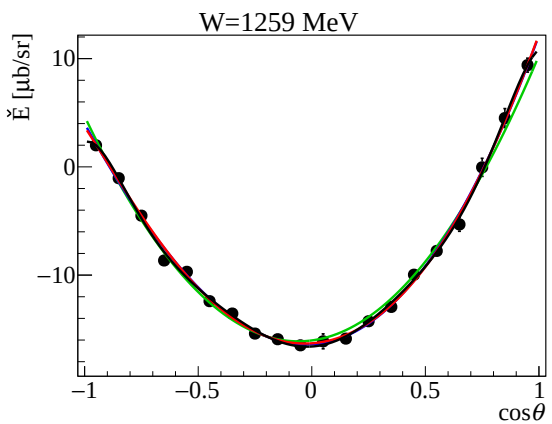

Dominant partial wave contributions (E (A2), $\gamma p \to p\pi^0$)

$$\check{\mathrm{E}}(W,\cos\theta) = \mathrm{E}(W,\cos\theta)\cdot\frac{d\sigma}{d\Omega}(W,\cos\theta) = \sum_{k=0}^{2L_{max}+1}(a_L(W))_k \cdot P_k^0(\cos\theta)$$

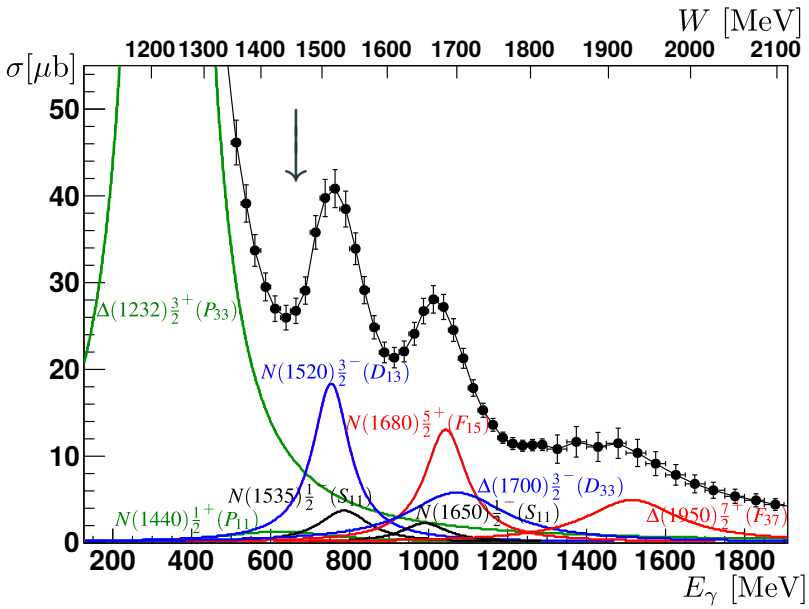

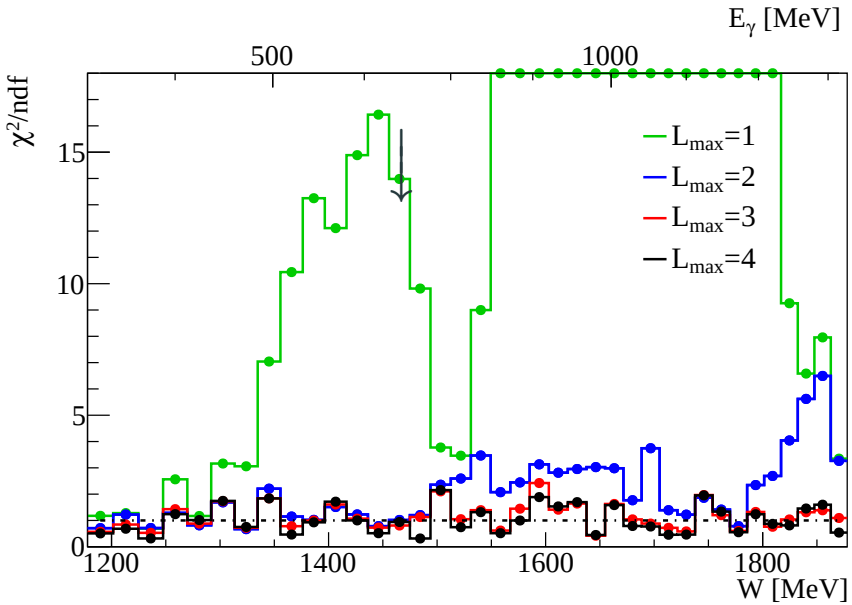

Y. Wunderlich, F. Afzal et al., EPJA 53 (2017) 86

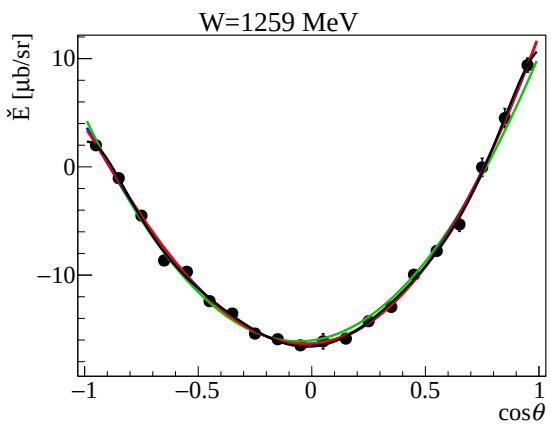

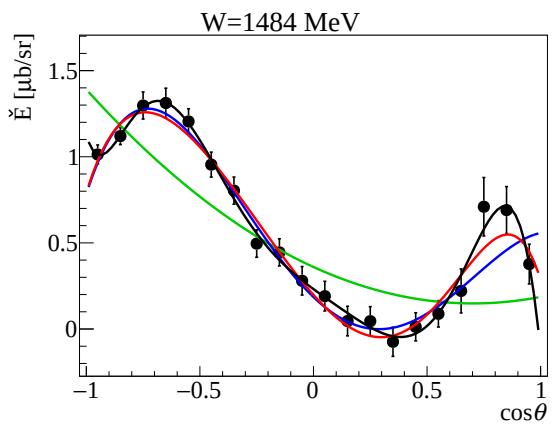

Dominant partial wave contributions (E (A2), $\gamma p \to p\pi^0$)

$$\check{\mathrm{E}}(W,\cos\theta) = \mathrm{E}(W,\cos\theta)\cdot\frac{d\sigma}{d\Omega}(W,\cos\theta) = \sum_{k=0}^{2L_{max}+1}(a_L(W))_k \cdot P_k^0(\cos\theta)$$

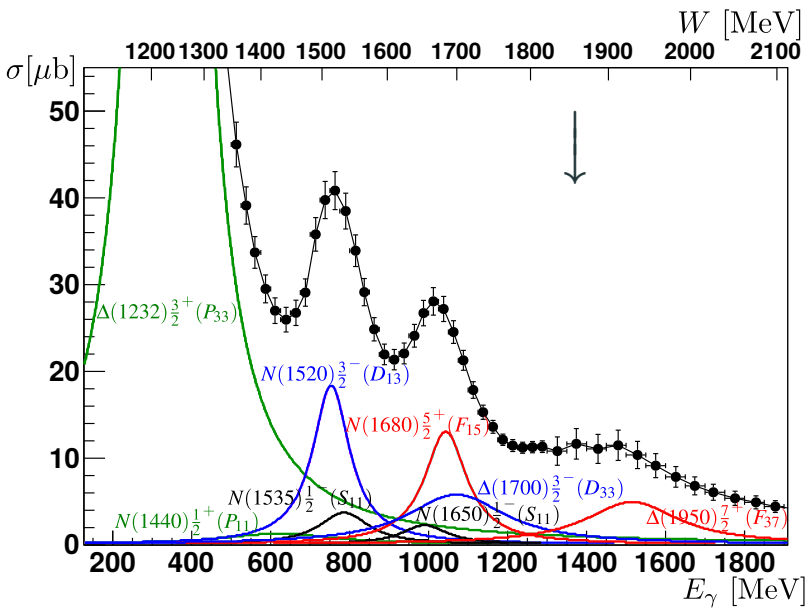

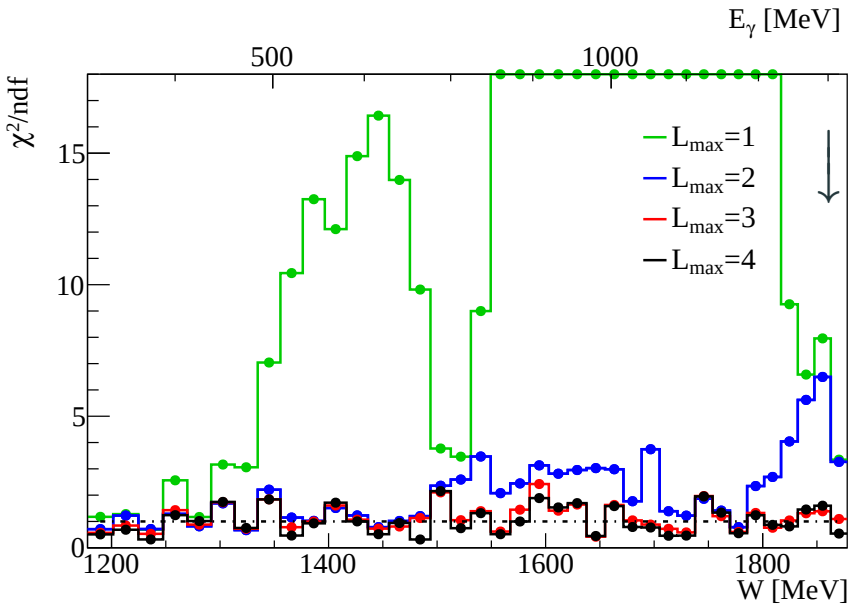

Y. Wunderlich, F. Afzal et al., EPJA 53 (2017) 86

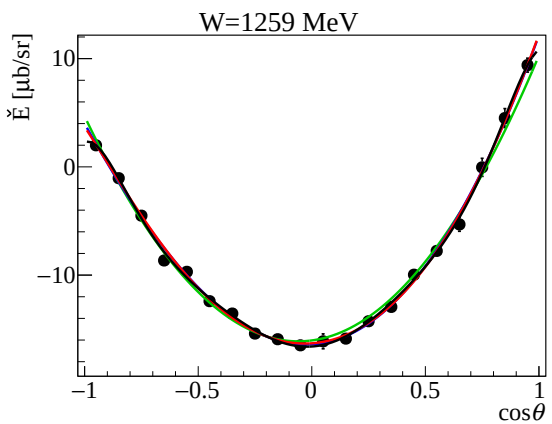

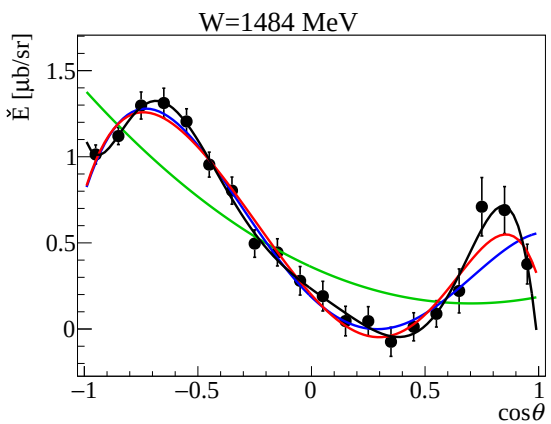

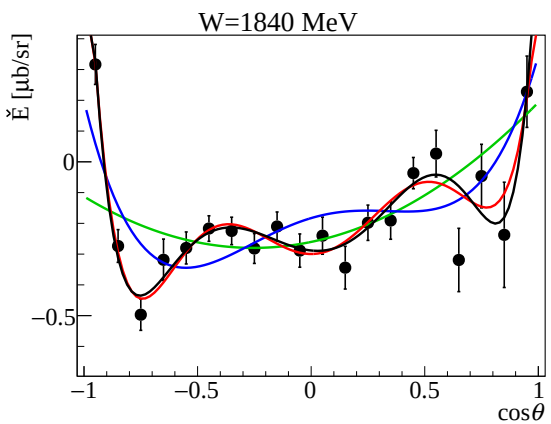

Dominant partial wave contributions (E (A2), $\gamma p \to p\pi^0$)

$$\check{\mathrm{E}}(W,\cos\theta) = \mathrm{E}(W,\cos\theta)\cdot\frac{d\sigma}{d\Omega}(W,\cos\theta) = \sum_{k=0}^{2L_{max}+1}(a_L(W))_k \cdot P_k^0(\cos\theta)$$

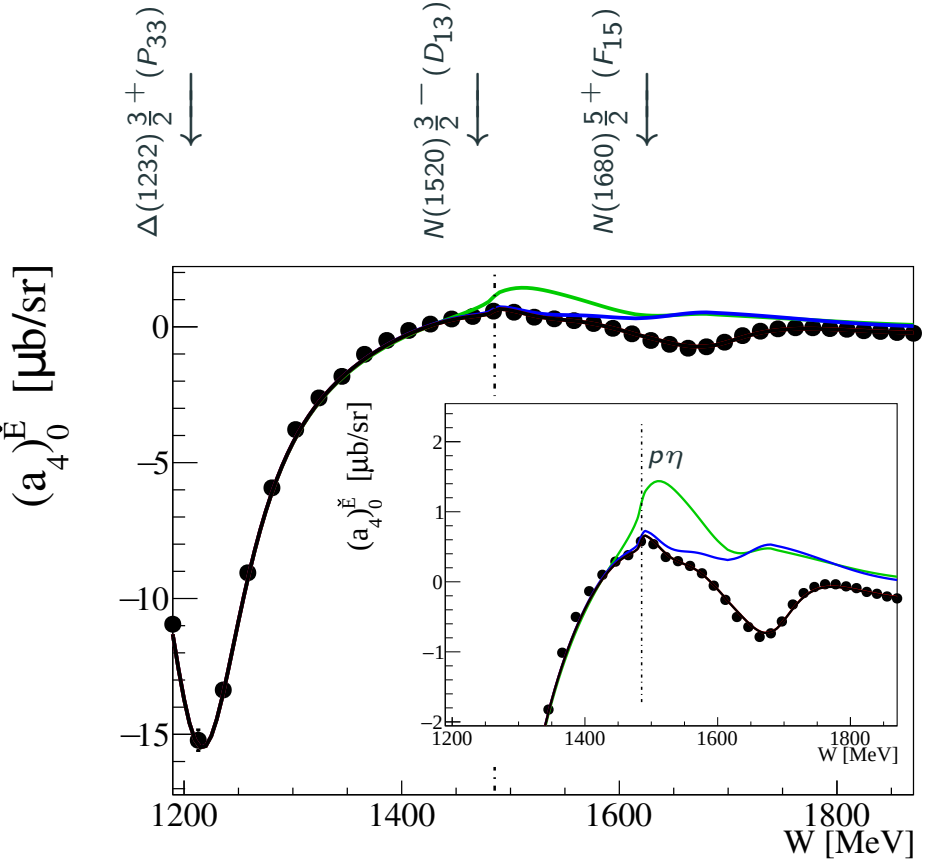

$$(a_4)_0^{\check{E}} = \langle S,S\rangle + \langle P,P\rangle + \langle D,D\rangle + \langle F,F\rangle + \langle G,G\rangle$$

Only interference terms of the same L. Similar to differential cross section.

Dominant partial wave contributions (E (A2), $\gamma p \to p\pi^0$)

$$\check{\mathrm{E}}(W,\cos\theta) = \mathrm{E}(W,\cos\theta)\cdot\frac{d\sigma}{d\Omega}(W,\cos\theta) = \sum_{k=0}^{2L_{max}+1}(a_L(W))_k \cdot P_k^0(\cos\theta)$$

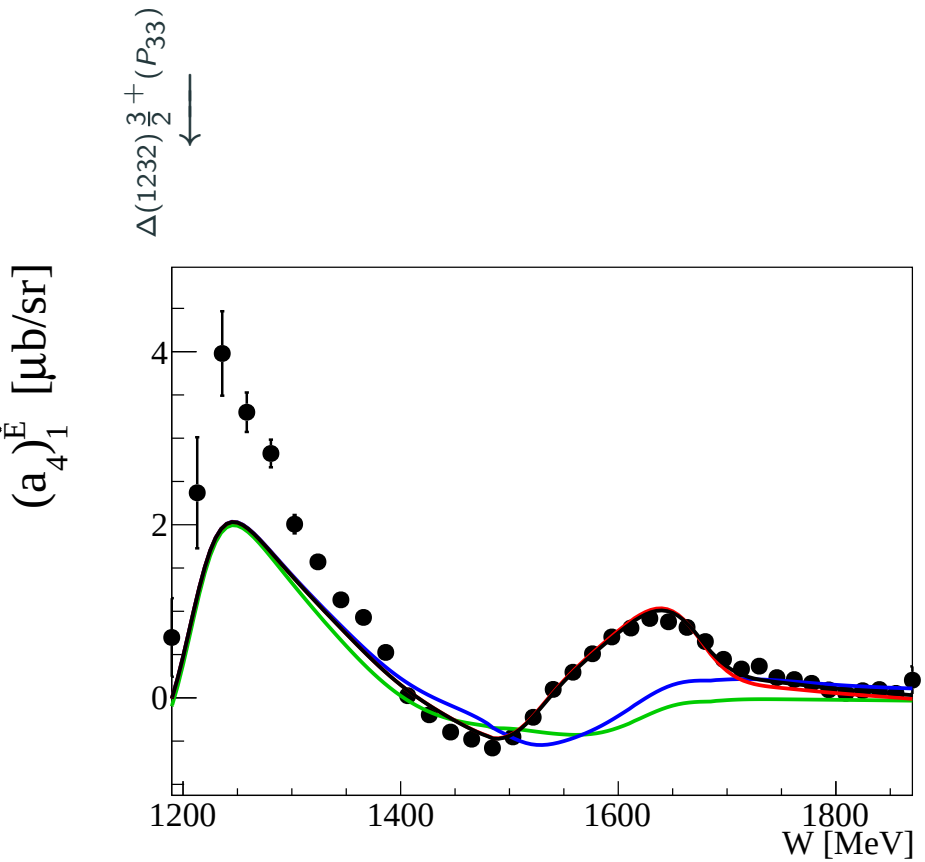

$$(a_4)_1^{\check{E}} = \langle S,P\rangle + \langle P,D\rangle + \langle D,F\rangle + \langle F,G\rangle$$

E_{0+} multipole (S-wave) needs modification in PWA models.

Dominant partial wave contributions (E (A2), $\gamma p \to p\pi^0$)

$$\check{\mathrm{E}}(W,\cos\theta) = \mathrm{E}(W,\cos\theta)\cdot\frac{d\sigma}{d\Omega}(W,\cos\theta) = \sum_{k=0}^{2L_{max}+1}(a_L(W))_k \cdot P_k^0(\cos\theta)$$

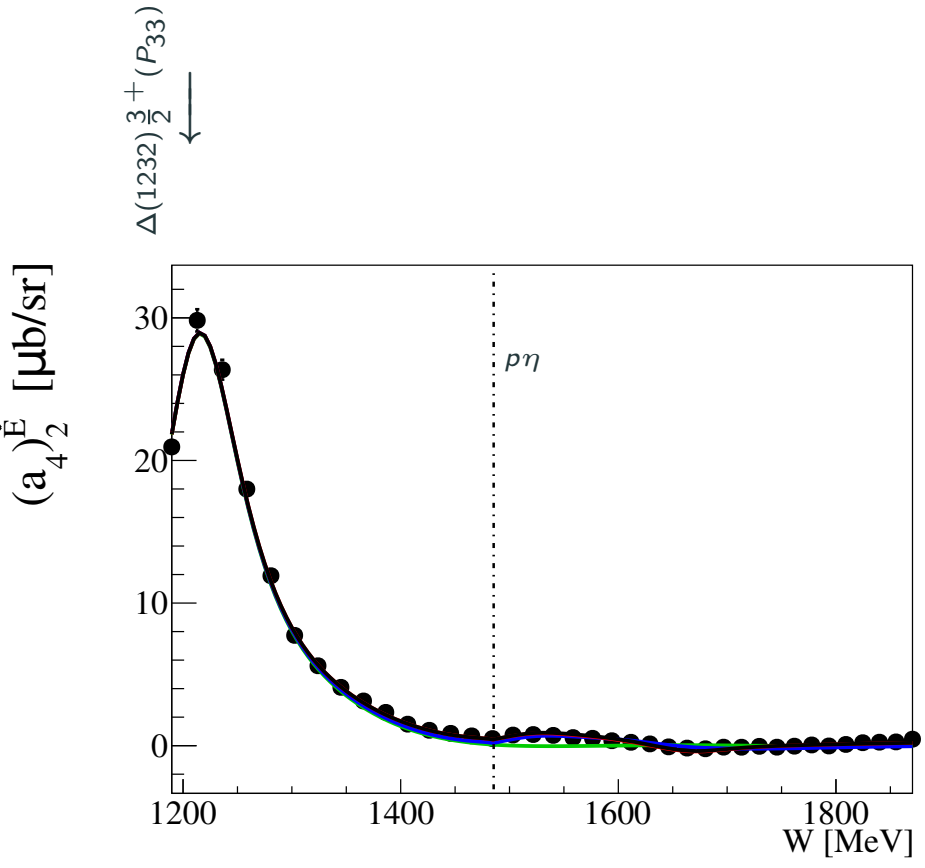

$$(a_4)_2^{\check{E}} = \langle P,P\rangle + \langle S,D\rangle + \langle D,D\rangle + \langle P,F\rangle + \langle F,F\rangle + \langle D,G\rangle + \langle G,G\rangle$$

$p\eta$ cusp is well visible in the data and BnGa-2014-02 PWA ($< S,D >$).

Dominant partial wave contributions (E (A2), $\gamma p \to p\pi^0$)

$$\check{\mathrm{E}}(W,\cos\theta) = \mathrm{E}(W,\cos\theta)\cdot\frac{d\sigma}{d\Omega}(W,\cos\theta) = \sum_{k=0}^{2L_{max}+1}(a_L(W))_k \cdot P_k^0(\cos\theta)$$

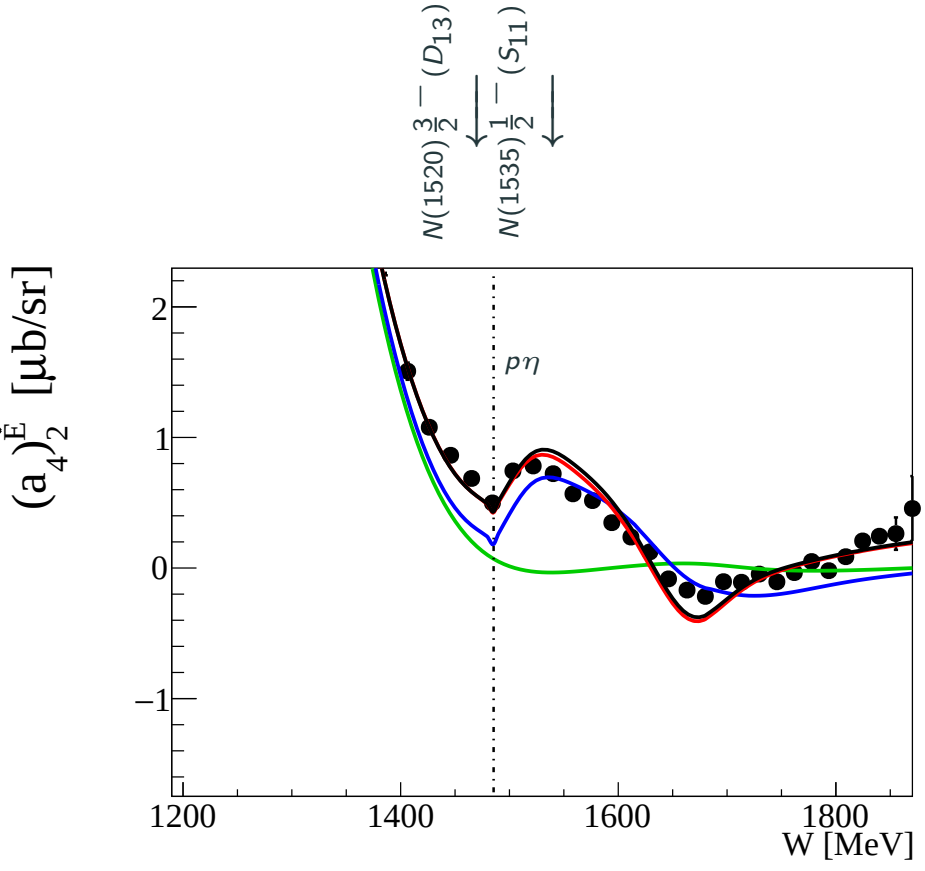

$$(a_4)_2^{\check{E}} = \langle P,P\rangle + \langle S,D\rangle + \langle D,D\rangle + \langle P,F\rangle + \langle F,F\rangle + \langle D,G\rangle + \langle G,G\rangle$$

$p\eta$ cusp is well visible in the data and BnGa-2014-02 PWA ($< S,D >$).

Dominant partial wave contributions (E (A2), $\gamma p \to p\pi^0$)

$$\check{\mathrm{E}}(W,\cos\theta) = \mathrm{E}(W,\cos\theta)\cdot\frac{d\sigma}{d\Omega}(W,\cos\theta) = \sum_{k=0}^{2L_{max}+1}(a_L(W))_k \cdot P_k^0(\cos\theta)$$

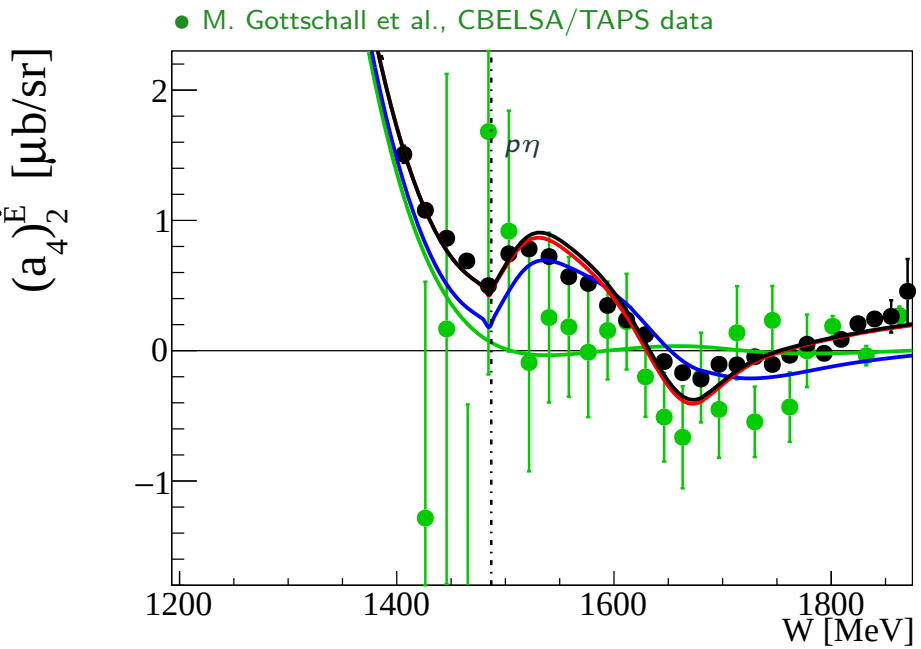

$$(a_4)_2^{\check{E}} = \langle P,P\rangle + \langle S,D\rangle + \langle D,D\rangle + \langle P,F\rangle + \langle F,F\rangle + \langle D,G\rangle + \langle G,G\rangle$$

Very precise new A2 data shows the $p\eta$ cusp.

It is important to cover the entire angular range.

Dominant partial wave contributions (E (A2), $\gamma p \to p\pi^0$)

$$\check{\mathrm{E}}(W,\cos\theta) = \mathrm{E}(W,\cos\theta)\cdot\frac{d\sigma}{d\Omega}(W,\cos\theta) = \sum_{k=0}^{2L_{max}+1}(a_L(W))_k \cdot P_k^0(\cos\theta)$$

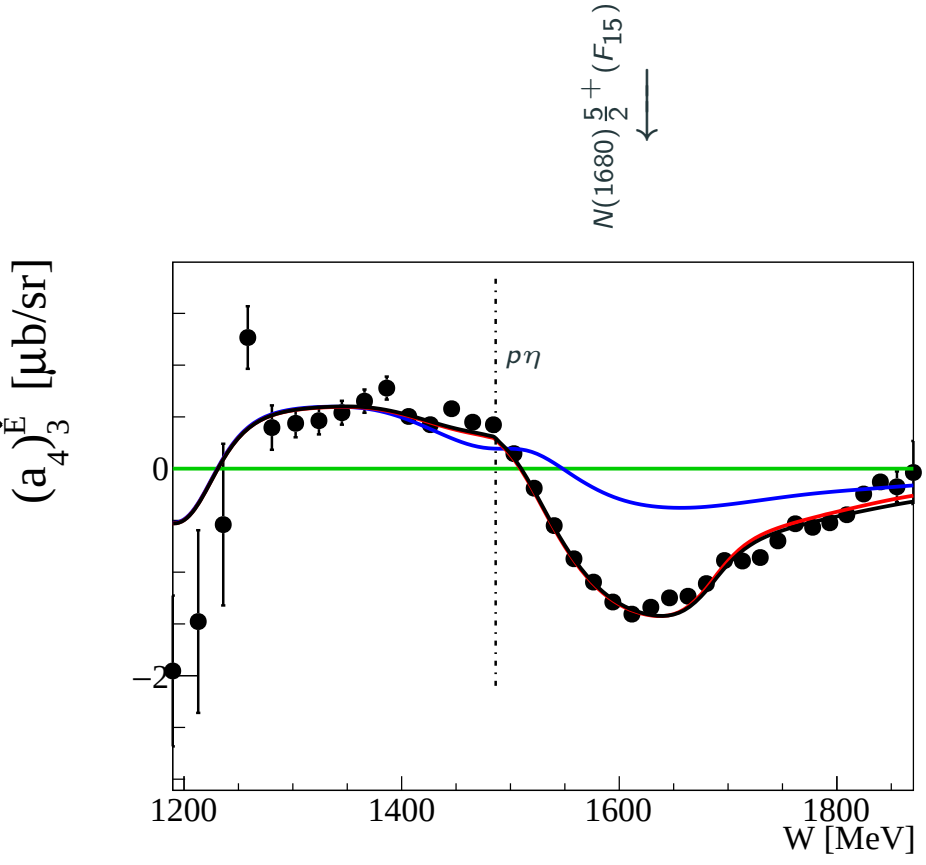

$$(a_4)_3^{\check{E}} = \langle P, D\rangle + \langle S, F\rangle + \langle D, F\rangle + \langle P, G\rangle + \langle F, G\rangle$$

$p\eta$ cusp is well visible in the data and BnGa-2014-02 PWA ($< S, F >$).

Dominant partial wave contributions (E (A2), $\gamma p \to p\pi^0$)

$$\check{\mathrm{E}}(W,\cos\theta) = \mathrm{E}(W,\cos\theta)\cdot\frac{d\sigma}{d\Omega}(W,\cos\theta) = \sum_{k=0}^{2L_{max}+1}(a_L(W))_k \cdot P_k^0(\cos\theta)$$

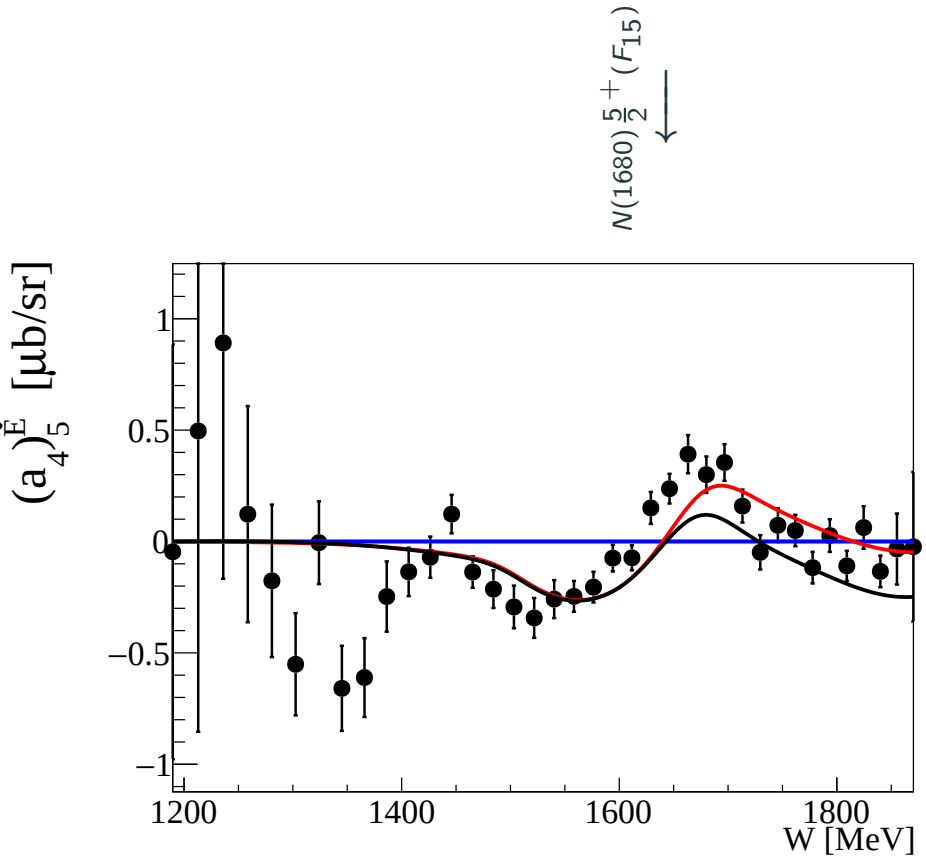

$$(a_4)_5^{\check{E}} = \langle D,F\rangle + \langle P,G\rangle + \langle F,G\rangle$$

$< D, F >$-term not well described by BnGa-2014-02 PWA.

Dominant partial wave contributions (E (A2), $\gamma p \to p\pi^0$)

$$\check{\mathrm{E}}(W,\cos\theta) = \mathrm{E}(W,\cos\theta)\cdot\frac{d\sigma}{d\Omega}(W,\cos\theta) = \sum_{k=0}^{2L_{max}+1}(a_L(W))_k \cdot P_k^0(\cos\theta)$$

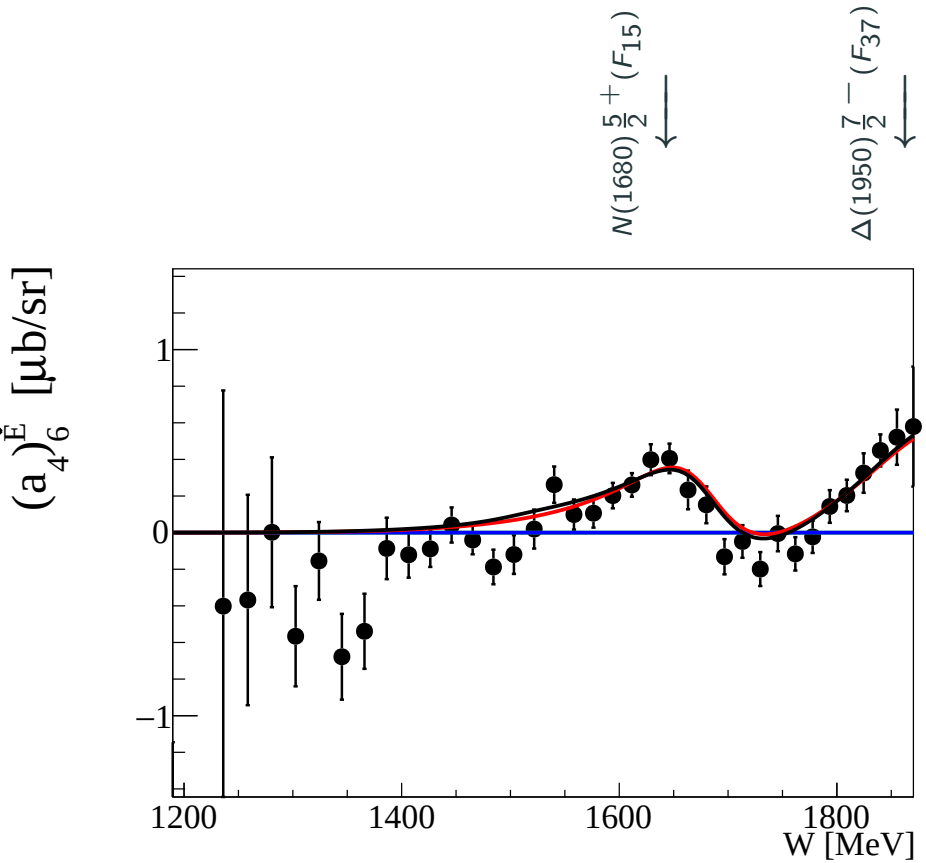

$$(a_4)_6^{\check{E}} = \langle F,F\rangle + \langle D,G\rangle + \langle G,G\rangle$$

F-waves are important above $W = 1450$ MeV and are well described by BnGa-2014-02 PWA.

Conclusion

Conclusion

- There are discrepancies between theory (quark models and lattics QCD calculations) and experiment regarding the nucleon excitation spectra
- Study of photoproduction reactions is important experimental tool to probe the nucleon excitation spectra
- Polarization observables need to be measured. They are sensitive to the interference terms of the partial waves
- Analysis of A2 data
  - Successful measurement of the double polarization observables E and G within the same beamtime using the A2 experiment
  - First experimental evidence that E can be measured with elliptically polarized photons
  - The obtained results of E comprise the most precise data set for both final states
  - $p\eta$ cusp can be observed in several Legendre coefficients of the $p\pi^0$ final state

Backup Slides

E_{0+} multipole in $\gamma p \to p\eta$

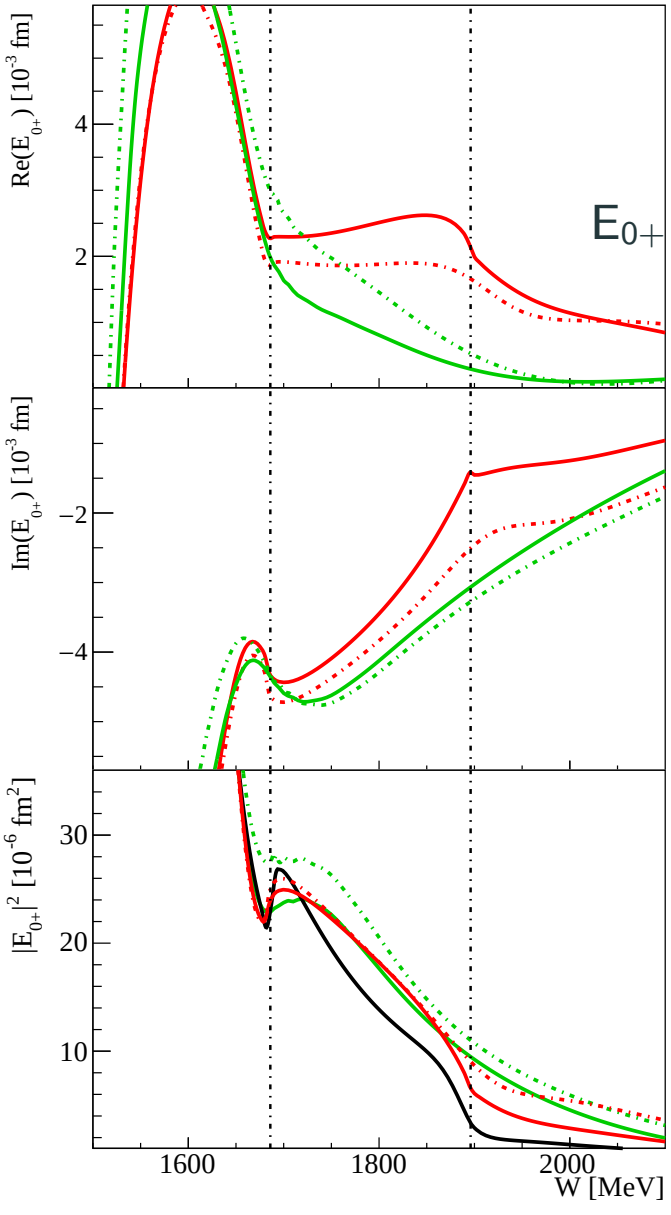

Mott measurement

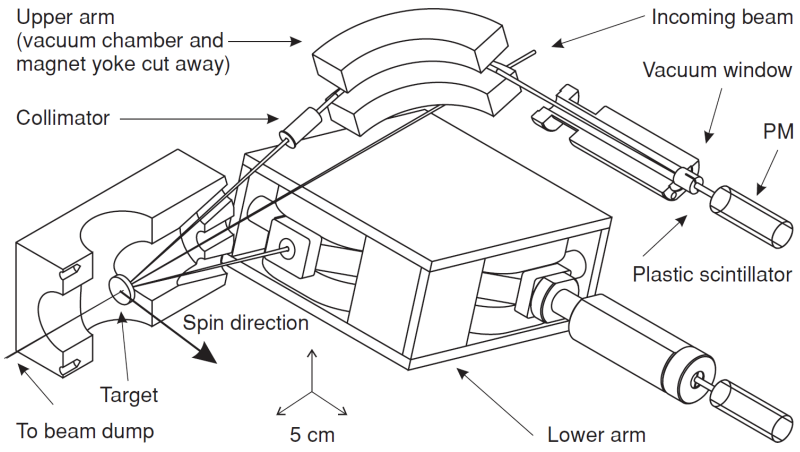

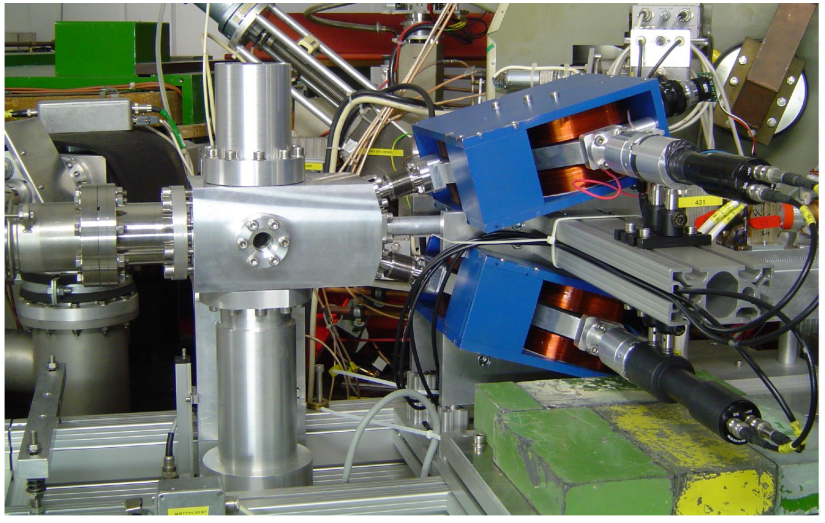

- Mott-scattering: elastic scattering of electrons in the Coulomb field of a heavy target nucleus (gold (Z=79)).
- interact via spin-orbit coupling $\rightarrow$ asymmetry in backscattering!
  $\rightarrow$ polarization degree of electrons
- helicity transfer from electrons to photons $\rightarrow$ circularly polarized photons

Elliptically polarized photons

- Calculation of photon circular polarization degree in crystals by I. M. Nadzhafov, Bull. Acad. Sci. USSR, Phys. Ser. Vol. 14, No. 10, p. 2248 (1976).

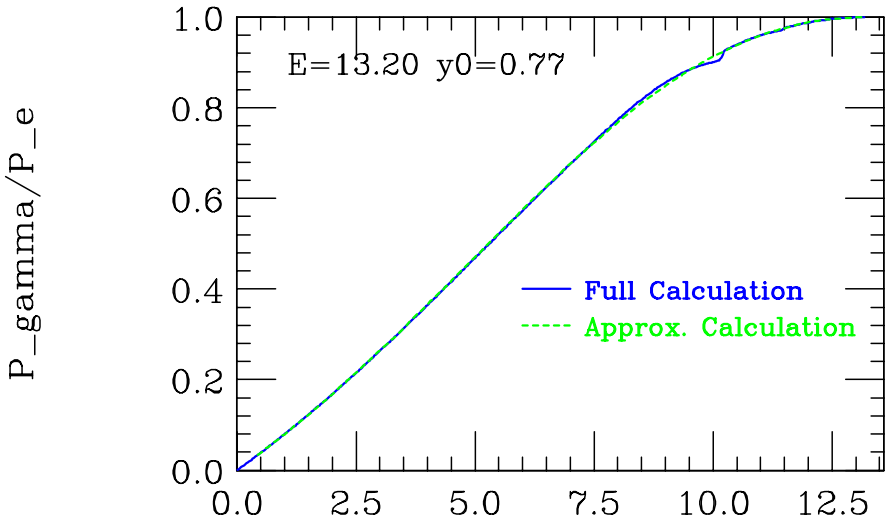

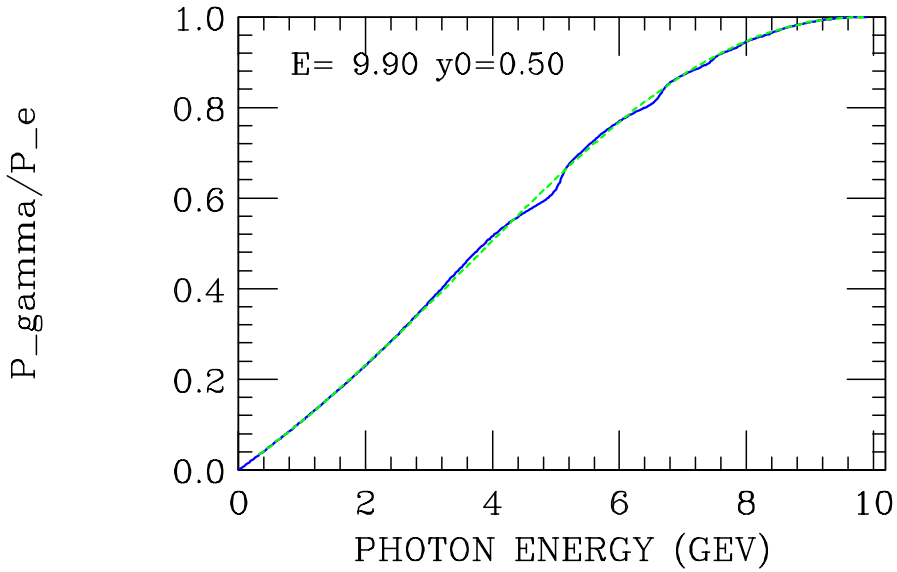

Bosted et al. (SLAC)

Comparison of diamond and amorphous data

- diamond runs with coherent edge at 450 MeV (elliptically polarized photons)
- Møller runs (amorphous radiator with circularly polarized photons)

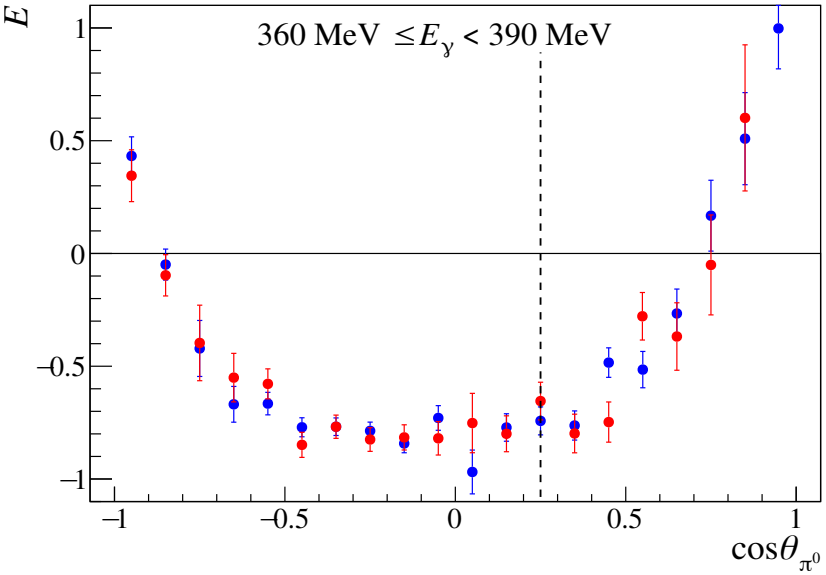

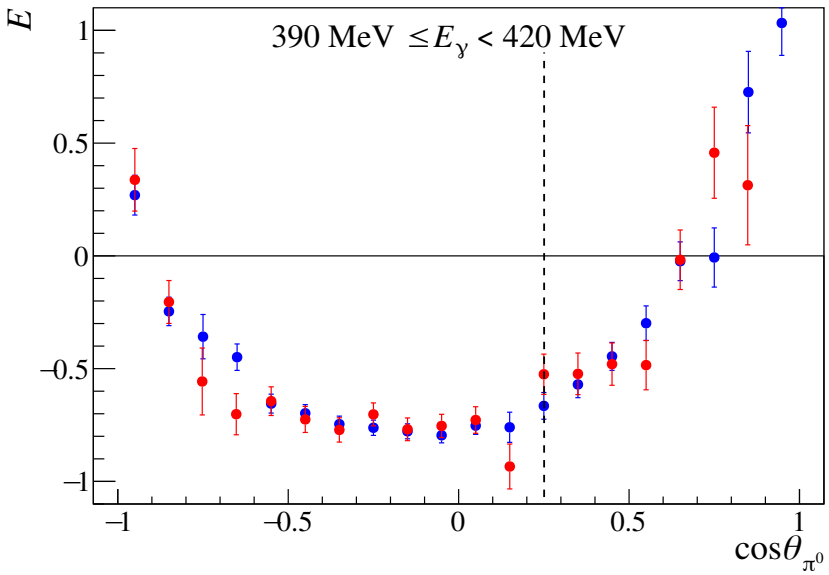

Comparison of diamond and amorphous data

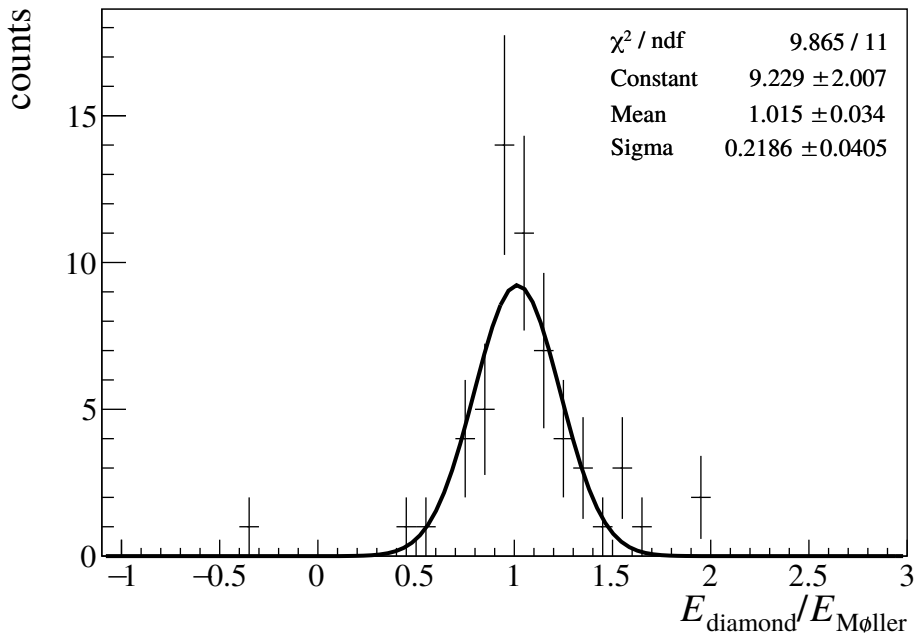

- first experimental evidence that the degree of circular polarization can be calculated in the same way for a diamond radiator as it is done for an amorphous radiator in a first approximation
- E can be determined using longitudinally polarized electrons and a diamond radiator

Dominant partial wave contributions (E (A2), $\gamma p \to p\eta$)

$$\check{\mathrm{E}}(W,\cos\theta) = \mathrm{E}(W,\cos\theta)\cdot\frac{d\sigma}{d\Omega}(W,\cos\theta) = \sum_{k=0}^{2L_{max}+1}(a_L(W))_k \cdot P_k^0(\cos\theta)$$

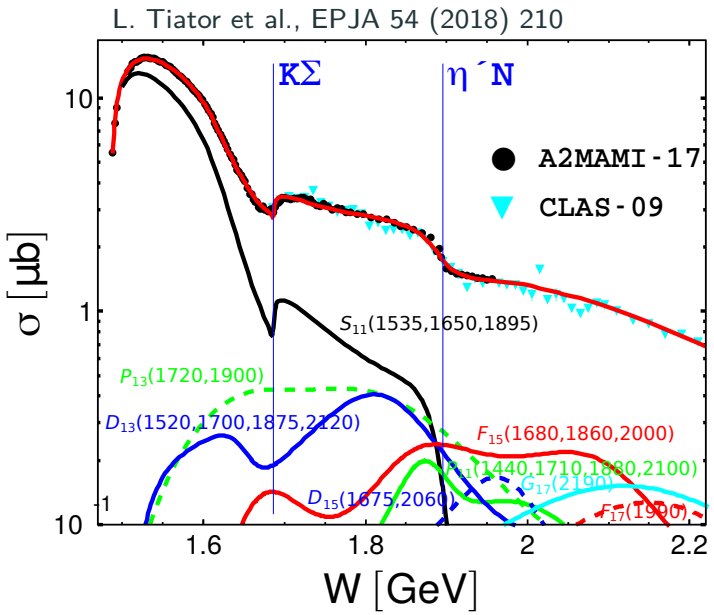

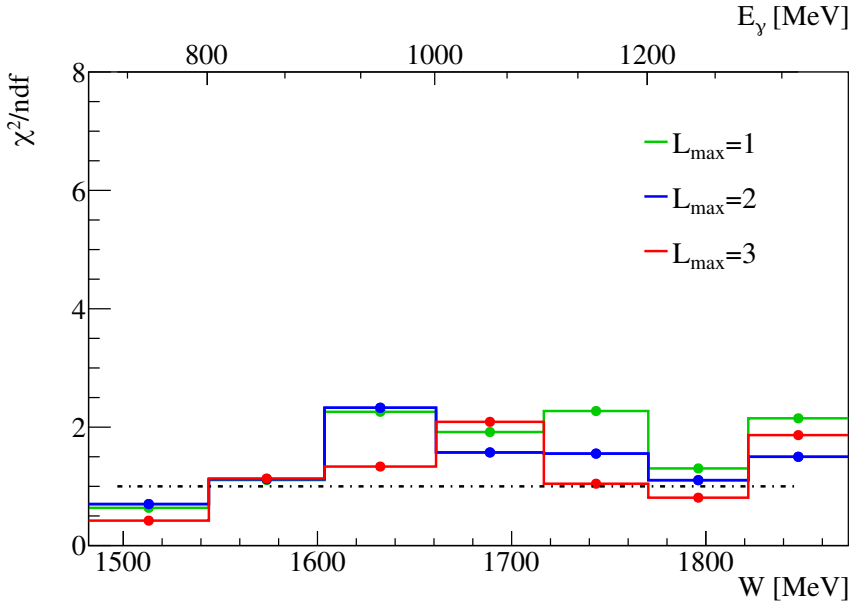

Dominant partial wave contributions (E (A2), $\gamma p \to p\eta$)

$$\check{\mathrm{E}}(W,\cos\theta) = \mathrm{E}(W,\cos\theta)\cdot\frac{d\sigma}{d\Omega}(W,\cos\theta) = \sum_{k=0}^{2L_{max}+1}(a_L(W))_k \cdot P_k^0(\cos\theta)$$

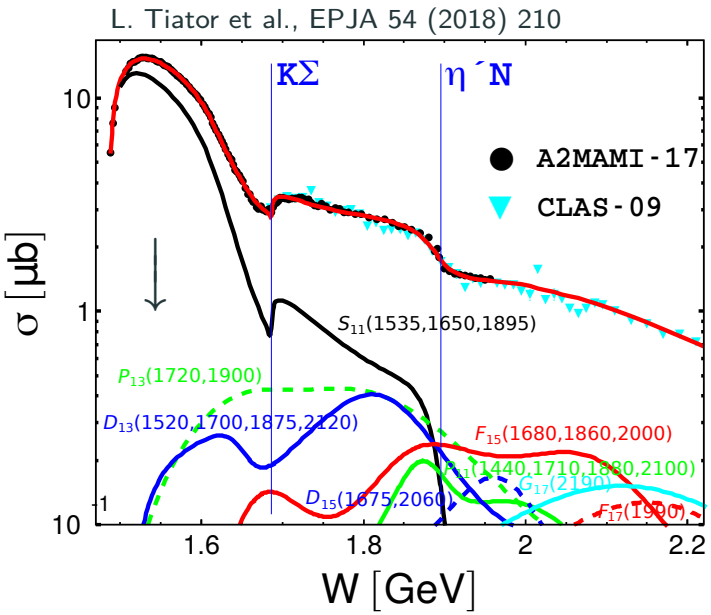

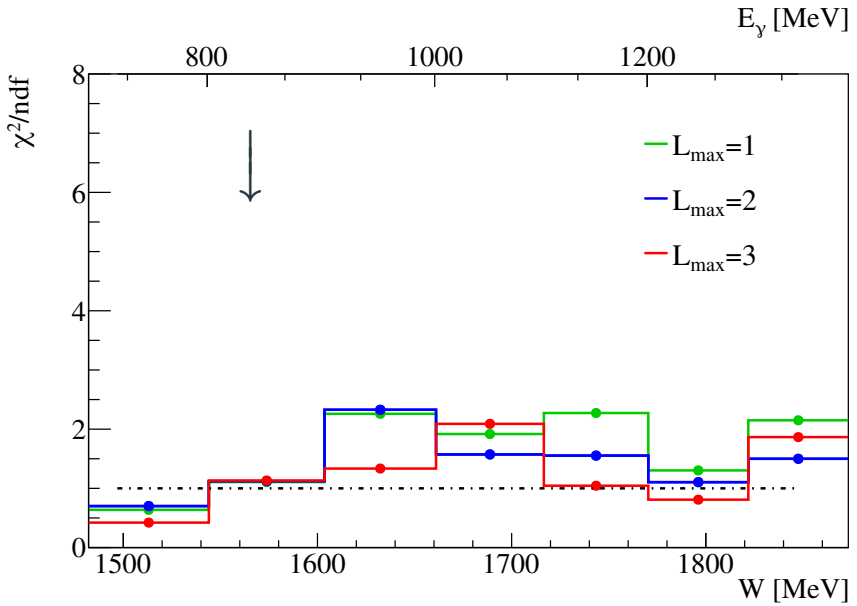

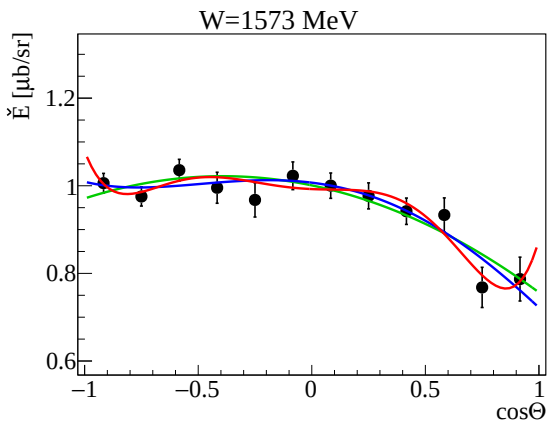

Dominant partial wave contributions (E (A2), $\gamma p \to p\eta$)

$$\check{\mathrm{E}}(W,\cos\theta) = \mathrm{E}(W,\cos\theta)\cdot\frac{d\sigma}{d\Omega}(W,\cos\theta) = \sum_{k=0}^{2L_{max}+1}(a_L(W))_k \cdot P_k^0(\cos\theta)$$

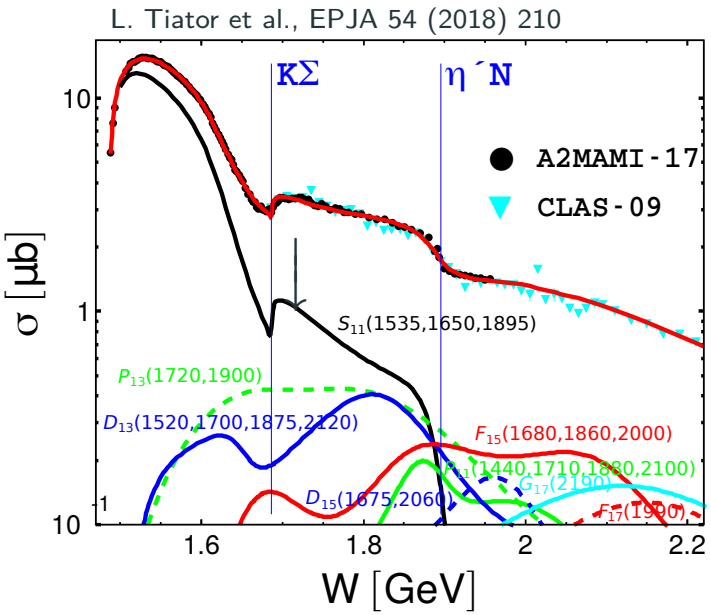

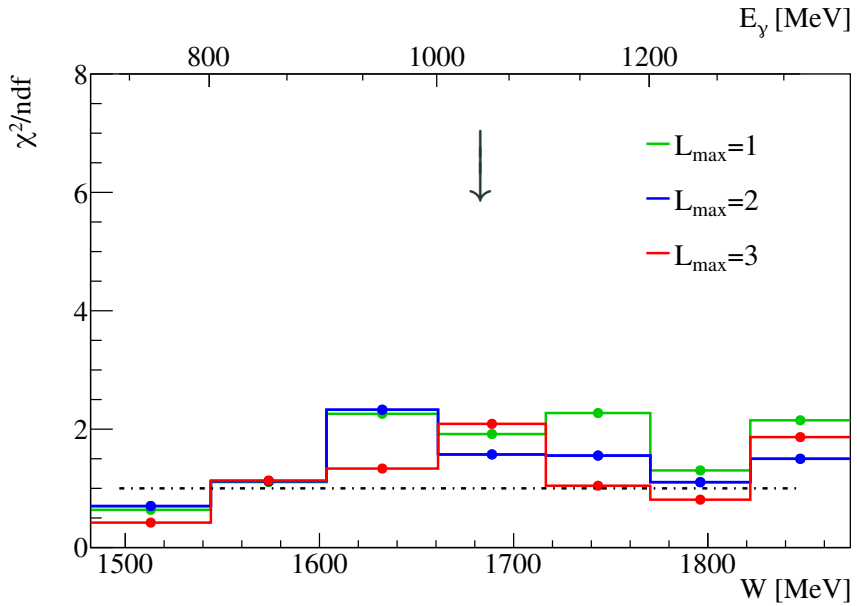

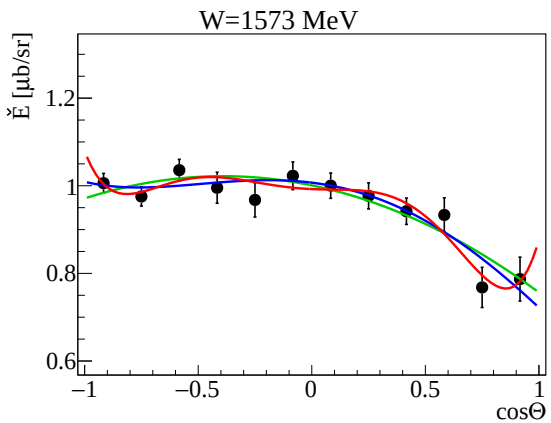

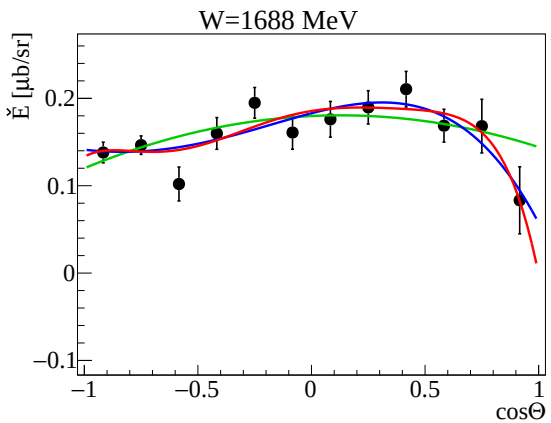

Dominant partial wave contributions (E (A2), $\gamma p \to p\eta$)

$$\check{\mathrm{E}}(W,\cos\theta) = \mathrm{E}(W,\cos\theta)\cdot\frac{d\sigma}{d\Omega}(W,\cos\theta) = \sum_{k=0}^{2L_{max}+1}(a_L(W))_k \cdot P_k^0(\cos\theta)$$

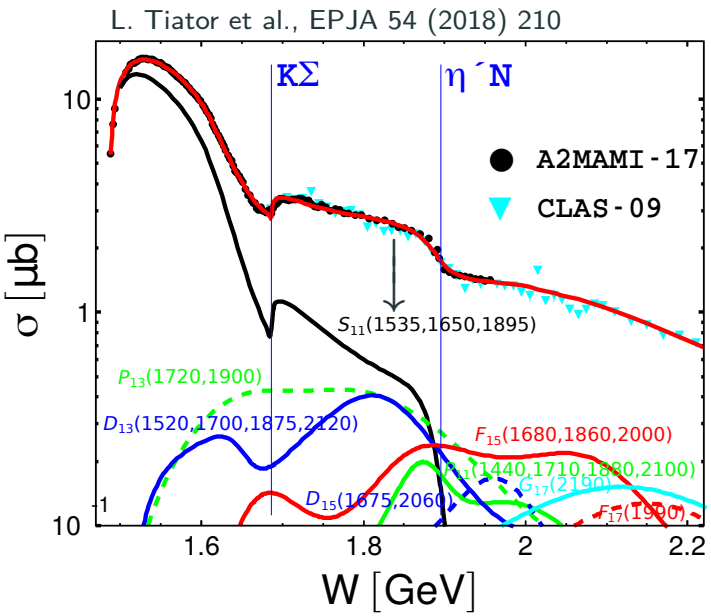

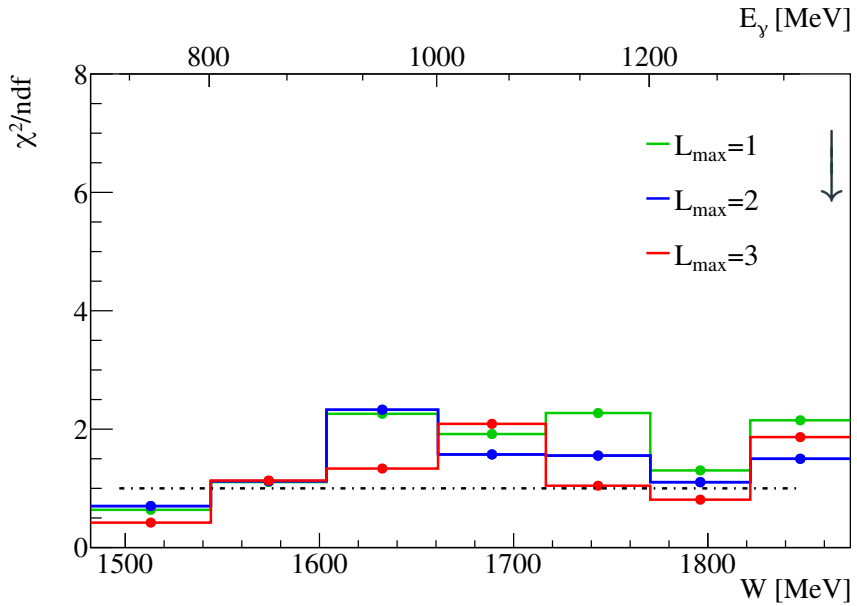

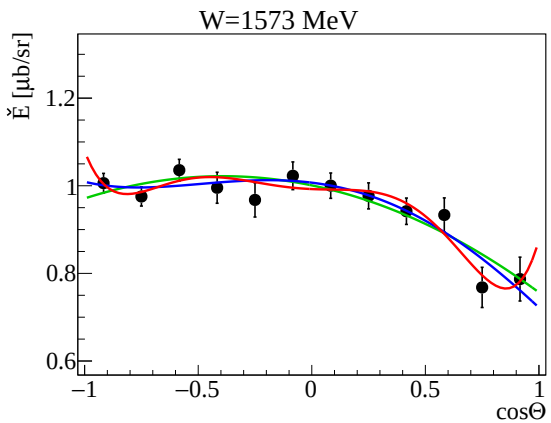

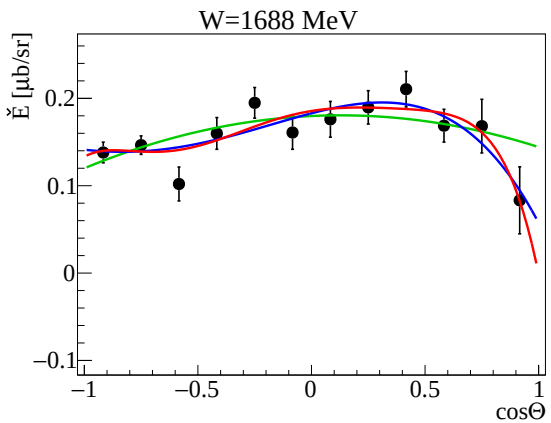

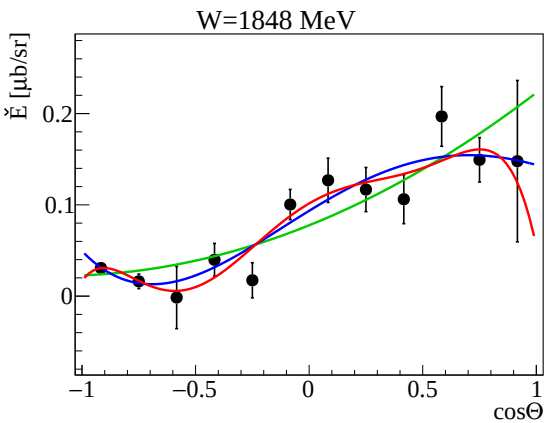

Dominant partial wave contributions (E (A2), $\gamma p \to p\eta$)

$$\check{\mathrm{E}}(W,\cos\theta) = \mathrm{E}(W,\cos\theta)\cdot\frac{d\sigma}{d\Omega}(W,\cos\theta) = \sum_{k=0}^{2L_{max}+1}(a_L(W))_k \cdot P_k^0(\cos\theta)$$

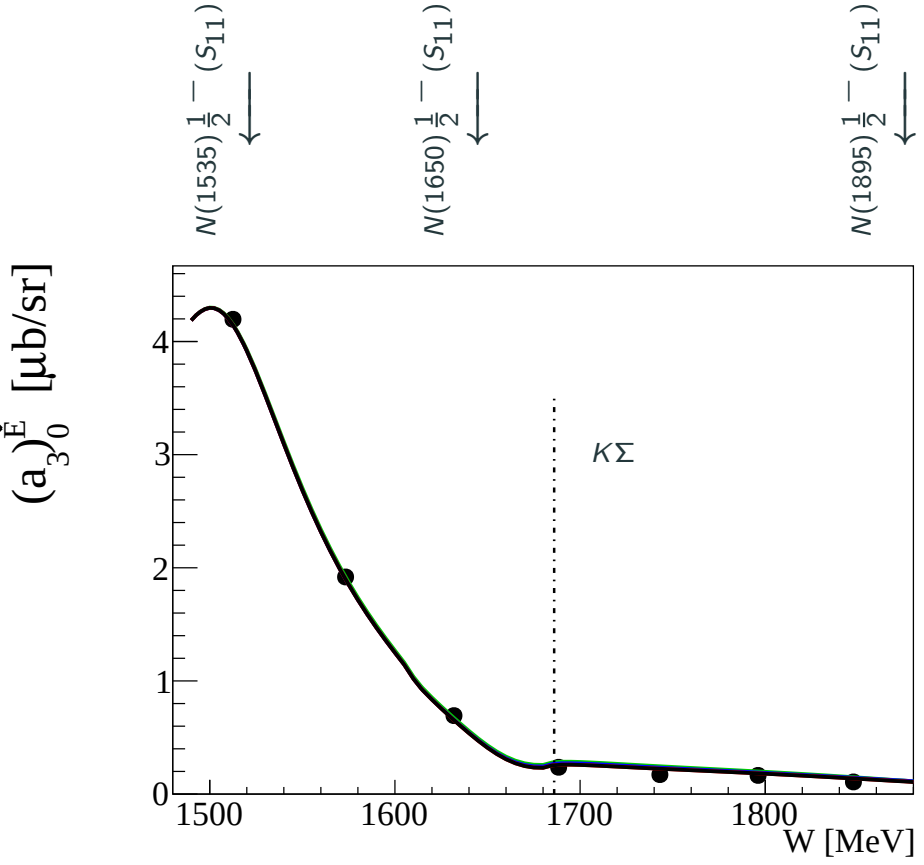

$$(a_4)_0^{\check{E}} = \langle S,S\rangle + \langle P,P\rangle + \langle D,D\rangle + \langle F,F\rangle + \langle G,G\rangle$$

Only interference terms of the same L. Similar to differential cross section.

S-wave dominates in η photoproduction.

Dominant partial wave contributions (E (A2), $\gamma p \to p\eta$)

$$\check{\mathrm{E}}(W,\cos\theta) = \mathrm{E}(W,\cos\theta)\cdot\frac{d\sigma}{d\Omega}(W,\cos\theta) = \sum_{k=0}^{2L_{max}+1}(a_L(W))_k \cdot P_k^0(\cos\theta)$$

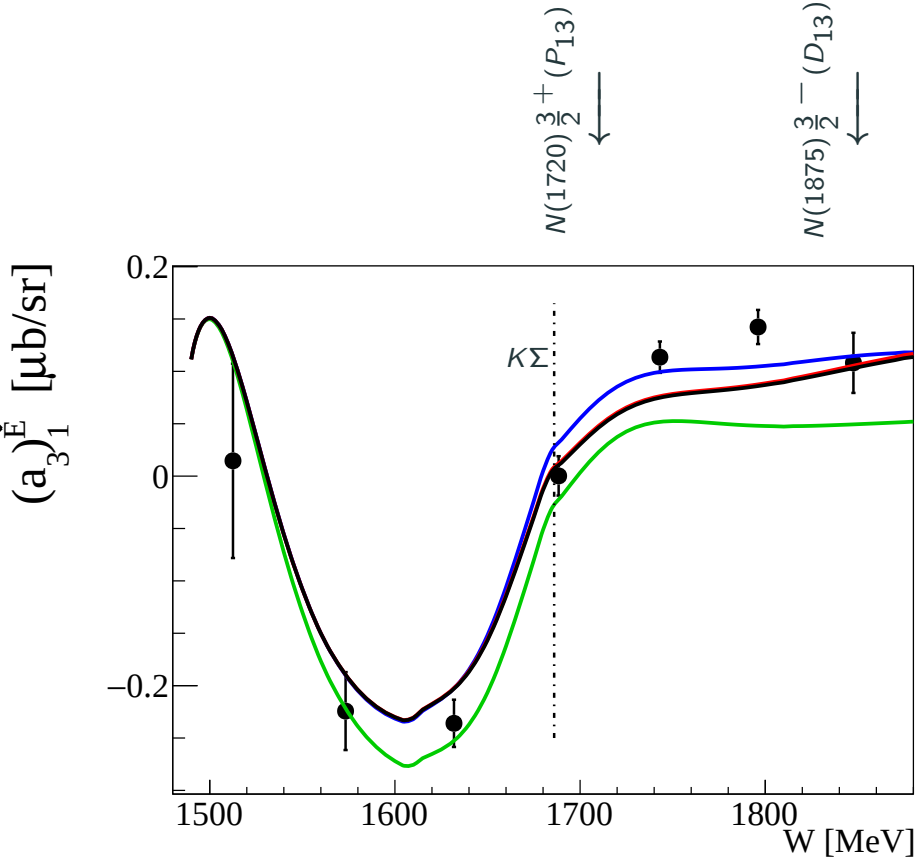

$$(a_4)_1^{\check{E}} = \langle S,P\rangle + \langle P,D\rangle + \langle D,F\rangle + \langle F,G\rangle$$

$< S, P >$ interference term dominates here.

Indications for $K\Lambda$ and $K\Sigma$ cusps.

Dominant partial wave contributions (E (A2), $\gamma p \to p\eta$)

$$\check{\mathrm{E}}(W,\cos\theta) = \mathrm{E}(W,\cos\theta)\cdot\frac{d\sigma}{d\Omega}(W,\cos\theta) = \sum_{k=0}^{2L_{max}+1}(a_L(W))_k \cdot P_k^0(\cos\theta)$$

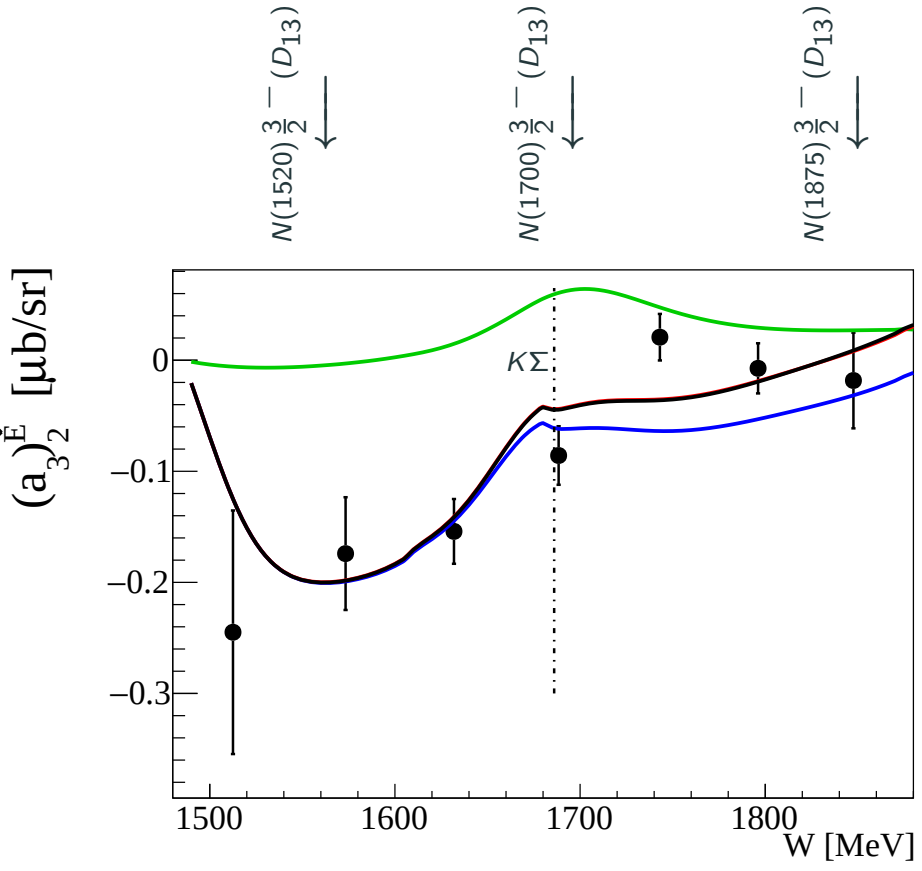

$$(a_4)_2^{\check{E}} = \langle P,P\rangle + \langle S,D\rangle + \langle D,D\rangle + \langle P,F\rangle + \langle F,F\rangle + \langle D,G\rangle + \langle G,G\rangle$$

$< S, D >$ interference term dominates here.

Indications for $K\Lambda$ and $K\Sigma$ cusps.

Dominant partial wave contributions (E (A2), $\gamma p \to p\eta$)

$$\check{\mathrm{E}}(W,\cos\theta) = \mathrm{E}(W,\cos\theta)\cdot\frac{d\sigma}{d\Omega}(W,\cos\theta) = \sum_{k=0}^{2L_{max}+1}(a_L(W))_k \cdot P_k^0(\cos\theta)$$

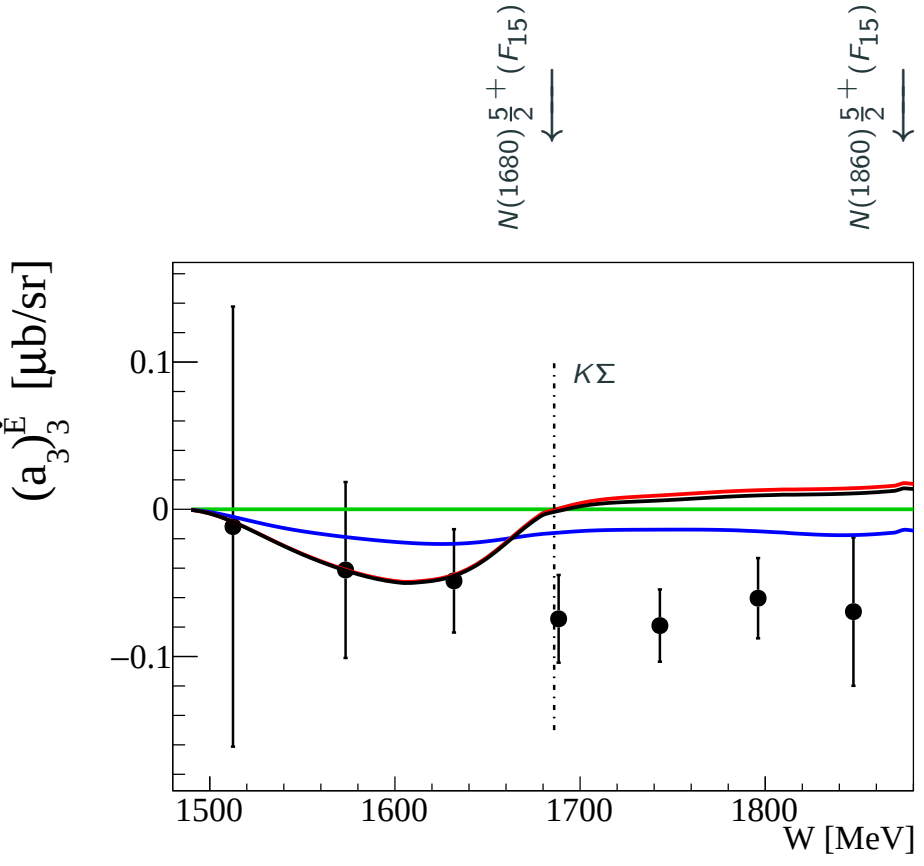

$$(a_4)_3^{\check{E}} = \langle P, D\rangle + \langle S, F\rangle + \langle D, F\rangle + \langle P, G\rangle + \langle F, G\rangle$$

Above $K\Sigma$ threshold the $< S, F >$ and $< D, F >$ terms do not describe the data.

How to determine the scaling factor?

$$s^C(E_\gamma, \cos\theta) = \frac{\epsilon^{\text{but}}(E_\gamma, \cos\theta) \cdot n_\gamma^{\text{but}}(E_\gamma) \cdot n_T^{\text{but}}}{\epsilon^C(E_\gamma, \cos\theta) \cdot n_\gamma^C(E_\gamma) \cdot n_T^C}$$

$$s^C(E_\gamma) \approx \frac{n_\gamma^{\text{but}}(E_\gamma) \cdot n_T^{\text{but}}}{n_\gamma^C(E_\gamma) \cdot n_T^C}$$

How to determine the scaling factor?

$$s^C(E_\gamma, \cos\theta) = \frac{\epsilon^{\text{but}}(E_\gamma, \cos\theta) \cdot n_\gamma^{\text{but}}(E_\gamma) \cdot n_T^{\text{but}}}{\epsilon^C(E_\gamma, \cos\theta) \cdot n_\gamma^C(E_\gamma) \cdot n_T^C}$$

$$s^C(E_\gamma) \approx \frac{n_\gamma^{\text{but}}(E_\gamma) \cdot n_T^{\text{but}}}{n_\gamma^C(E_\gamma) \cdot n_T^C}$$

$$s^C \cdot N^C_{\text{non-hydrogen region}} = N^{\text{but}}_{\text{non-hydrogen region}}$$

$$s^C = \frac{N^{\text{but}}_{\text{non-hydrogen region}}}{N^C_{\text{non-hydrogen region}}}$$

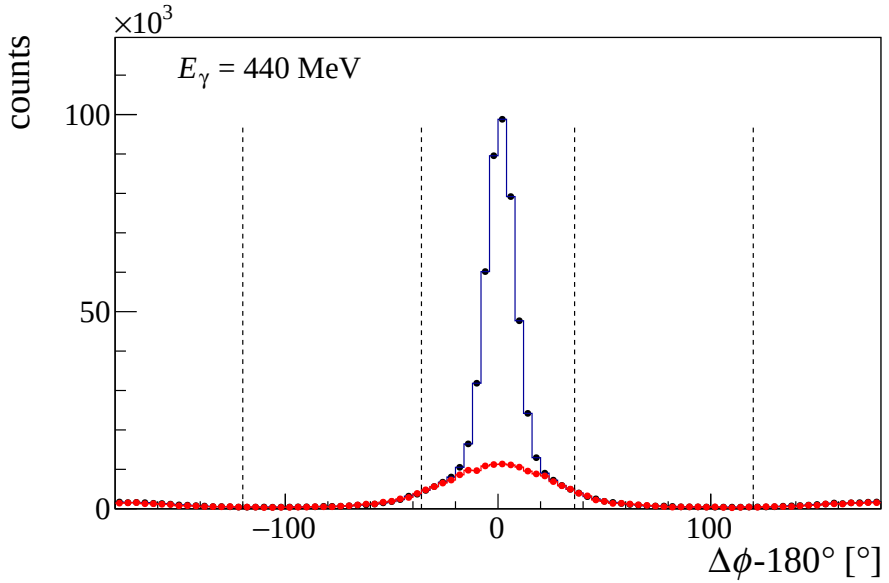

Scaling factor - Comparison of methods

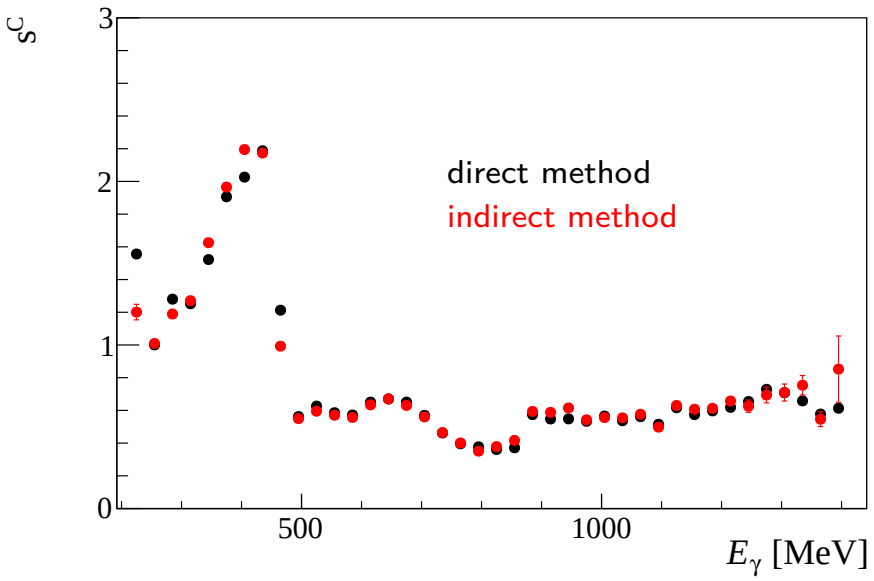

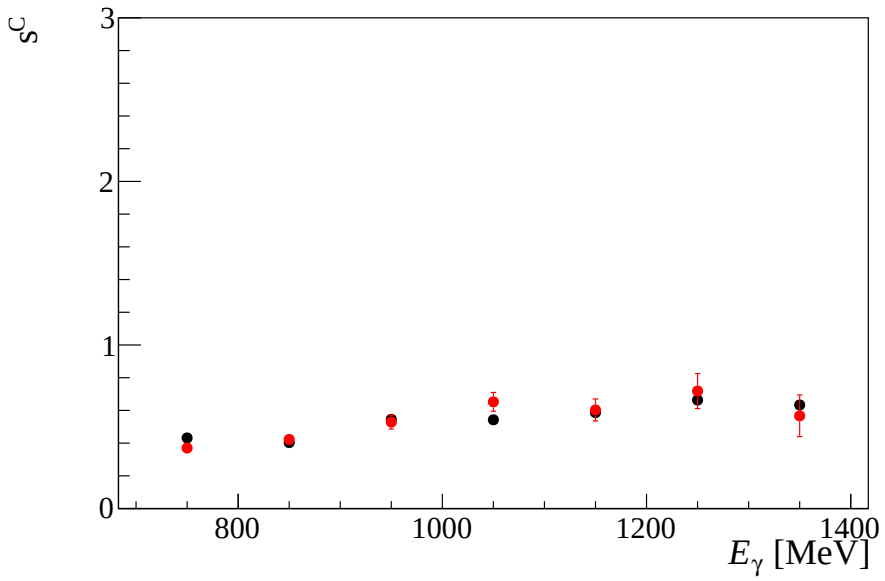

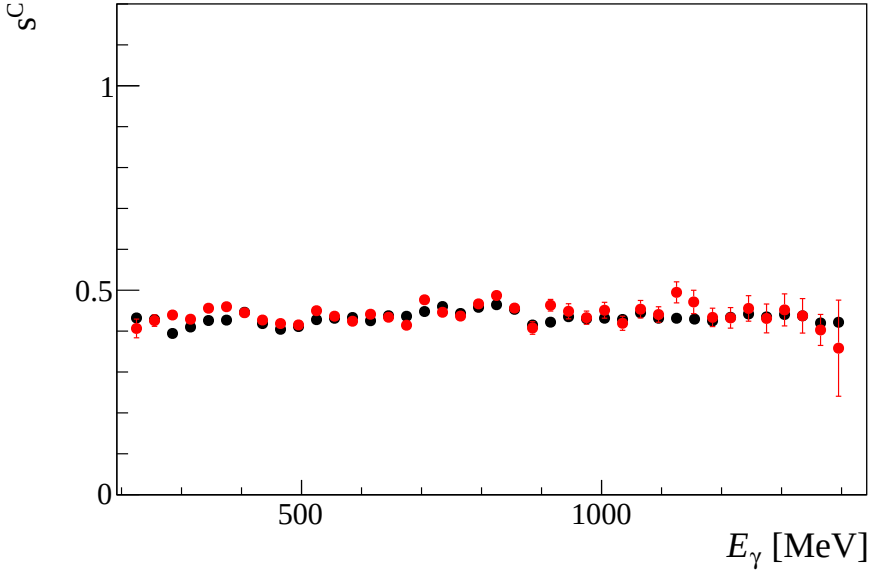

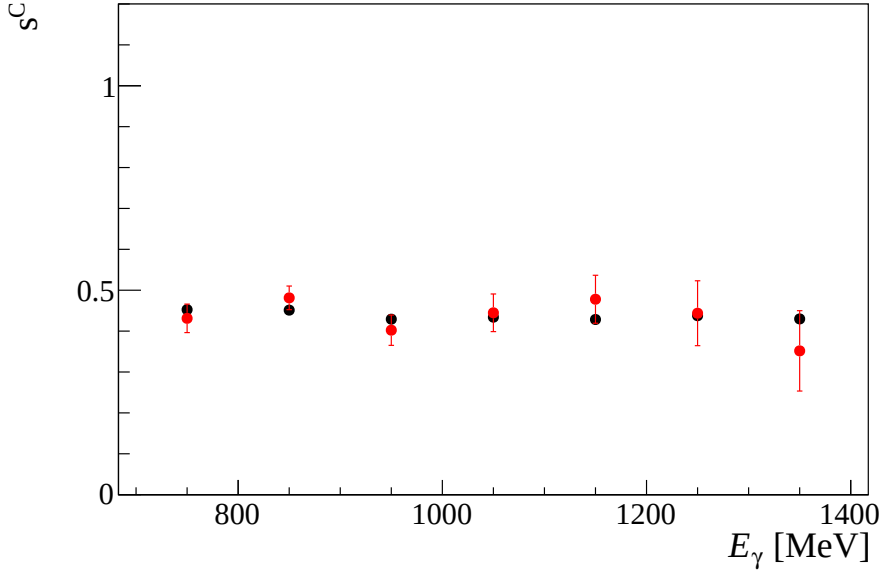

Scaling factor - Comparison of final states

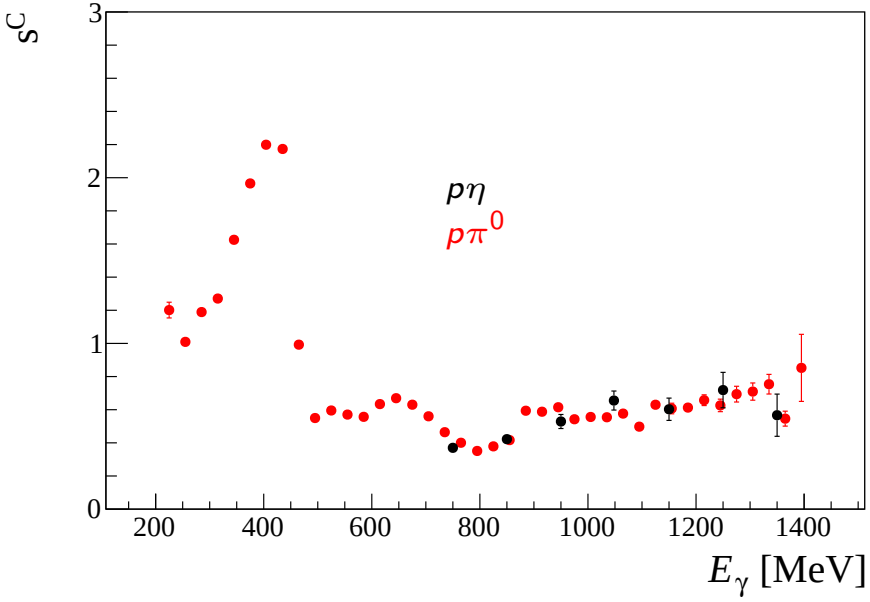

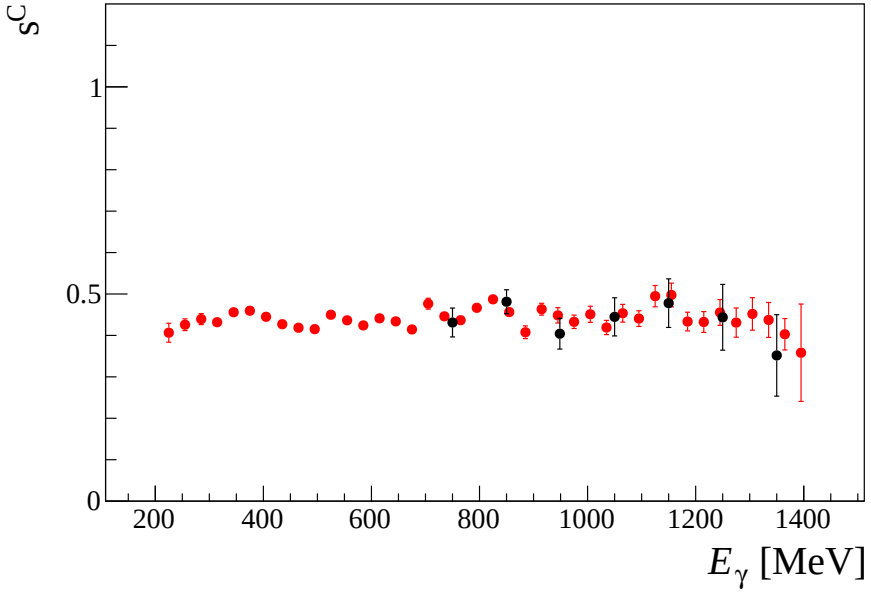

Dilution factor

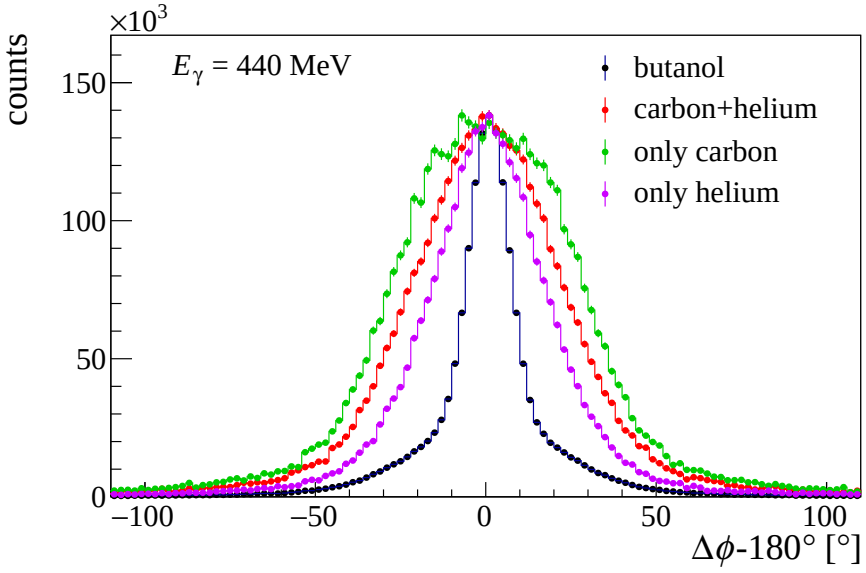

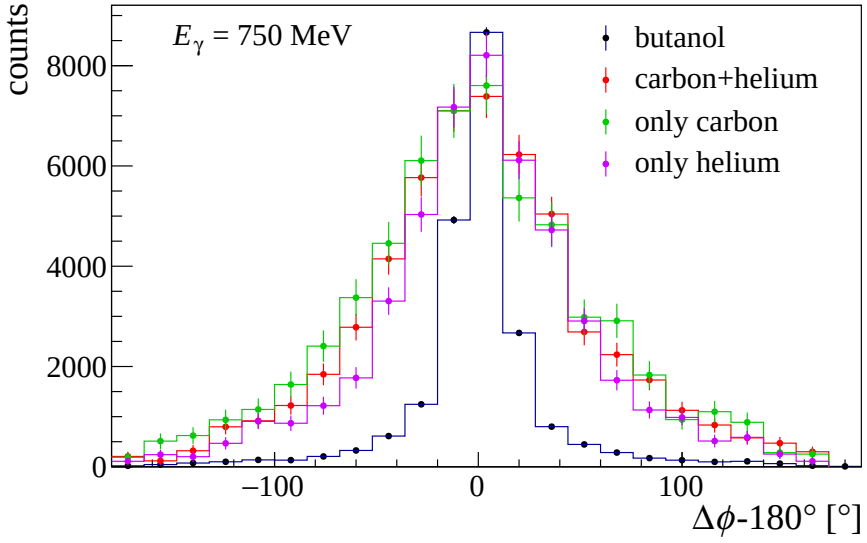

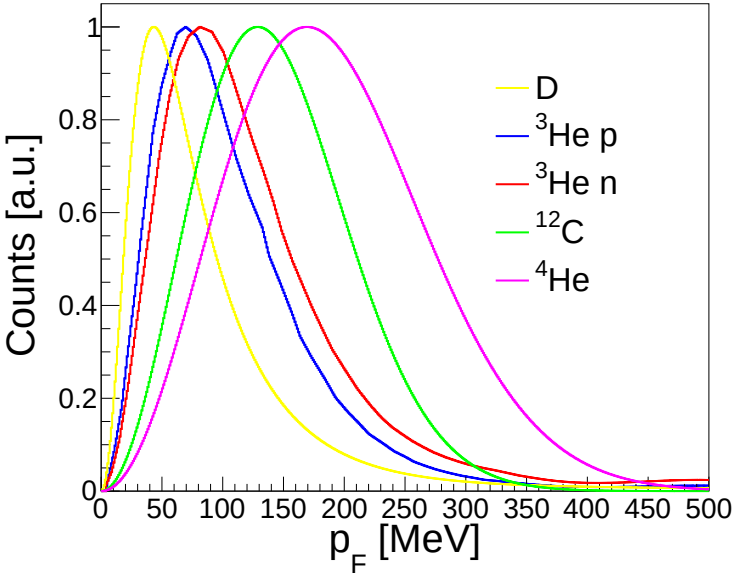

Dilution factor

It is important to measure with helium!

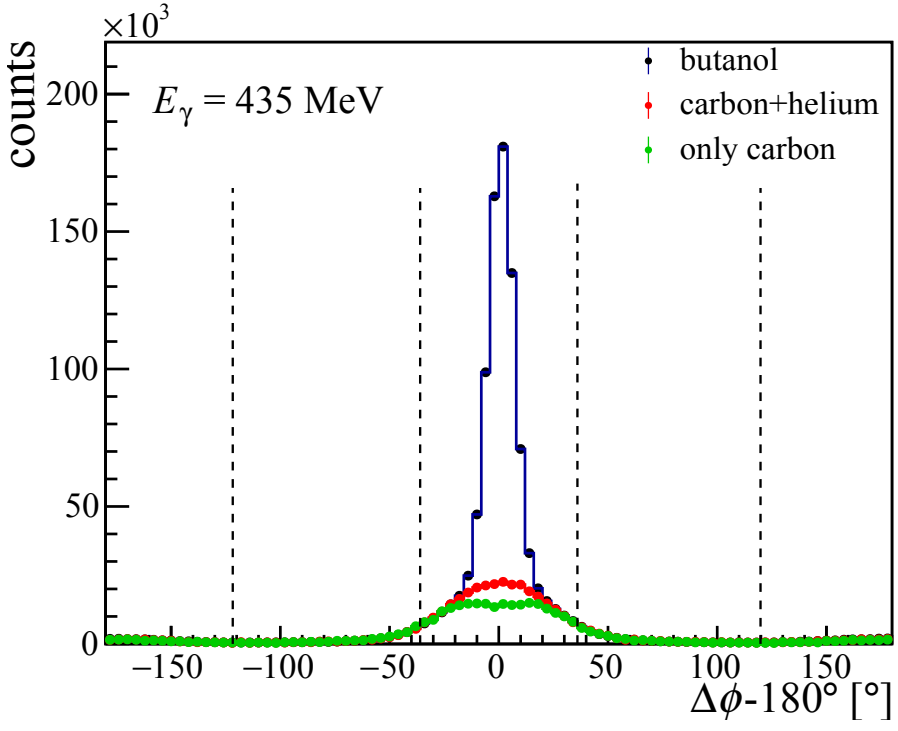

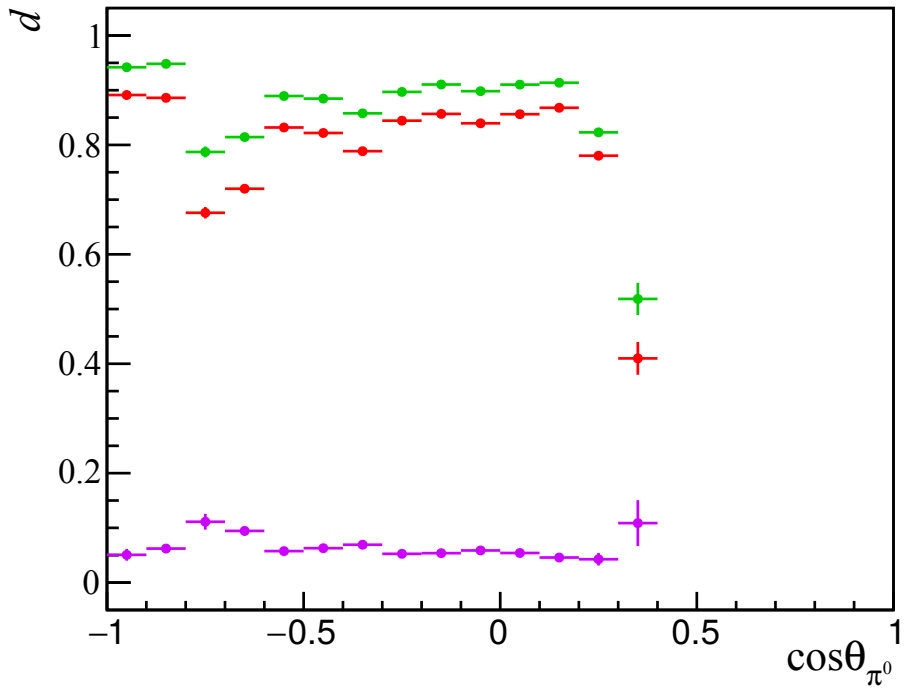

Dilution factor ($p\pi^0$ final state)

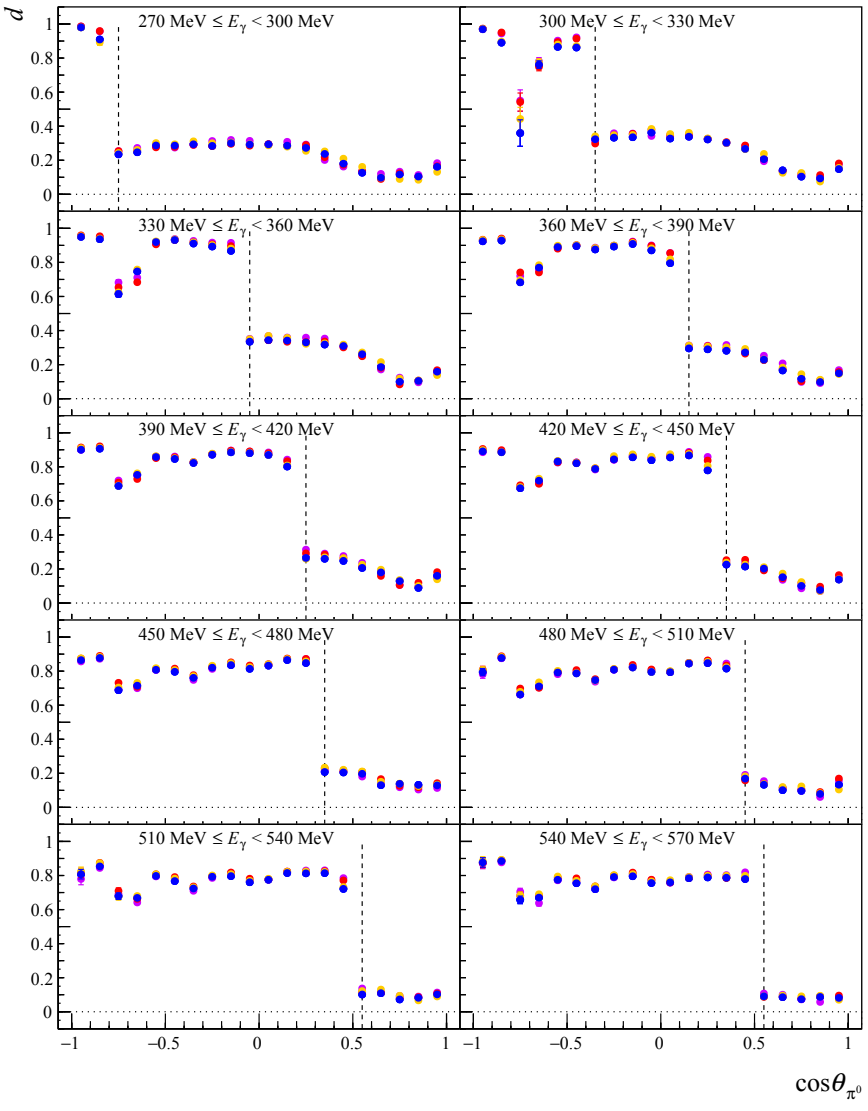

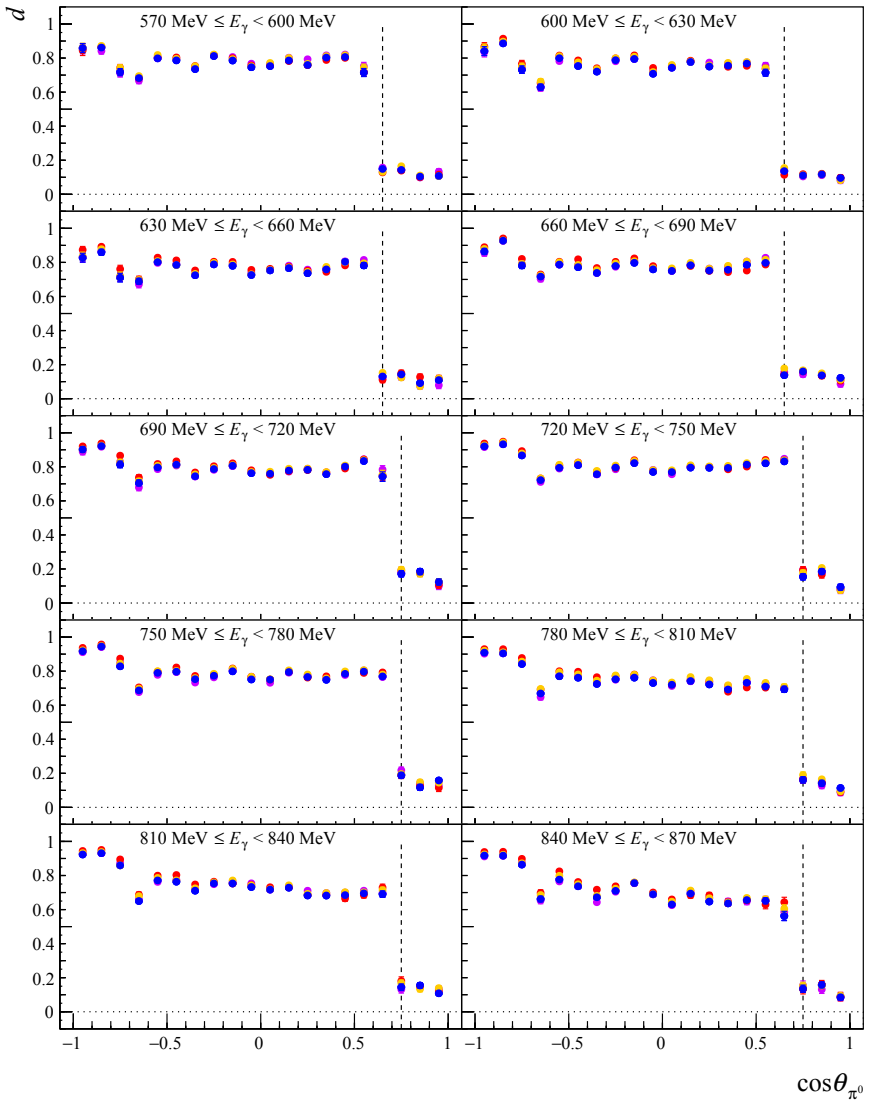

Problems with the target polarization degree (A2 data) (I)

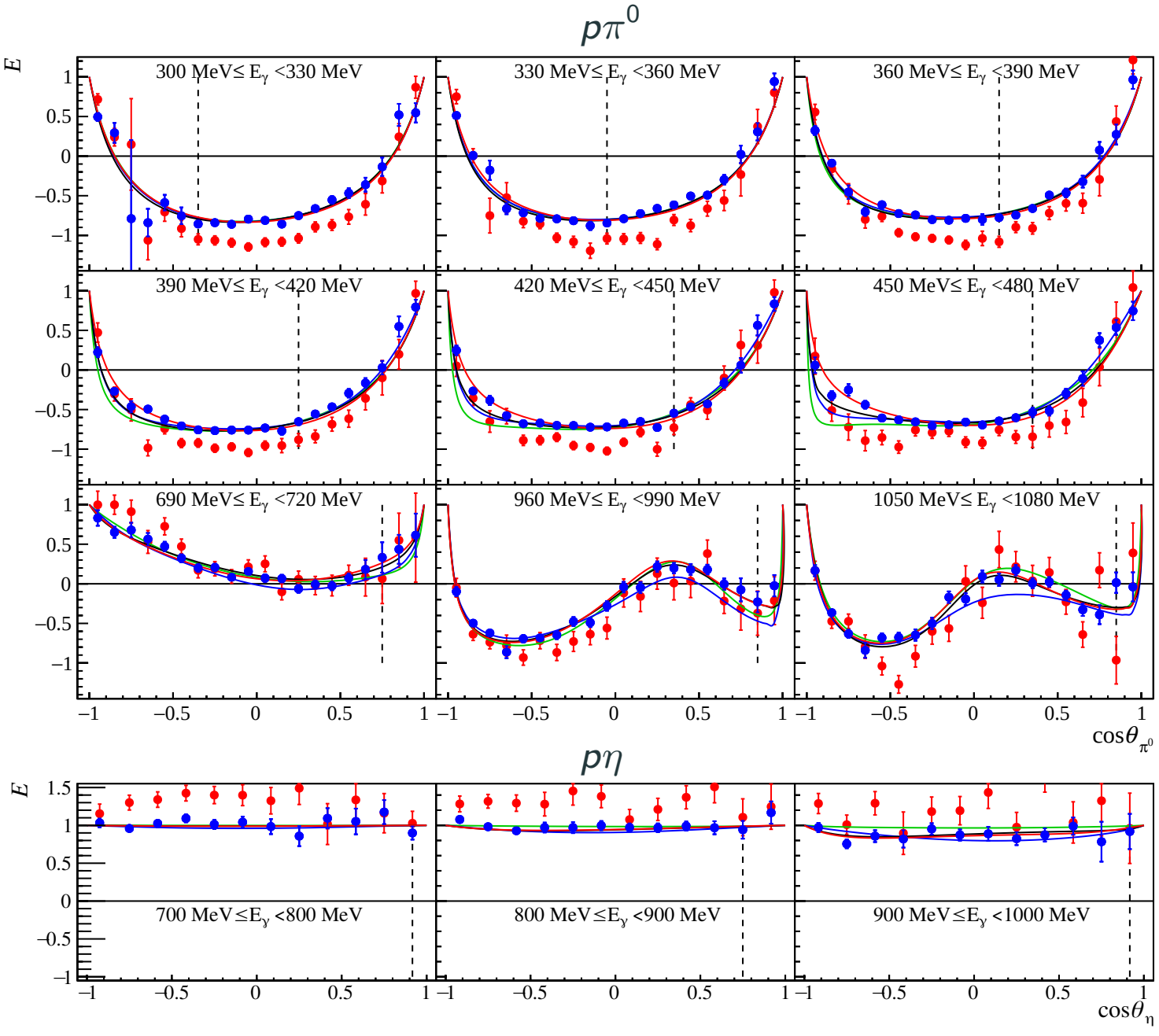

- November 2013
- September 2015

Problems with the target polarization degree (A2 data) (II)

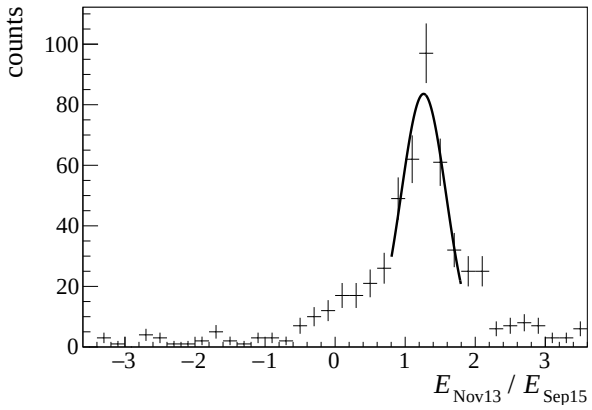

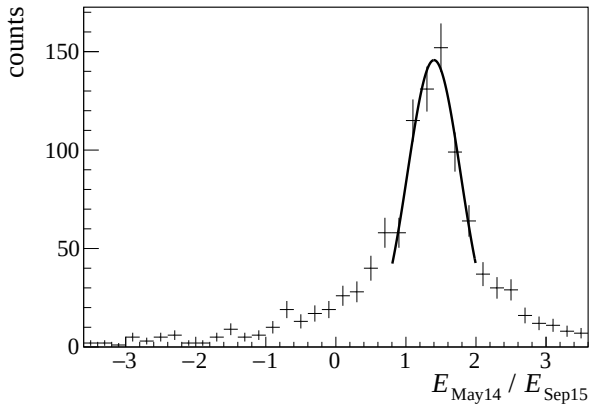

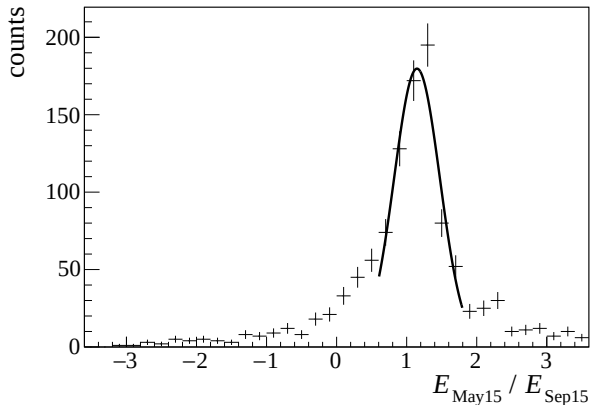

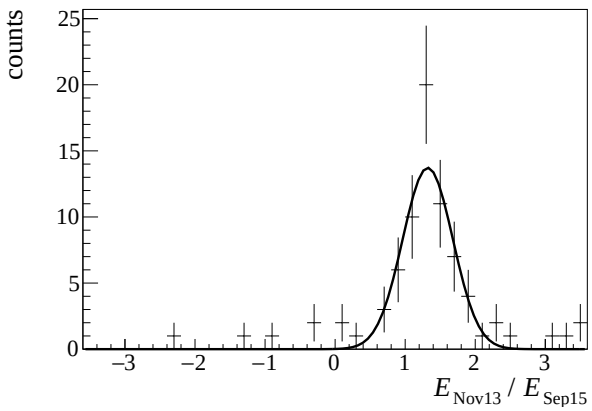

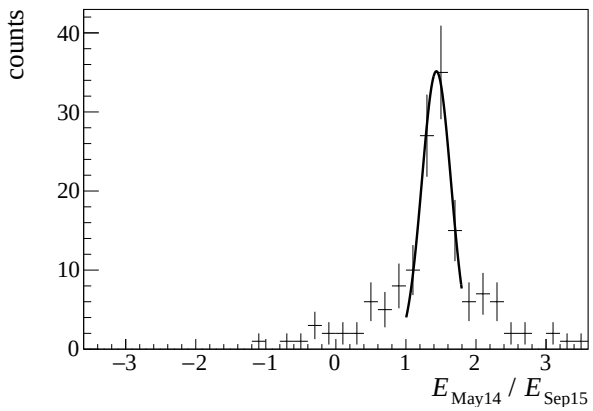

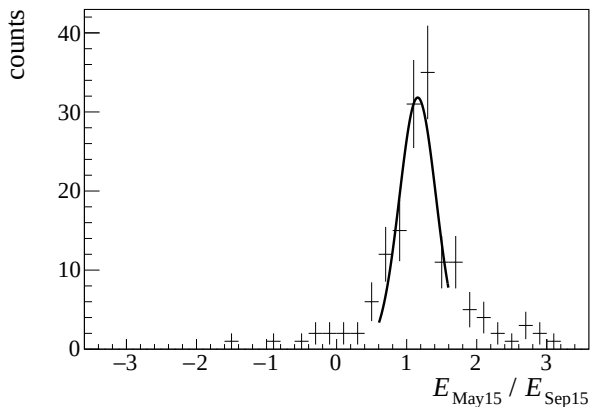

channel/beamtime	November 2013	May 2014	May 2015
$p\pi^0$	1.27 ± 0.03	1.40 ± 0.03	1.15 ± 0.02
$p\eta$	1.30 ± 0.05	1.39 ± 0.04	1.17 ± 0.03
mean	1.29 ± 0.02	1.40 ± 0.01	1.16 ± 0.02

Problems with the target polarization degree (A2 data) (III)

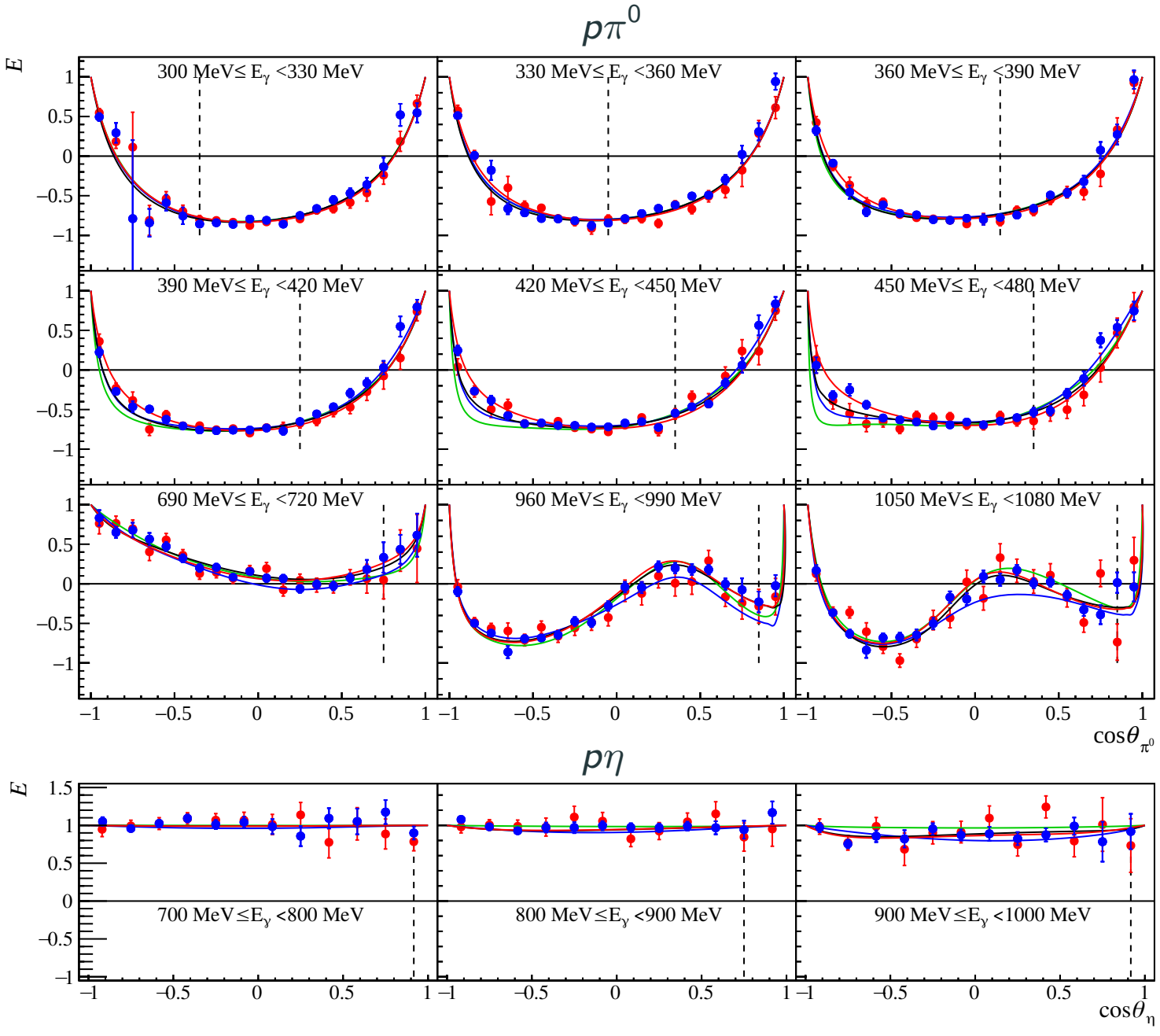

- November 2013
- September 2015

Systematic error - circular and target pol. degree (A2 data)

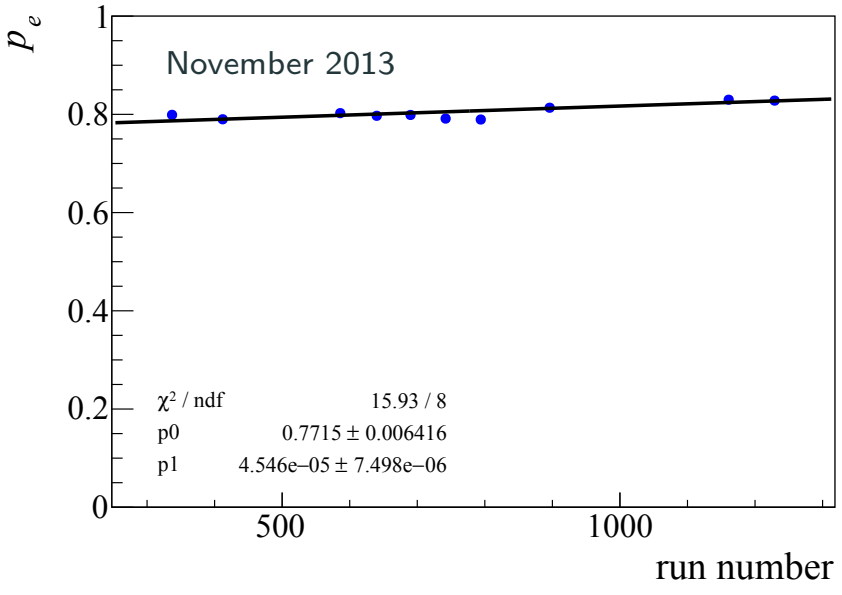

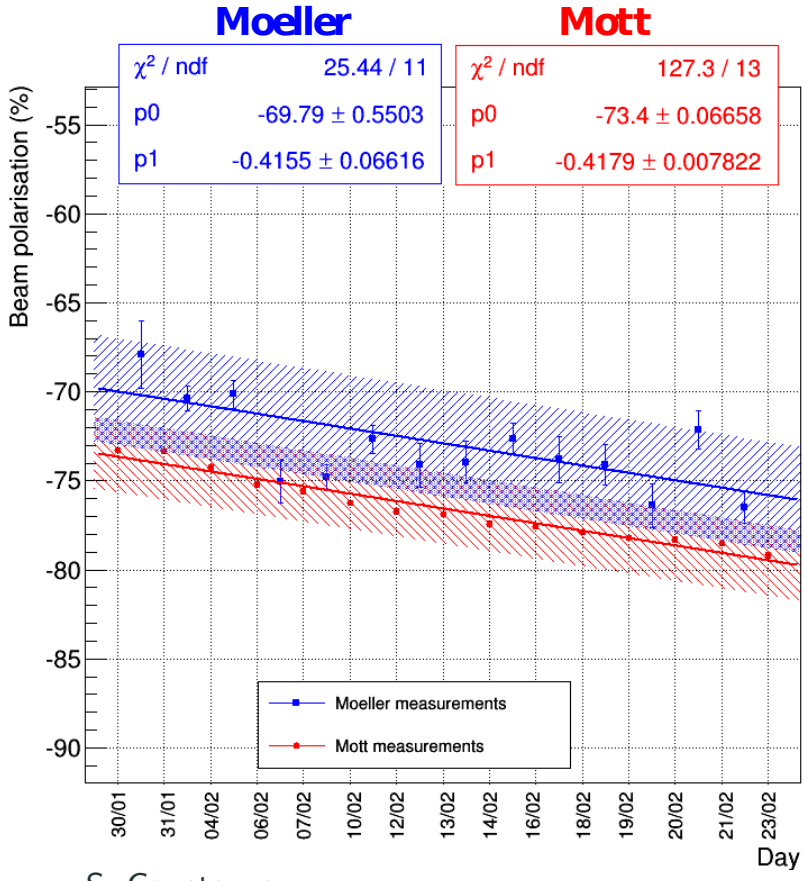

S. Constanza

$$\frac{\Delta p_\gamma^{\text{circ}}}{p_\gamma^{\text{circ}}} = 2.7\%.$$

Systematic error - circular and target pol. degree (A2 data)

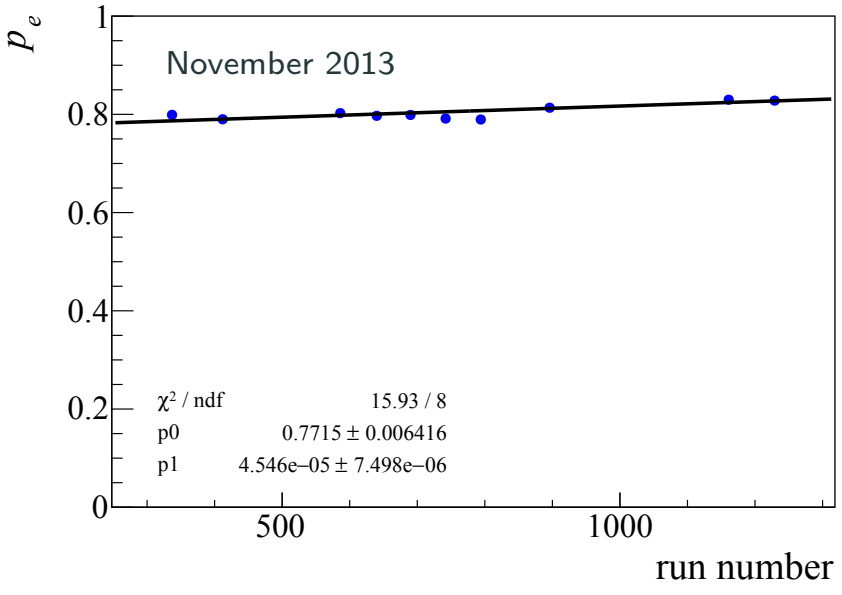

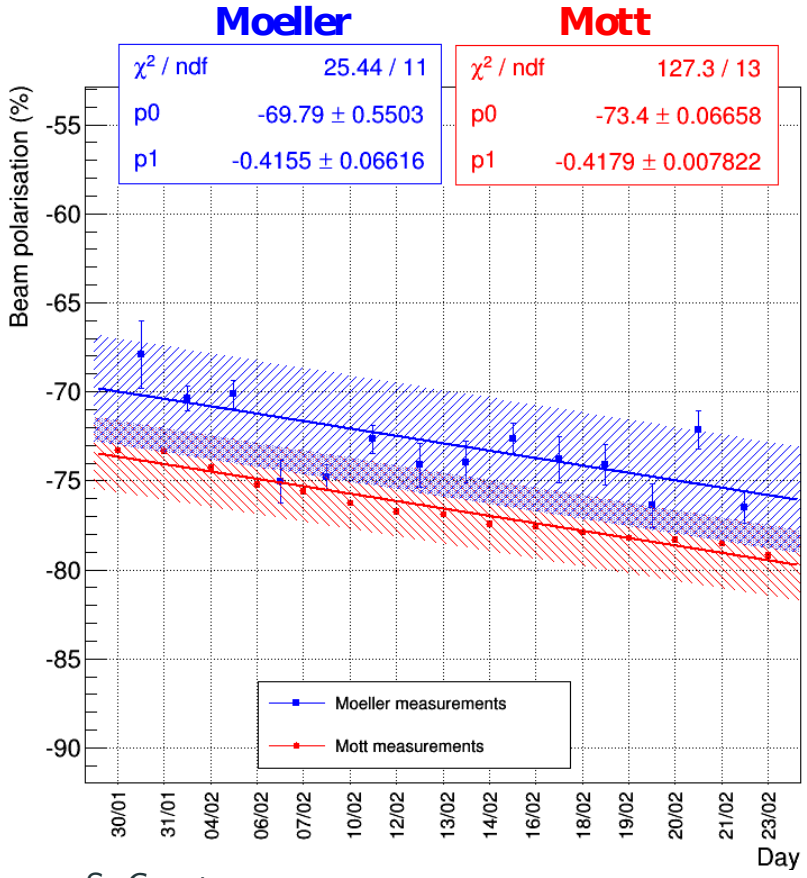

S. Constanza

$$\frac{\Delta p_\gamma^{\text{circ}}}{p_\gamma^{\text{circ}}} = 2.7\%.$$

$$\frac{\Delta p_T}{p_T} = \sqrt{(2\%)^2 + (2\%)^2} = 2.8\%.$$

Systematic error - background and dilution factor (A2 data)

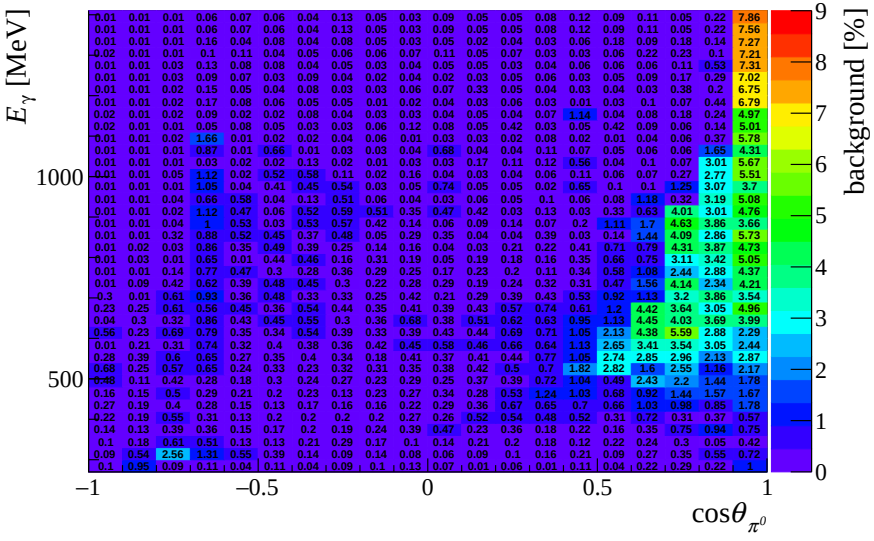

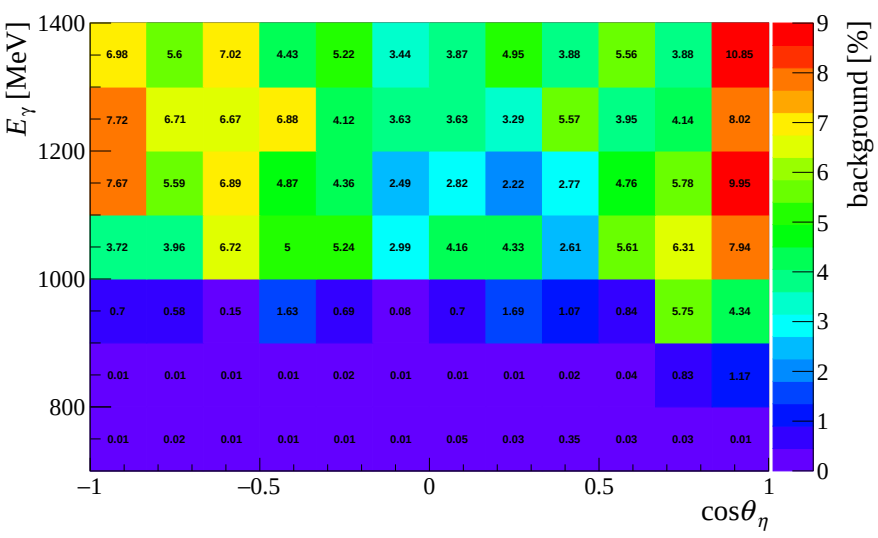

$$\Delta E^{\text{bg, abs}} \lesssim \delta^{\text{bg}}$$

Systematic error - background and dilution factor (A2 data)

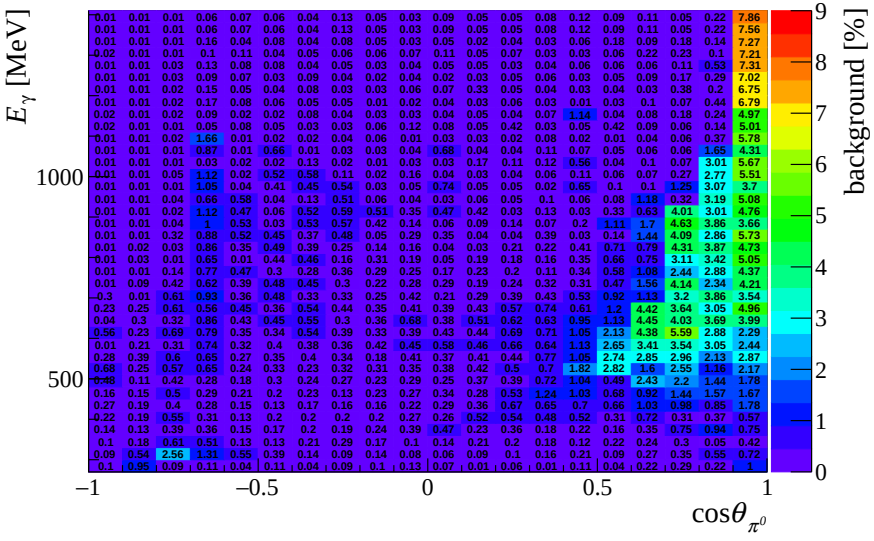

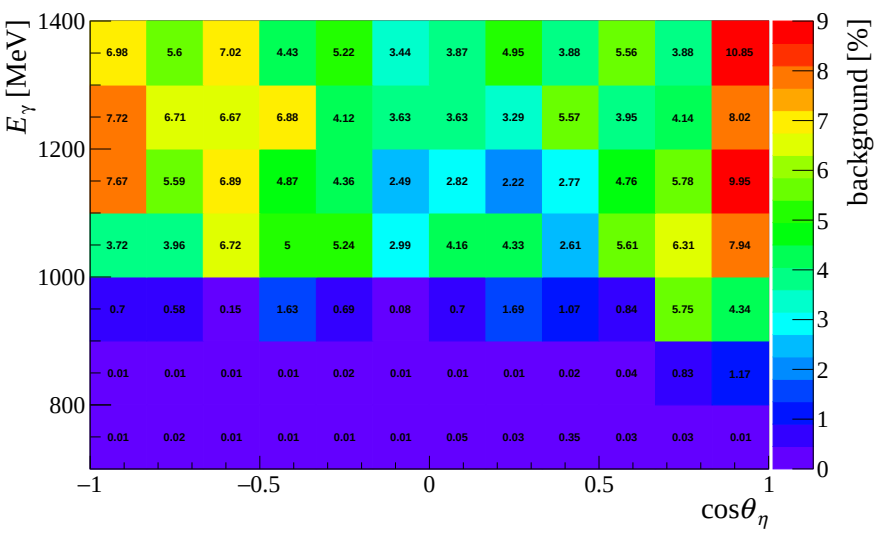

$$\Delta E^{\text{bg, abs}} \lesssim \delta^{\text{bg}}$$

$$\frac{\Delta d}{d} = \frac{1-d}{d}\frac{\Delta s^C}{s^C}, \qquad \frac{\Delta s^C}{s^C} = \sqrt{(0.03)^2 + (0.015)^2} \approx 0.034$$

The helicity asymmetry E in η photoproduction

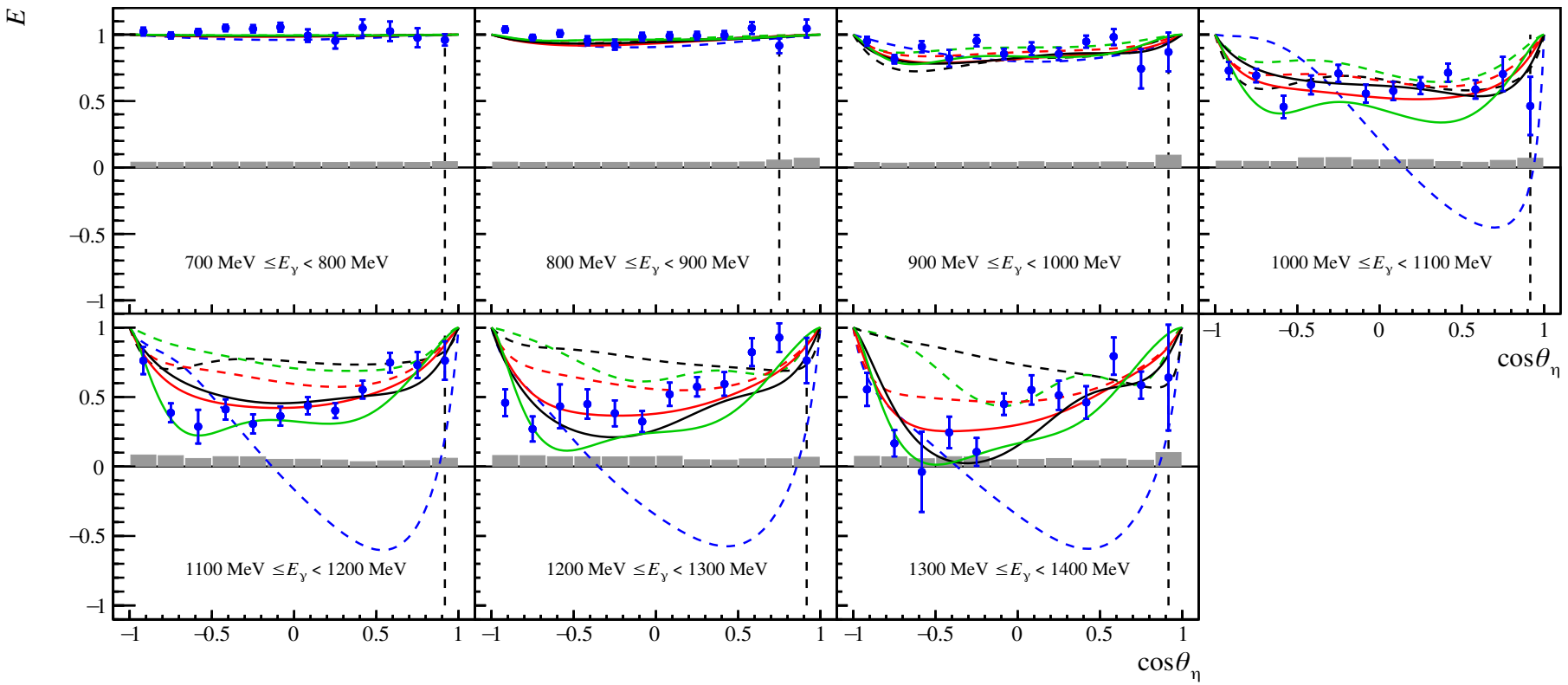

- A2 data (this work)
- BnGa-2014-02
- JüBo-2015-FitB
- ηMAID
- SAID-GE09
- BnGa-2017
- JüBo-2017
- ηMAID-2018